Thesis Report

Strength classification of Okan from Gabon by the combination of visual and machining grading

Xianyue Chen

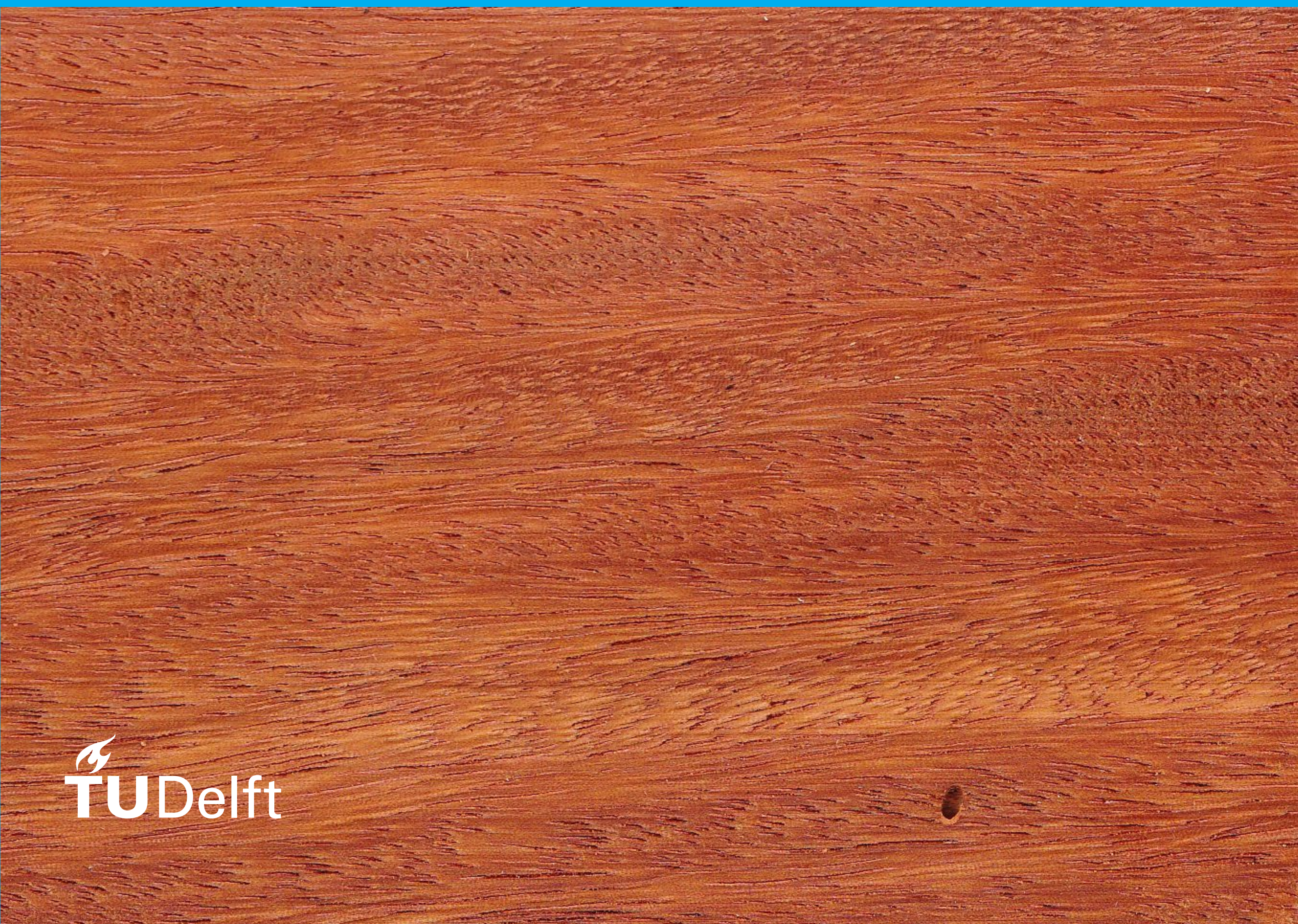

TU Delft

Thesis Report

Strength classification of Okan from Gabon by the combination of visual and machining grading

by

Xianyue Chen

Student number:	4911482	
Thesis committee:	Prof.dr.ir. J.W.G. van de Kuilen	TU Delft
	Dr.ir. G.J.P. Ravenshorst	TU Delft
	Ir. C. Noteboom	TU Delft
	Drs. Wolfgang Gard	TU Delft

TU Delft

Acknowledgement

I would like to express my very great appreciation to the following persons who made this MSc graduation thesis possible. First I would like to express my special thanks to Dr.ir. G.J.P. Ravenshorst for his valuable and constructive suggestions and guidance. Especially, during the COVID outbreak period, the proper arrangement of the experiment made the thesis go smoothly. Then I would like to thank Prof.dr.ir. J.W.G. van de Kuilen influenced me with his critical ideas and provide me with professional insights regarding the 3D fiber orientation strategy. Furthermore, I would like to thank Ir. C. Noteboom for his insightful opinions and taking time out of their busy schedules to be a part of the thesis committee. Then, advice given by Drs.W.F.Gard helped me understand the microlevel of timber. Also, many thanks to the company which offers the tested Okan. Finally, I would like to extend my thanks to the researcher Giorgio Pagella and the technicians of the laboratory of the Stevin Lab for their help in assisting me in running the experiments.

Last but most important, many thanks to friends and family for supporting me through this journey.

Xianyue Chen
Delft, September 2020

Abstract

Timber as a renewable source has been extensively applied among European countries in the construction field. Among more than 1000 available wood species which could be potentially applied as engineered wood, tropical hardwood takes up a significant portion and has advantages of high mechanical resistance and remarkable biological durability against micro-organisms compared to coniferous species and European grown hardwood. Okan has been part of this development, as a hardwood species mostly from the West African regions.

The objective of this thesis is to investigate the strength influencing features, calculate corresponding characteristic values and establish the correlation between the influencing factors and the bending strength with the least deviation and create a representative Okan strength predicting model. Abstracted from literature and dataset, geographically speaking, climate, precipitation, soil quality, water sources are expected to have varying degrees of impacts on mechanical properties. From the material perspective, knot ratio, fiber orientation (slope of grain & ring angle), moisture content, density, Modulus of elasticity (dynamic, static) are important factors. Several experiments about hardwood bending strength have been conducted. However, none of those focus on the growth ring angle and the 3D effect of the fiber orientation. To dive deep into Okan, a series of laboratory tests are conducted, including non-destructive inspection, a four-point bending test on 20 beams (10 stored in the dry condition, 10 stored in the wet condition) with the assistance of digital image correlation technology [DIC]). Except for the regulated experimental procedure, two innovative visual inspection methods based on image processing via Matlab were conducted and verified, which turns out the automation method has preferable efficiency and precision. However, this method could hardly identify compression failure. To avoid the compression failure, beams with the dynamic modulus of elasticity less than $18500N/mm$ are supposed to be checked again by the inspector. All possible influencing factors are well determined by the above-mentioned testing.

Influencing factors of the fracture section form could be concluded from the observation of damaged samples. The slope of grain and growth ring work together to determine the form of the governing crack section. From the experimental outcome, it is clear to observe the linear correlation between mechanical properties and moisture content grouped by the slope of grain. Constant $k_{mc} = 0.13$ for bending strength is found, $k_{mc} = 0.05$ is found for dynamic modulus of elasticity. The experimental results yield the following adjusted characteristic values: bending strength $63.56N/mm^2$, dynamic modulus of elasticity $21134.55N/mm^2$, density $866.58kg/m^3$. Based on 20 beams, this batch of Okan could be graded to D55 which is higher than D30-D35 yielded from the dataset. Besides, Okan beams from Gabon could also be graded into D55. Current European standards advise that the reasonable slope of grain range for tropical hardwood is 0 to 0.1. Through the calculation of the theoretical slope of grain of the dataset and experimental samples, increasing the threshold of the slope of grain to 0.3 should be considered in the testing program. Further promotion to 0.2 doesn't improve the grading outcome and even worsen it.

The linear regression result of modulus of elasticity and bending strength is more preferable than density and bending strength in literature and experimental results, which proves the modulus of elasticity is a good indicator of bending strength. Large scatter happens in the regression of the Hankinson formula. In the combination of two basic models, the new proposed model has an optimized coefficient of determination ($R^2 = 0.685$). The distribution function of the bending strength of the dataset has preferrable overlapping with the theoretical bending strength calculated from the new strength model. To keep the model on the safe side, a safety factor $\gamma = 0.9$ is applied.

It is still unclear if the growth ring angle has a clear numerical relationship with mechanical properties. However, the growth ring angle does bring apparent influences on the form of the fracture section. The

3D effect of fiber orientation needs further investigation.

List of Symbols

Greek letters

α	angle between the beam axis and grain direction
φ	annual ring angle
ρ	density
σ	stress(N/mm^2), or standard deviation of a population
μ	mean value of a population

Latin Letters

a	distance between support and nearest point load [mm]
b	width of beam in mm or constant in regression line
COV	coefficient of variance
E_{dyn}	dynamic modulus of elasticity [N/mm^2]
E_{glob}	global modulus of elasticity [N/mm^2]
E_{loc}	global modulus of elasticity [N/mm^2]
f_e	eigenfrequency [Hz]
$f_{m,k}$	characteristic value of Okan [N/mm^2]
$f_{m,0}$	bending strength parallel to the grain [N/mm^2]
$f_{m,90}$	bending strength perpendicular to the grain [N/mm^2]
$f_{m,\alpha}$	bending strength under angle α to grain [N/mm^2]
$f_{i,\alpha}$	bending strength of NO.i Okan with α slope of grain [N/mm^2]
$f_{t,0}$	tensile strength parallel to the grain [N/mm^2]
$f_{t,90}$	tensile strength perpendicular to the grain [N/mm^2]
$f_{t,\alpha}$	tensile strength under angle α to grain [N/mm^2]
F	Force [N]
G	shear modulus [N/mm^2]
I	second moment of Inertiia [mm^4]
k_α	linear regression factor of NO.i Okan beam
k_{mc}	moisture content factor
l	length of beam [mm]
m	mass of samples
$m.c.$	moisture content [%]
m_k	characteristic value of bending strength [N/mm^2]
$MOE_{i,\alpha}$	modulus of elasticity of NO.i Okan with α slope of grain [N/mm^2]
N	number of samples
r^2	coefficient of determination
R	Resistance
s	standard deviation of a sample
S	solicitation (load)
W	section modulus [mm^3]

Contents

1 Introduction

This chapter articulates the proposed topic and background.

Timber as a renewable source has been extensively applied among European countries in the construction field. Compared to other alternative loading bearing materials, it could achieve maximum sustainability. Among more than 1000 available wood species which could be potentially applied as engineered wood, tropical hardwood takes up a significant portion and has advantages of high mechanical resistance and remarkable biological durability against micro-organisms compared to coniferous species and European grown hardwood[29] [13]. In civil engineering projects, hardwood structures are more applied in bridges, sheet pile walls, jetties, fenders, etc[33]. In Netherlands, researches and developments in guard rails and glued laminated beams for roof structures are ongoing[13]. Okan has been part of this development, as a hardwood species mostly from the West African regions.

In European construction market, most tropical woods rely on importing from tropical areas like Africa, Indonesia, South-America, part of which are barely known in terms of their identification characteristics and/or wood properties[13]. To be able to use those timber species for structural purposes complying with regulations, proper testing and strength grading in terms of mechanical properties need to be done. Strength grading refers to 'the process of sorting sawn timber into groups to which the same mechanical and physical properties can be assigned, based on quantified characteristics.' In reality, several parameters could influence the strength of timber including wood species, origin, moisture content, knot, slope of grain, density, etc. Currently, strength assigning by machine grading or visual grading for wood grading is the most common methodologies to quantify those parameters' influences. However, based on existing regulations, for tropical hardwoods, only strength properties connected with visual assessment are regulated[27]. Hence, for more precise grading, laboratory testing and strength predicting models based on specific hardwood species, like Okan are essential.

This main objective of this thesis is to grade a batch of Okan from Gabon and formulate a strength predicting model by the combination of visual and machine grading based on previous database and laboratory testing, but also according to standards' requirements.

2

Research Design

The main purpose of this chapter is to introduce problems this thesis is going to tackle with, subsequently state the research objectives and questions, at last position the research scope.

2.1. Problem analysis

Using timber as a construction material has been a tendency in the EU for a long time. There are several reasons behind it. On the one hand, wood is a sustainable material and could satisfy people's various structural and esthetical demands. On the other hand, economic globalization makes timber trade easier for EU countries recently which brings more possibilities in engineered wood innovation and development. Demands bring the market. A large amount of tropical hardwoods imported from certified forests entered the European market. Those kinds of tropical timber are called Lesser-Known Timber Species (LKTS)[32]. The object of this thesis is Okan from Gabon, one of lesser-known timber species, which needs to be graded and assigned to existing strength class.

Like other in-homogeneous wood material, see Fig.2.1, Okan's mechanical properties vary from direction to direction. In parallel to the grain direction, namely, the longitudinal direction of the tree stem, material is relatively stronger than any other direction, which is shown in Fig.2.2. On the contrary, at a certain angle to the grain, the strength is far lower than the parallel to the grain. For instance, the tensile strength parallel to the grain is around 40 times higher than perpendicular to the grain[9]. In addition, Okan has a mixture of straight and highly interlocked grain,which is one of the peculiar features of tropical hardwoods. Moreover, knots and other irregular defects might exist. As consequences, irregular knots interrupting the direction of grain and interlocked grain are responsible for many mechanical failures for the sake of complex stress distributions within wood or an irregular sheared surface etc. In practice, Okan will be applied as pile underwater or beams exposed to sunshine, where the variety of moisture content could also bring uncertainty.

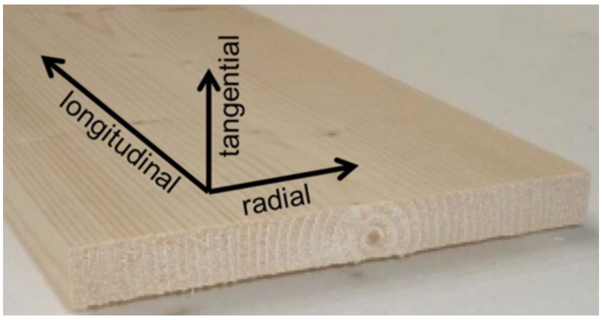

Figure 2.1: Timber's inhomogeneity

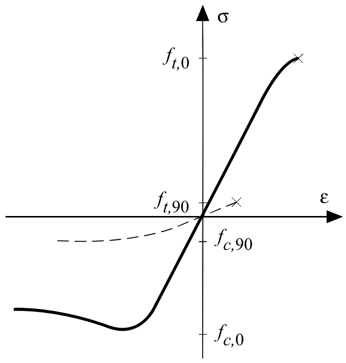

Figure 2.2: Stress-strain curve of clear wood exposed to tensile (t) and compressive stresses (c) parallel to the grain (solid line) and perpendicular to the grain (dashed line) at constant strain increase [9].

In the grading procedure, the above-mentioned features should be taken into account when determining influencing factors. However, current standards outline a few general influencing factors obtained by visual and machine grading, which is not detailed and specified for Okan and any other tropical hardwood. Hence, in order to apply Okan more economically, figuring out associated influencing factors and a strength predicting model should come into play as a solution.

2.2. Research objective

The objective of this thesis is to establish the correlation between the influencing factors and the bending strength with the least deviation and create a representative Okan strength predicting model. Moreover, to find out proper thresholds for those influencing factors to achieve higher and more economical grading results. Beginning from literature review and material property assessment, through analyzing the existing dataset by statistical methods, influencing factors and sample characteristics will be articulated. By laboratory testing, more data could be obtained for analyzing failure mechanisms, based on which, mechanical model and predicting model of Okan could be computed. Ending on developing the grading theory for Okan. All phases are essential and determine the accuracy of the final strength predicting model.

In this thesis, the main questions are:

- Which influencing factors could be correlated to the Okan's mechanical properties?
- What relationship between those influencing factors and Okan's mechanical properties?

Several sub-questions could be proposed from the main questions:

- How physical features (knots, interlocked grain, etc.) of Okan by visual grading could be quantified and simplified during the measurement?
- What is the relationship between parameters including machine grading (modulus of elasticity, density) and visual grading (knots, slope of grain)?
- What is the best mathematical way to adjust testing data to reference moisture content and size?
- What is the fitting effect of theoretical predicting model?
- What are the most suitable thresholds of those influencing factors in the view of producer?
- Is the current class D40 as defined in NEN-EN 338(2016) a suitable assignment for this batch of Okan from Gabon?
- What could be added or improved for current grading method (procedure) for Okan?

2.3. Research scope

The final strength predicting model mainly focuses on the specific Okan from Gabon. The test data consist of 20 pieces from the region near Lastourville and Makokou. Thus, the research has limitations for the sake of testing number, origin and timber species, meaning that the conclusion might be not representative for all Okan.

During testing, only two types of specific moisture content ambient which represent dry and moist environment will be set. Then, the adjustment to the reference standard condition will be done. In the machine grading stage, the MTG handheld from Brookhuis Micro Electronics will be used. The tensile strength, compressive strength, and shear strength are also significant indicators for engineered timber application, but in this research, the main focus is bending strength model.

The following physical and mechanical properties will be mainly focused:

- Physical properties (weight, length, width, height etc.)
- Density
- The fibre orientation
- Surface defects
- Modulus of elasticity (MOE), including global, local and dynamic.
- Bending strength

The following mechanical properties will not be covered in this these:

- Tension strength
- Compression strength
- (Rolling) shear strength and modulus

3

Background and literature review

3.1. Background of Okan and development in civil engineering works

Okan (Cylicodiscus gabunensis Harms) is a trade name for a tropical hardwood belongs to Leguminosae family, sometimes called denya. It is native to West Africa, from Sierra Leone to Gabon, see in Fig.3.1. Biologically, Okan is a deciduous species with a height up to 50-60m, of which the first 25m or more is the straight, cylindrical and clear bole. Common trunk diameter attains from 100 to 130cm. The wood is heavy and hard. One big tree could provide high-quality usable timber around 15-20 m^3. Okan timber is characterized by its strength and durability. Consequently, it has been used for load-bearing elements from hydraulic structure to building structure. To be specific, important application in marine field includes lock gates, see Fig.3.2, bridges, piles, decking, etc. In building and road construction, furniture, roof structures, flooring, railway sleepers, guard rails all need Okan. In other aspects, it used for making mine props, pontoons, etc. Structurally, according to NEN-EN 1912, Okan from Congo Brazaville and Cameroon is assigned to D40, meaning that based on edgewise bending tests, the 5-percentile characteristic values of bending strength value is $40 N/mm^2$ and the mean modulus of elasticity is $13000 N/mm^2$.

Figure 3.1: Okan distribution map

Figure 3.2: Hydraulic work: Lock gate

*Fig3.2 : Retrieved from: `https://slideplayer.com/slide/13524883/`

3.2. Hardwoods grading

Visual grading and machine grading are two parallel methods of strength grading in the non-destructive way[11]. The standard EN338 regulates certain strength classes for hardwoods. Each class is indicated by the value of the edgewise bending or tensile strength in N/mm^2. Statistically, the existing grading system only could assign a type of timber with a wide spectrum of possible strength to a certain strength class.

In terms of hardwood species, based on edgewise bending tests, the characteristic values of strength, stiffness, and density for the strength classes Dxx, where xx refers to the 5-percentile characteristics bending strength value, are given in EN338[12].

3.2.1. Visual grading

Visual grading has been widely used since the beginning of the timber industry. By visual inspection and assessment, into grades to which characteristic values of strength, stiffness, and density can be allocated. Electronic or mechanical instruments can be used to assist the visual grader in this process[11]. Currently, national standards and grading rules outline the visual grading system. In the EU, standards of visual grading vary from country to country, but basically, they have more or less the same indicators and characteristics with different threshold levels and measurement approaches[13]. To be specific, knots, slope of grain, wane, fissures, boxed heart, distortion, etc. are common important grading features but with different restrictions, which could trace back to individual countries' timber industry development, engineer's experiences and building codes. Characteristics mentioned above are not necessarily related to strength but also have relation to durability classification as well. It is important to note that this thesis will mainly focus on grading of tropical hardwood about bending strength class of dutch standards.

Researches show that the slope of grain and knot are the most important characteristics during visual grading, which brings a reduction of strength. Usually, tropical hardwood species have few knots with relatively small size compared to softwood, which slightly influences the tropical hardwood's mechanical properties. Thus, the slope of grain is the dominant factor when assigning strength classes to certain hardwood species, However, because of difficult quantifying by a visual grading, standards only regulate the threshold value, above which the beam should be rejected. Numerically, only Hankinson relations[15] could roughly articulate the correlation between the slope of grain and timber strength, which is derived from softwood[15]. According to approved standards, the procedure of allocating tropical hardwood species to strength classes is presented in Fig.3.3[13].

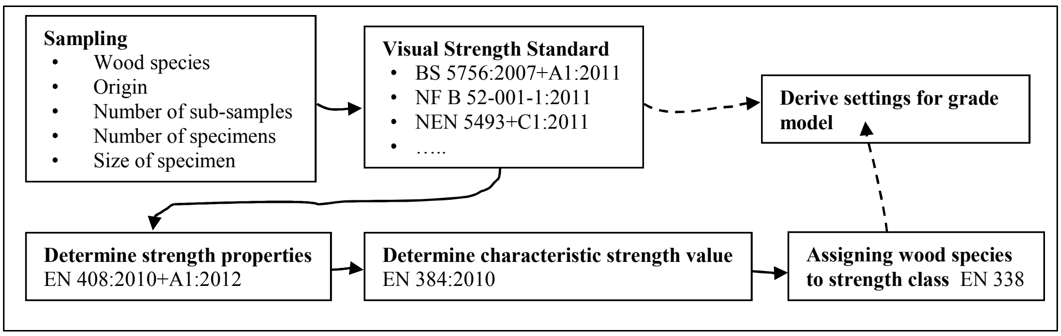

Figure 3.3: Procedure of allocating tropical hardwood species to strength classes[13]

3.2.2. Machine grading

As we know, the visual strength grading is characterized by subjectivity of graders and inevitable ambiguity. Thus, grading machine was developed and machine grading comes into play in the timber industry. Machine grading is one of the common non-destructive methods of grading including two basic systems, namely, output control and machine control, both requiring the combination of visual inspection to obtain strength-reducing parameters that cannot be sensed by the machine automatically[11]. Generally, machine grading could acquire physical and mechanical properties of timber, among which density and dynamic modulus of elasticity (MOE) are most correlated to strength classes. Mathematical and/or statistical models could be derived from machine grading resultants and link timber properties to measured parameters.

In comparison with visual grading, the measured resultants MOE and density could capture the other physical parameters' effects referred to the knots and slope of grain[28]. However, there are no established machine grading rules/ standards for tropical hardwoods in the EU.

3.2.3. FEM grading

Timber as an inhomogeneous material, to fully utilize the load-bearing capacity, the Finite Element Method (FEM) has been introduced to analyze its characteristics. The FEM simulation aims to assess how the failure mechanism develops and what the governing features are when capturing growth inhomogeneities, namely modeling the knots and the grain course in the structural timber.

Several types of modelling principles are developed, among which streamline meshing (shown in Fig.3.4) has been proved to be effective without considering the radial and tangential direction. To improve the abovementioned defects, the equipotential lines method was introduced for improving transverse direction meshing[16]. However, existing models are still built based on ideal assumption and simplification. There is a long way to go to tackle some anatomical issues like how to model knots more accurately, connection of knots and surrounding wood.

By application of the FEM method, the strength grading system could be improved, especially, in the future, with the development of automation of the simulation procedure.

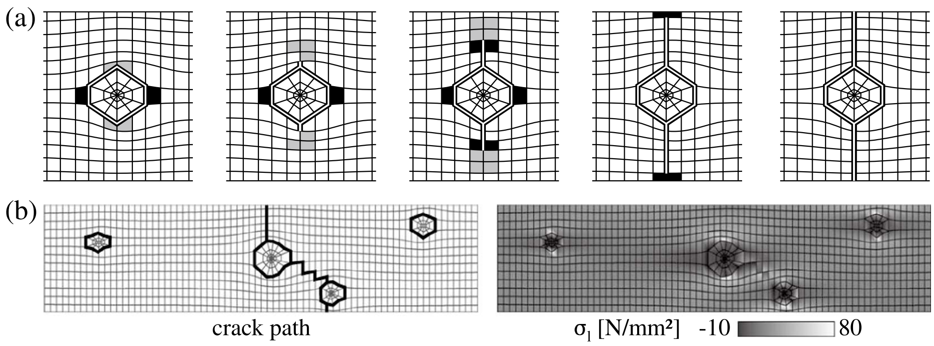

Figure 3.4: SL-mesh: (a) determination of crack path, (b) simulation results for timber board [16]

3.3. Strength modelling

In this section, according to the thesis[27], a series of steps about setting up a tropical hardwood mathematical model are articulated.

3.3.1. Mechanical model

In this section, a mechanical model for tropical hardwood is derived from the thesis[27] is introduced. Timber is simulated as the Bernoulli-Euler beam which has characteristics that the plan sections remain plane and any section of a beam is perpendicular to the neutral axis. Hooke's Law works in an elastic range for stresses and strains relationship. Elastic range and brittle failure could happen in tension zone and bi-linear stress-strain relation is considered in the compression zone.

For four-point bending test the following equation is given to calculate the bending strength:

$$f_m = \frac{3Fa}{bh^2} = \frac{M}{W} \tag{3.1}$$

During visual override inspection which happened in the preliminary phase of grading, samples with compression failures, fissures, etc. would be removed. Thus, only the mechanical model of clear wood, timber with grain angle deviation and timber with knot are articulated in this section.

For clear wood, the compression zone acts in plastics range and brittle behavior shows in the tension zone. For simplification during calculation, the bending strength behavior is assumed as a linear stress distribution usually, see in Fig.3.5.

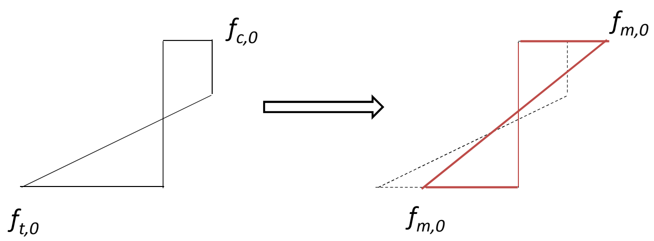

Figure 3.5: Stress distribution for tropical hardwood failure mechanism [27]

The bending strength could be expressed as follows:

$$f_{m,o,cw} = \frac{f_{c,o^*}\left(3f_{t,o} - f_{c,o}\right)}{f_{t,o} + f_{c,o}} \tag{3.2}$$

The anisotropic behavior of timber caused by its natural properties like grain angle deviation, knot, fissures, etc. For structural timber with grain angle deviations, Hankinson and Norris equation are explanation in most cases. In tropical hardwood cases where shear strength is not governing in the interaction of stresses, Hankinson equation is more suitable in the modeling to formulate the bending strength and modulus of elasticity with grain angle deviation (Eq.3.3 & Eq.3.4), especially over the range from 0 to 20 degree. Based on the Hankinson equation, the relationship between the MOE and the bending strength at a certain grain angle could be formulated by further experimental assistance.

$$f_{m,\alpha} = \frac{f_{m,0}}{\frac{f_{m,0}}{f_{m,90}}\sin^2(\alpha) + \cos^2(\alpha)} \tag{3.3}$$

$$MOE_\alpha = \frac{MOE_0}{\frac{MOE_0}{MOE_{90}}\sin^2(\alpha) + \cos^2(\alpha)} \tag{3.4}$$

Apart from grain angle deviation, knots could reduce the section modulus of the cross-section as well. Stress redistribution and brittle behavior failure in the tension zone happen mostly due to the occurrence of knots. According to the thesis[27], for tropical hardwood with knots, the mechanical model could be described as a clear wood equipped with a weak zone with a concept that assuming the knot as a hole, namely removed material. By introducing a linear reduction factor combined with the simplification in Fig.3.6, the stiffness could be formulated in the safe side (Eq. 3.5)

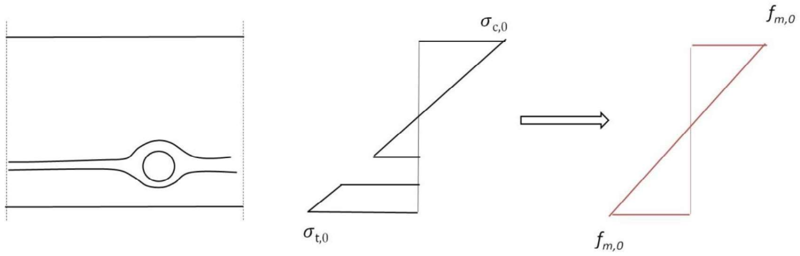

Figure 3.6: Stress distribution for tropical hardwood with knot [27]

$$f_{m,red} = f_{m,cw} \frac{W_{red}}{W_{full}} (2.5) \tag{3.5}$$

where:

W_{full} is the unreduced section modulus

W_{red} is the reduced section modulus

$f_{m,cw}$ is the clear wood strength

Theoretically, above models could predict tropical hardwood mechanical and physical properties. However, the large portion of the accuracy of the output depends on the visual measurement input which, in practice, is hard to be obtained precisely, especially the existence of 3D effect.

3.3.2. Mathematical model

In this section, a mathematical model for tropical hardwood is derived from the thesis[27] is introduced. A large number of experimental data shows the bending strength and MOE for clear wood are correlated with density respectively, see Eq.3.6 & Eq.3.7, which could also derive the good relationship between the MOE and the bending strength.

$$f_{m,0} = \rho C_1 + \varepsilon_f \tag{3.6}$$

$$MOE_0 = \rho C_2 + \varepsilon_M \tag{3.7}$$

Where constant C_n can be obtained by data analysis and regression.

Without taking knots into account

Researchers concluded that MOE measurement could capture 3D-effect well. Meanwhile, the grain angle from practical measurement could bring more measuring error resulting in a sensitive model. Hence, from Eq.3.3 & Eq.3.4 & Eq.3.6 & Eq.3.7, the prediction model between the bending strength and the density & MOE_α without taking knots into account could be derived as (Constant D_n can be obtained by data analysis and regression.):

$$f_{m,\alpha} = \frac{\rho MOE_{\alpha}}{D_1\rho + D_2 MOE_{\alpha}} + D_3 \tag{3.8}$$

Assuming the grain angle deviation is 0

In addition, $f_{m,\alpha}$ could also be formulated as linear correlation with MOE by

$$f_{m,\alpha} = A * MOE + B \tag{3.9}$$

It is assumed that the grain angle deviation is 0 when building a prediction model for structural timber with knots, the bending strength and MOE could be formulated in linear reduction form as follow:

$$f_{KR} = f_{m.0} * (1 - A_1 * KR) + B_1 \tag{3.10}$$

$$MOE_{KR} = MOE_0 * (1 - A_2 * KR) \tag{3.11}$$

By combing above formulas and Eq.3.6 & Eq.3.7, f_{KR} could be rewritten as Eq.3.12

$$f_{KR,\,\mathrm{mod}} = K_1\rho + K_2 MOE_{KR} + K_3 \tag{3.12}$$

Overall model

In practice, the grain angle deviation and knots occur at the same time, to present them in one single model, knot-reduction oriented model and grain angle deviation reduction-oriented model could be combined and formulated as followed form:

$$f_{m,\alpha,KR} = \frac{\rho C_1\,(1 - A_1 KR)}{(C_3 - 1)\sin^2(\alpha) + 1} + C_5 \tag{3.13}$$

$$MOE_{m,\alpha,KR} = \frac{\rho C_2\,(1 - A_2 KR)}{(C_4 - 1)\sin^2(\alpha) + 1} + C_6 \tag{3.14}$$

Obviously, density and measured MOE are needed for formulating the bending strength at the same time.

3.4. Statistical method

Timber is a natural material characterized by high deviation and randomness. Thus, to analyze the reliability of this kind of material, statistical methods come into play. In this section, the probabilistic design principle and related statistical methods are explained.

3.4.1. Probabilistic design principle

In civil engineering, the reliability of a system usually is defined by comparing two stochastic variables: the resistance R of the structure or material and the load (or solicitation) S[17]. To make sure no failure occurs, a reliable system could be defined as the resistance should be larger than the load, which could be indicated as follows:

$$R > S \tag{3.15}$$

However, in practice, it is impossible to get the deterministic values of resistance(R_d) and load(S_d), but random variables, which are described by certain distribution types and accompanying parameters in probabilistic approach. When the probability density function of R and S are known, the failure probability P_f can be formulated as Eq.3.16, and be graphically expressed in Fig.3.7.

$$P_f = P[S > R] \tag{3.16}$$

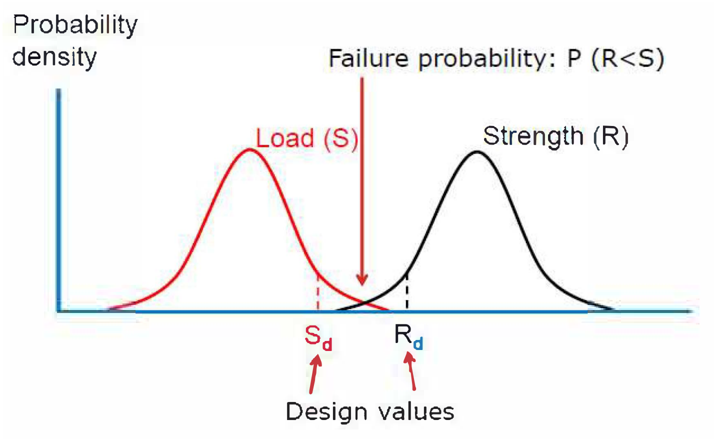

Figure 3.7: Ilustration of relationship between strength and load [31]

Among several reliability calculation methods, semi-probabilistic design is specified in Eurocode: the uncertain parameters are modelled by one characteristic value based on partial coefficient ($\gamma's$) concept. In this concept, γ adjusts for deviation from the characteristic value, uncertainty in the calculation model, and scattering in dimensioning, etc. To be specific, in this case, the characteristics value of load S_k is defined as the 95^{th} percentile value and the characteristics value of resistance R_k is defined as the 5^{th} percentile value. Then, according to the definition of semi-probabilistic design and Eurocodes, design value load and design value resistance for material properties could be formulated as follows, respectively:

$$R_d = R_k/\gamma_M \tag{3.17}$$

$$S_d = S_k \cdot \gamma_s \tag{3.18}$$

In this thesis, characteristic values are defined as:

- Bending strength: the 5% fractile at 12% moisture content and a certain size.
- Modulus of Elasticity: mean value at 12% moisture content and a certain size.
- Density: the 5% fractile at 12% moisture content and a certain size.

As a type of structural material, when timber is applied in projects, based on the probabilistic design principle, the structural reliability could be computed.

3.4.2. Data distribution types

Characteristic values are the key indicators in strength grading. Before determining the characteristic value of timber, correct data distribution should be assumed. The most common distribution types for civil engineering work are normal distribution, lognormal distribution, Weibull distribution or ranking. EN14358:2016[22] regulates two types of calculation methods for determining characteristics values: parametric calculation and non-parametric calculation, mainly focusing on normal distribution/ lognormal distribution and ranking, respectively.

Normal (Gaussian) distribution

Normal distribution is the most common distribution function in real life, which is reflected in, for example, height, blood pressure, measurement error, IQ scores ,etc.

The probability density function is:

$$f_X(x) = \frac{1}{\sqrt{2\pi}} \frac{1}{\sigma} e^{\left\{-\frac{(x-\mu)^2}{2\sigma^2}\right\}} \tag{3.19}$$

Where:

μ: the mean value

σ: the standard deviation

The normal distribution graph, see Fig.3.8, is symmetrized by the mean value. The area between the belt-shape curve and the horizontal axis is always equal to 1, and the probability corresponding to the function of the probability density function from positive infinity to negative infinity is 1, meaning that the sum of the frequencies is 100%.

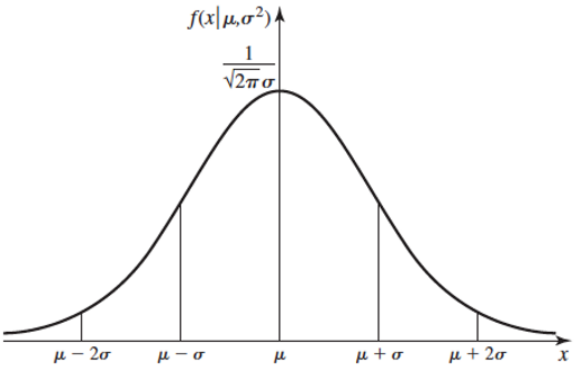

Figure 3.8: Normal distribution diagram

Lognormal distribution

If X follows lognormal distribution, then $Y = ln(X)$ is a normal distribution. Fig.3.9 shows the lognormal distribution under different mean values and standard deviation values. The probability density function is:

$$f_X(x) = \frac{1}{\sigma_Y x\sqrt{2\pi}} e^{\left\{\frac{(\ln(x)-\mu_Y)^2}{2\sigma_Y^2}\right\}} \tag{3.20}$$

Statistically, the lognormal distribution is the result of a nonlinear transformation of normal distribution.

When the standard deviation is much less than the mean value the corresponding transformation could be formulated as follows Eq.3.21 & Eq.3.22:

$$E(X) = \exp\left\{E(Y) + \frac{1}{2}\sigma^2(Y)\right\} \approx \exp\{E(Y)\} \quad (3.21)$$

$$\sigma(X) = E(X)\sqrt{\exp\{\sigma^2(Y)\} - 1} \approx E(X)\sigma(Y) \quad (3.22)$$

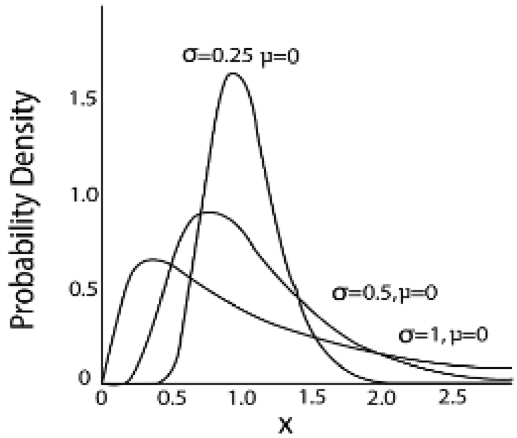

Figure 3.9: Lognormal distribution diagram (retrieved from:https://quantra.quantinsti.com/glossary/Lognormal-Distribution)

Ranking

NEN-EN 14358:2016[22] prescribed: non-parametric calculation can be applied in the sample whose distribution of data is unclear. This approach only focuses on the dataset's lower tail part value and by ranking the data in ascending order, the 5 percentile could be determined [27].

4

Statistical method to determining 5th percentile value

To assign the Okan to specific strength grade, the 5% fractile characteristic value, which is regulated in relevant standards, of bending strength and density must be determined by statistical methods. In accordance with NEN-EN14358[22], the 5% characteristic value shall be determined at α=75%, where α is the confidence level, indicating as the probability of 75% the 5% population is greater than the estimator on the characteristic value.

The procedure of determining the 5^{th} percentile value of population and each sample consists of the following steps:

- Find out the distribution of the population (all existing detailed Okan dataset).
- Find out the sample's distribution.
- Calculate the 5^{th} percentile value of samples with a 75% confidence level based on the sample's distribution.
- Determine the 5^{th} percentile value of the population with a 75% confidence level based on the population's distribution.

4.1. Distribution based on the population

Before destructive testing, in the existing dataset, there are 286 peices from 6 samples with detailed data available. In this section, in terms of the density and the bending strength, those samples will be checked which distribution fits best.

In Fig.4.1, Fig.4.2 and Fig.4.3, the histograms of the population show the desirable normal distribution bell curves. On the basis of the three rough diagrams, normal distribution is assumed. In this case, the population is around but less than 300 samples. Usually, for small or medium size sample (n<300), the Shapiro-Wilk is the most common assessment method, however, which is more reliable when n< 50. Even though, sometimes, skewness and kurtosis's outcome will be affected by abnormal value. Under comprehensive consideration, to address the unreliability introduced by size, Skewness, and Kurtosis with their corresponding Z-score will be used for normality test of population and the P-P plot will be plotted as well as one of the indicators.

Theoretically speaking, skewness presents the degree of the asymmetry and kurtosis is the indicator of the distribution curve peak sharpness. Skewness (Kurtosis) Z-score is defined as skewness (Kurtosis) value divided by its standard error. Moreover, P-P plot plots observed and expected cumulative distribution function against each other which reflects the degree of congruence between the actual data and theoretical data distributed normally. Technically, a perfect normal distribution has zero kurtosis value and zero skewness value. In practice, the closer the two values are to zero, the stronger the normality is. Abstracting from literature[18], for medium size samples (50< n<300), with confidence level 0.05, when the z-value is over 3.29, the sample could be concluded as non-normal distribution.

Firstly, the adjusted mechanical properties including bending strength and dynamic MOE were analyzed by the software SPSS. In the P-P plot of adjusted bending strength and dynamic MOE, see Fig.4.4 and Fig.4.5, two tiles ends fit the straight line well and the deviation in the middle zone is in the acceptable range. Regarding the adjusted bending strength, in the Tab.4.1, the value of skewness is -0.254 (standard error: 0.144), Z-score = -0.254 /0.144 = 1.764, Kurtosis is -0.388 (standard error is 0.287), Z-score = -0.388/0.287 = 1.352. Regarding the adjusted dynamic MOE, in the Tab.4.2, the value of skewness is -0.299 (standard error: 0.144), Z-score = -0.299 /0.144 = 2.076, Kurtosis is -0.374 (standard error is 0.286), Z-score = -0.374 /0.286 = 1.308. Skewness and Kurtosis are around zero, Z-score is between ±3.29. Thus, both series of data could be considered as normal distributions.

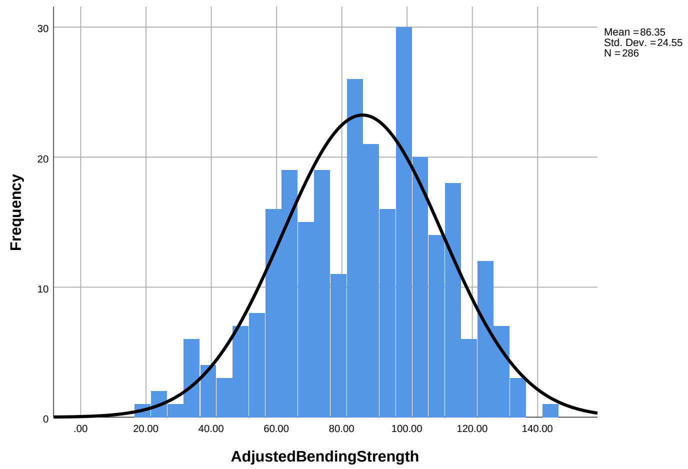

Figure 4.1: Fitting normal distribution curve of adjusted bending strength

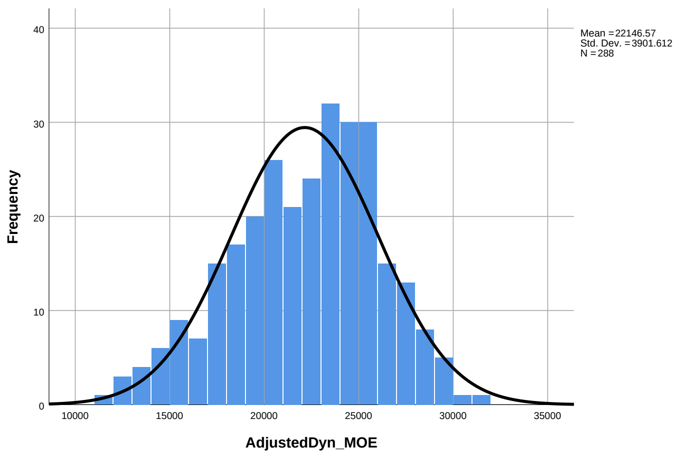

Figure 4.2: Fitting normal distribution curve of adjusted dynamic MOE

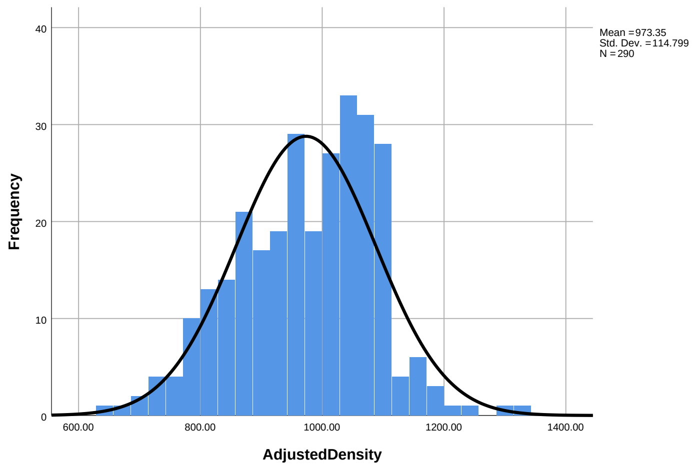

Figure 4.3: Fitting normal distribution curve of adjusted density

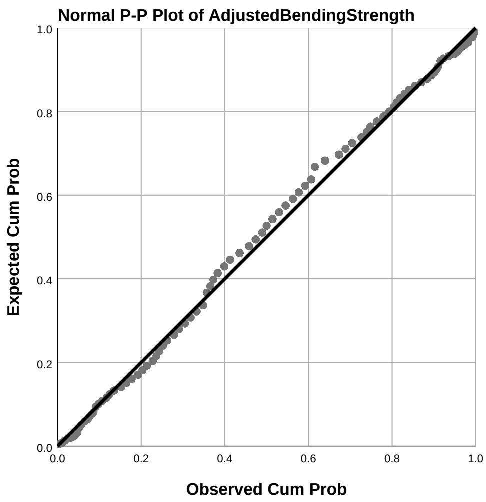

Figure 4.4: Normal P-P plot of adjusted bending strength

Table 4.1: Descriptive statistics of adjusted bending strength

	N	Skewness		Kurtosis	
	Statistic	Statistic	Std. Error	Statistic	Std. Error
AdjustedBendingStrength	286	-.254	.144	-.388	.287
Valid N (listwise)	286				

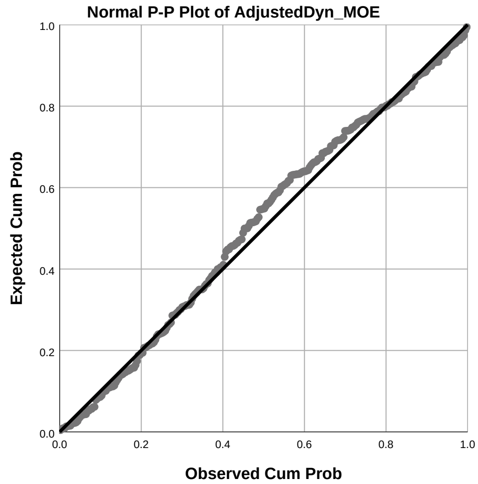

Figure 4.5: Normal P-P plot of adjusted dynamic MOE

Table 4.2: Descriptive statistics of adjusted dynamic MOE

	N	Skewness		Kurtosis	
	Statistic	Statistic	Std. Error	Statistic	Std. Error
AdjustedDyn_MOE	288	-.299	.144	-.374	.286
Valid N (listwise)	288				

In the P-P plot of adjusted density, see Fig.4.6, the tile has some deviation, but the overall tendency is in the acceptable range. In the Tab.4.3, the value of skewness is -0.228 (standard error: 0.143), Z-score = -0.228 /0.143 = 1.594, Kurtosis is -0.054 (standard error is 0.285), Z-score = -0.054/0.285 = 0.189. Skewness and Kurtosis are around zero, Z-score is between ±3.29. Thus, this series of data could be considered as normal distribution.

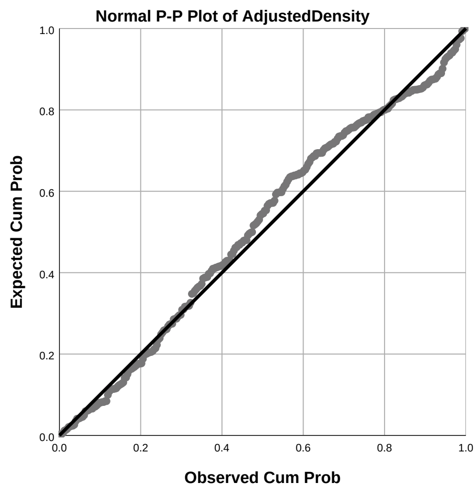

Figure 4.6: Normal P-P plot of adjusted density

Table 4.3: Descriptive statistics of adjusted density

	N	Skewness		Kurtosis	
	Statistic	Statistic	Std. Error	Statistic	Std. Error
AdjustedDensity	290	-.228	.143	-.054	.285
Valid N (listwise)	290				

4.2. Distribution based on samples

In this case, different from population with medium size, each single sample in population is mostly small size (<50 beams). Statistically, the Shapiro-Wilk test is more appropriate to handle small size sample. When the p-value, which is indicated as sig. in the Tab.4.4, is above the chosen alpha level, in this case, 0.05, the null hypothesis that the sample is normal distribution cannot be rejected.

In Tab.4.4, in terms of adjusted bending strength, aside from samples 1 and 5, other samples all follow the normal distribution. In terms of adjusted dynamic MOE, except for sample 3, all follow the normal distribution. However, only 50% of samples distribute normally in terms of adjusted density.

All in all, taking the standard requirement and above assessment into account, for all samples, the 5^{th} percentile value of samples with a 75% confidence level could be calculated in the light of the normal distribution.

Table 4.4: Shapiro-Wilk test results of adjusted bending strength and adjusted density (red font: rejected groups)

Tests of Normality

	AdjustedBendingStrength			AdjustedDensity			AdjustedDynamicMOE		
	Statistic	df	Sig.	Statistic	df	Sig.	Statistic	df	Sig.
Sample1	.927	54	.003	.945	54	.015	.985	54	.731
Sample2	.975	42	.483	.951	42	.072	.956	42	.105
Sample3	.973	44	.379	.985	44	.841	.947	44	.041
Sample4	.976	50	.387	.944	50	.020	.964	50	.132
Sample5	.945	47	.027	.972	50	.279	.969	48	.226
Sample6	.962	49	.118	.911	50	.001	.989	50	.910

4.3. Calculate the 5th percentile value of samples with a 75% confidence level based on normal distribution

In Section.4.2, it is derived that those samples are normally distributed and independent. Therefore, according to this distribution type, relevant characteristic values calculation method refers to NEN-EN 14358 Clause 3.2.2[22].

The mean value and standard deviation are formulated as below:

$$\bar{y} = \frac{1}{n}\sum_{i=1}^{n} m_i \tag{4.1}$$

$$s_y = \max \begin{cases} \sqrt{\frac{1}{n-1} \sum_{i=1}^{n} (m_i - \bar{y})^2} \\ 0,05\bar{y} \end{cases} \tag{4.2}$$

Then the 5^{th} percentile characteristic value is determined by the parametric method:

$$m_{\mathrm{k}} = \bar{y} - k_{\mathrm{s}}(n) s_{\mathrm{y}} \tag{4.3}$$

k_s is the confidence level factor under the assumption that the normal distributed samples are from one population. For the consistency of this thesis, k_s for N (>=1) sample(s) all refer to the Tab.4.5[27].

Table 4.5: Confidence level factor k_s for N

n	***N***				
	1	2	3	4	5
10	2.08	1.96	1.90	1.87	1.84
20	1.92	1.84	1.81	1.79	1.77
30	1.86	1.80	1.77	1.76	1.75
40	1.83	1.78	1.75	1.74	1.73
50	1.81	1.76	1.74	1.73	1.72
100	1.76	1.73	1.71	1.70	1.70
150	1.73	1.71	1.70	1.69	1.69
200	1.72	1.70	1.69	1.69	1.68
250	1.71	1.69	1.69	1.68	1.68
300	1.71	1.69	1.68	1.68	1.68
500	1.69	1.68	1.67	1.67	1.67
1000	1.68	1.67	1.67	1.66	1.66

4.4. Determine the 5th percentile value of the population with a 75% confidence level based on the normal distribution

In the last section, the confidence level factor k for one single sample was found out, based on which, for population, the confidence level factor k will be elaborated in this section. The derivation method could be checked in the literature [27]. Proved in the Section 4.1, the population is normal distribution, conforming to the derivation assumption for k, denoted as $k_{N,n}$. Here, the standard error still needs to be assumed as normal distribution.

Then $k_{N,n}$ can be calculated with: (where k can be found in Tab.4.5)

$$k_{N,n} = z_p + \frac{(k - z_p)}{\sqrt{N}} \tag{4.4}$$

Those samples in the existing dataset grew in Africa but different forests and regions. In other words, they are drawn from an inhomogeneous population. Thus, to make sure the final 5% fractile could represent the population, the chi-squared test should be conducted to guarantee samples could be regarded as a homogenous population. Eventually, only the weakest samples will be used to determine the 5% fractile of all samples. Detailed procedures refer to the literature [27] section 3.3.

Brief steps are explained as follows:

1. Calculate all samples' mean values and observed (O) percentage value (in every single sample, the percentage of boards below the population mean value)
2. Calculated the expected values (E) which is manipulated with the summation of all observed percentage value divided by the number of boards.
3. Calculate the Z value by: $Z = \sum_{i}^{N} \frac{(O_i - E_i)^2}{E_i}$
4. Calculate the significance value which could be obtained by dividing the sample-1 freedom from the Z value.
5. If the significance value is lower than 0.01, then remove the sample with the largest mean value and restart the procedure from step 1 until the significance value is above 0.01.

5

Data review - (evaluation of existing data)

In the past few years, researchers have conducted relative testings about Okan's properties in structural size. In this section, from the perspective of statistics, the mean value, standard deviation and characteristics values are mainly focused on to conclude the correlation between mechanical properties and physical properties. Six samples, from sample 1 to 6, namely first group data, with a detailed record of experiment data and four samples, from sample 7 to 10, namely second group data, only with outcomes, from different regions tested in different periods are analyzed, based on which the strength grade will be concluded in terms of 5^{th} percentile value.

According to the EN384 clause 5.4.1[23], data from the original test should be adjusted to reference moisture content and height, in this thesis, 12% and 150mm is used. In the data review stage, the adjustment method refers to the thesis[27].

In Tab.5.1, the overview of the existing dataset with available properties' information is given. The tick sign denotes that the sample is equipped with ticking cell property information.

Table 5.1: Available data per test specimen

Group	Sample ID	Source	Number	Density	m.c.	MOEdyn	MOEloc	MOEglob	Slope of grain	Knot ratio	Compression failure
1	1		√	√	√	√	√	√			√
	2	√	√	√	√	√	√				
	3	√	√	√	√	√		√	√	√	
	4	√	√	√	√	√		√	√	√	
	5	√	√	√	√	√		√	√	√	
	6	√	√	√	√	√		√	√	√	
2	7	√	√								
	8	√	√								
	9	√	√								
	10	√	√								

*Slope of grain is actual number measured after bending test based on the major failure crack which goes with the fiber direction

5.1. Properties correlation

From those basic parameters, a medium correlation was found between adjusted dynamic modulus of elasticity and adjusted bending strength (around $R^2 = 0.46$), even though with deviation among individual samples, see Fig.5.1 & 5.2 and Tab.5.2 & 5.3.

The relatively low correlation exists between adjusted density and bending strength in the first group($R^2 = 0.0045$), see Fig.5.4. Elasticity of Modulus positively correlated with density, but with considerable scatter ($R^2 = 0.05$) for the first group data, see Fig.5.5. Even though, the second group shows a good positive correlation ($R^2 = 0.58$) between the adjusted density and MOE, in this thesis, combined with two resultants, the density still is not an efficient sole grading parameter.

Apparently, the increment of the slope of grain has a non-linear negative impact on bending strength and modulus of elasticity, see Fig.5.6 & 5.7. Drawing two threshold lines in Fig.5.6, to achieve the objective D50 in terms of 5-percentile characteristic value, the limit of slope of grain could be up to around 0.4 rather than 0.1. However, in practice, visually assessing the slope of grain accurately is a challenge. On the other perspective, Modulus of Elasticity could capture the influence from the slope of grain to some extent, but not the density.

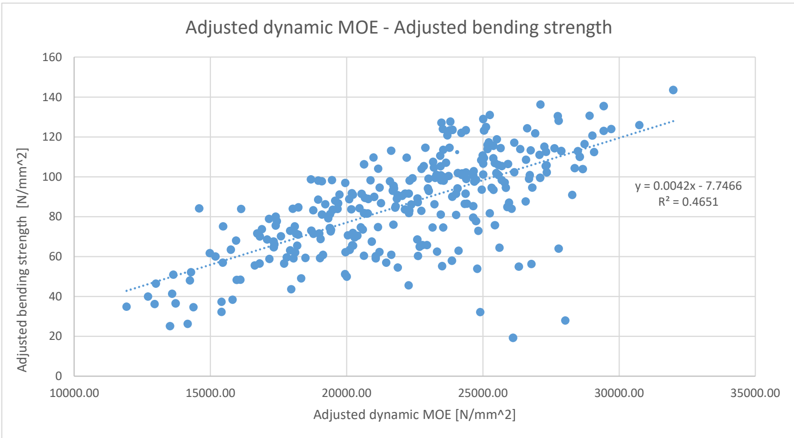

Figure 5.1: Adjusted bending strength vs. Adjusted modulus of elasticity (sample 1-6 in the first group)

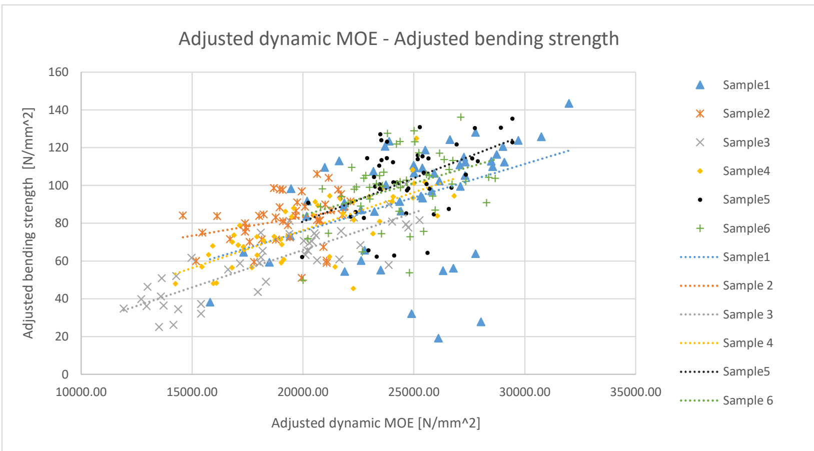

Figure 5.2: Adjusted bending strength vs. Adjusted modulus of elasticity (sample 1-6 in the first group)

Table 5.2: R^2 of Adjusted Bending strength vs. Adjusted modulus of elasticity (sample 1-6 in the first group)

Sample	1	2	3	4	5	6	All
R^2	0.183	0.086	0.719	0.248	0.556	0.158	0.465

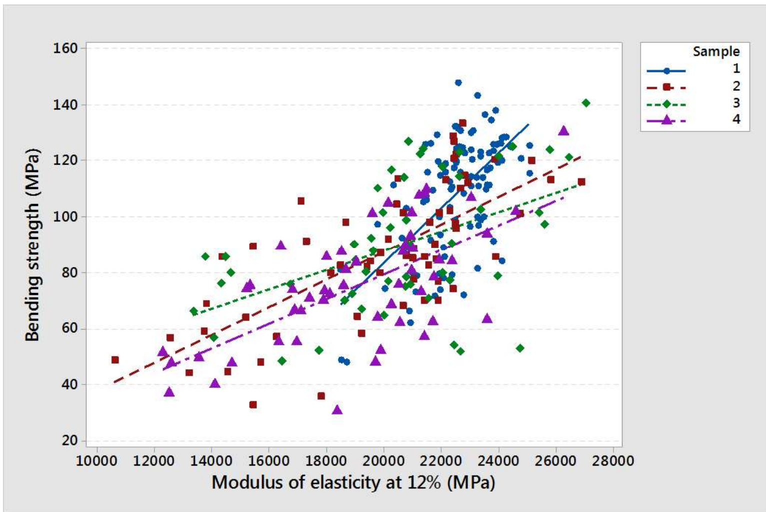

Figure 5.3: Adjusted bending strength vs. Adjusted modulus of elasticity (sample 7-10 in the second group)

Table 5.3: R^2 of Adjusted Bending strength vs. Adjusted modulus of elasticity (sample 7-10 in the second group)

Sample	1	2	3	4	All
R^2	0.36	0.5	0.22	0.42	0.46

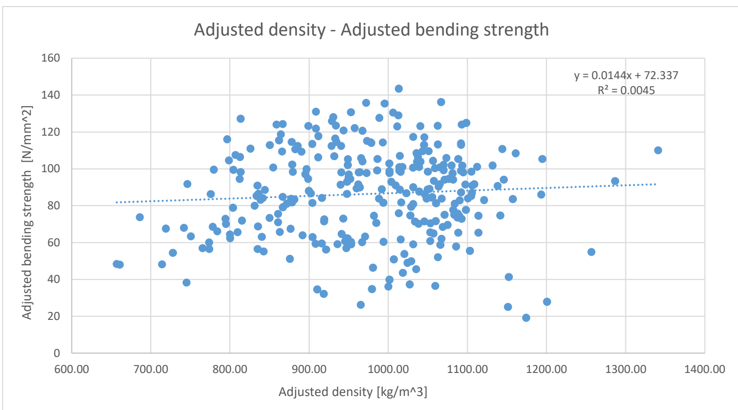

Figure 5.4: Adjusted bending strength vs. Adjusted density (sample 1-6 in the first group)

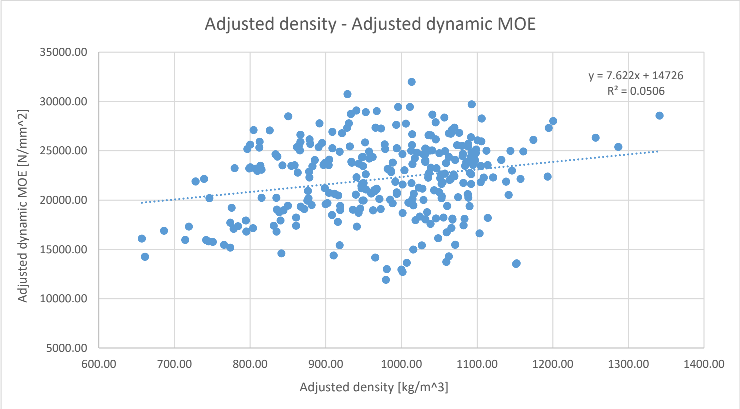

Figure 5.5: Adjusted modulus of elasticity vs. Adjusted density (sample 1-6 in the first group)

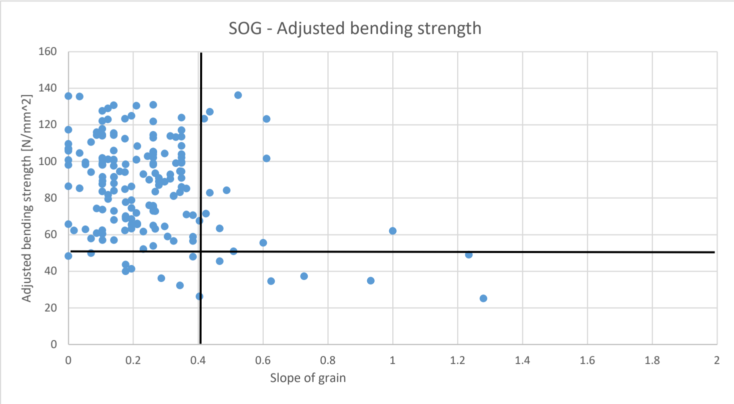

Figure 5.6: Adjusted bending strength vs. Adjusted slope of grain after test (sample 3-6 in the first group)

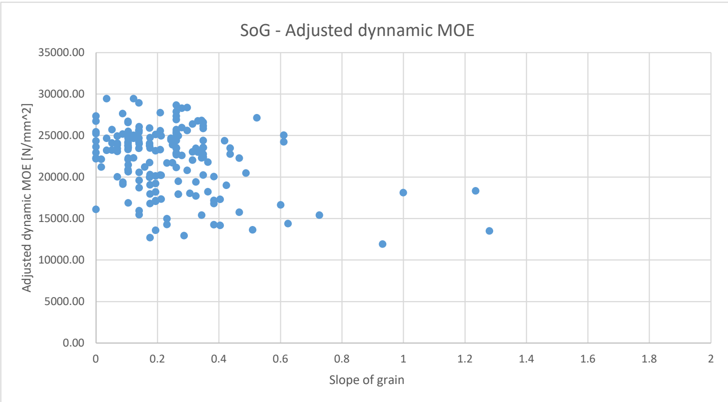

Figure 5.7: Adjusted modulus of elasticity vs. Slope of grain of after test (sample 3-6 in the first group)

5.2. Theoretical derivation of slope of grain

According to section 5.1, the threshold of the slope of grain could be adjusted to 0.4 from the statistical perspective for higher classification. From a mechanical point, this number needs further proof. It is clear that bending strength has a relatively good correlation with the modulus of elasticity and both mechanical properties are influenced by the slope of grain to a different extent. However, the system of the real slope of grain measurement is still imperfect. Thus, under this circumstance, the theoretical slope of grain is more informative and might provide a better insight into the threshold of slope of grain. Through rewriting the Hankinson formula where constants and density values are derived by non-linear regression analysis, see formula 5.1, the theoretical grain angle in radius could be calculated according to the formula 5.2 with inputting the bending strength and the density[30].

$$f_{m,\alpha} = \frac{(\rho C_1)}{(C_3 - 1)\sin^2(\alpha) + 1} \tag{5.1}$$

$$\sin^2(\alpha) = \left[\frac{(\rho C_1)}{f_{m,\alpha}} - 1\right]\frac{1}{(C_3 - 1)} \tag{5.2}$$

$$\text{Slope of grain } = \tan\alpha \tag{5.3}$$

Where: $\rho = 982$, $C1 = 0.12$, $C3 = 27.8$ [30]

The theoretical grain angle of sample 3–6 of the first group from the dataset with actual density and bending strength could be calculated based on the formula 5.2. By the transformation of the trigonometric function Eq.5.3, the theoretical slope of grain comes out in Fig. 5.8 in orange dots.

Fig.5.8 shows that, in light of the theoretical Hankinson, 0.3 slope of grain corresponds to $40N/mm^2$. The theoretical slope of grain up to 0.3 could make the dataset pass the D50 in terms of the 5-percentile characteristic value. Compared to the slope of grain measured after the test in Fig.5.6, the theoretical slope of grain is less scattering and concentrates alone on the theoretical Hankinson formula curve. The difference between the two types of the slope of grain could be caused by the difficulty of measurement which might be interfered with the interlocked grain. Moreover, the theoretical formula does not fully capture the effect of 3D fiber orientation, which could also contribute to the difference[30]. Therefore, in this assessment, in the consideration of safety reason, compared to 0-0.4, 0-0.3 is a reasonable range for the threshold of the slope of grain for higher classification in structural size.

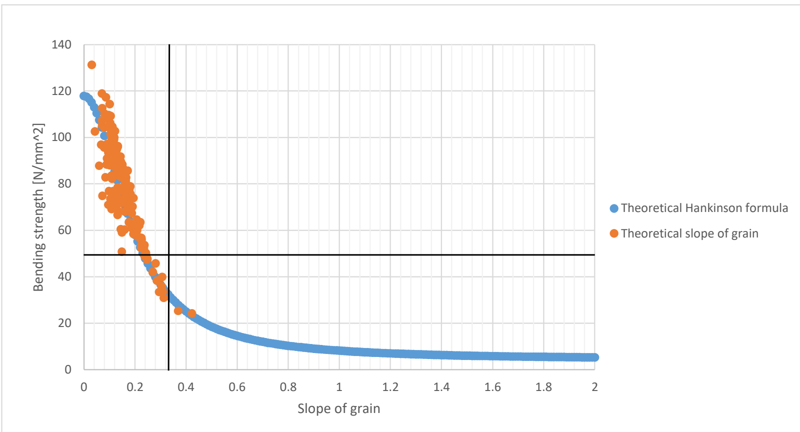

Figure 5.8: Bending strength against the theoretical slope of grain for 4 samples of Okan and the theoretical Hankinson drawn according to formula 5.1[30]

5.3. Influence of moisture content

The previous investigation shows the fiber saturation point of Okan is around 25%. Basically, above the 25% m.c., the environment is considered as 'wet' condition. In this section, the first group data was studied. Scatterplot 5.9 and 5.10 shows, with the change of moisture content, the range of mechanical properties barely has fluctuation. Moreover, there is no clear linear correlation between density and bending strength nor dynamic modulus of elasticity with $R^2 < 0.05$, see Fig.5.11 and Fig.5.12. Only a slight positive relationship could be observed. There is no denying the fact that, those data are not from experiments intended to figure out the correlation between moisture content and mechanical properties. Thus, those beams from different resources with different degrees of missing information might bring inaccuracy in this assessment.

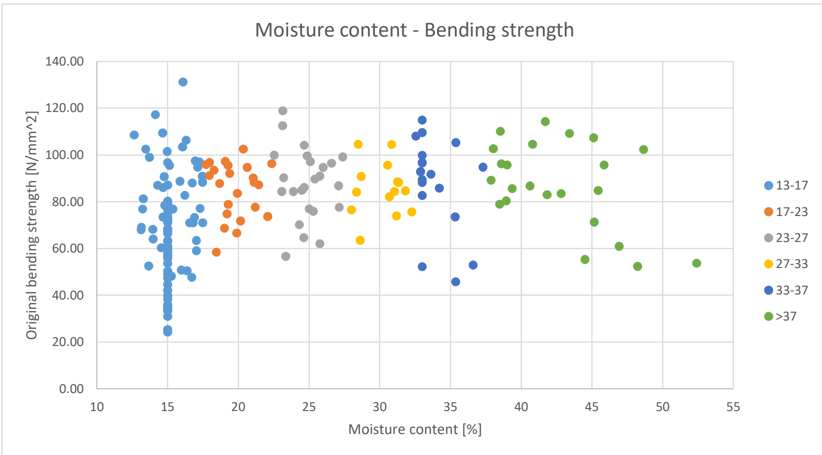

Figure 5.9: Moisture content vs. Original bending strength with grouping

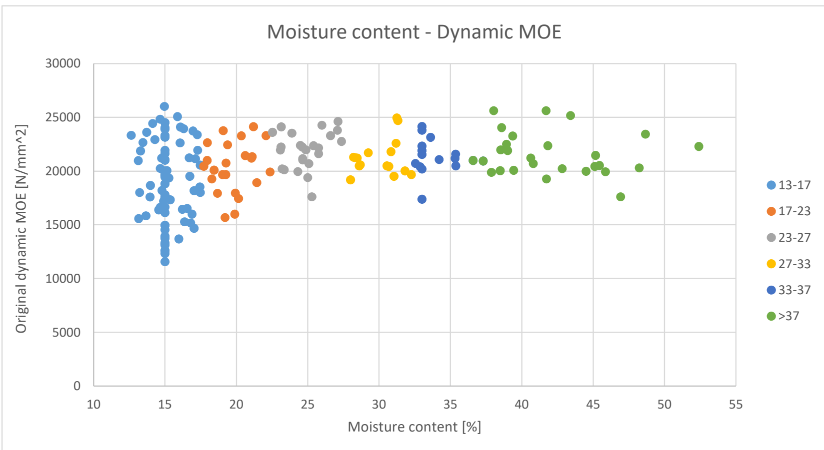

Figure 5.10: Moisture content vs. Original dynamic MOE with grouping

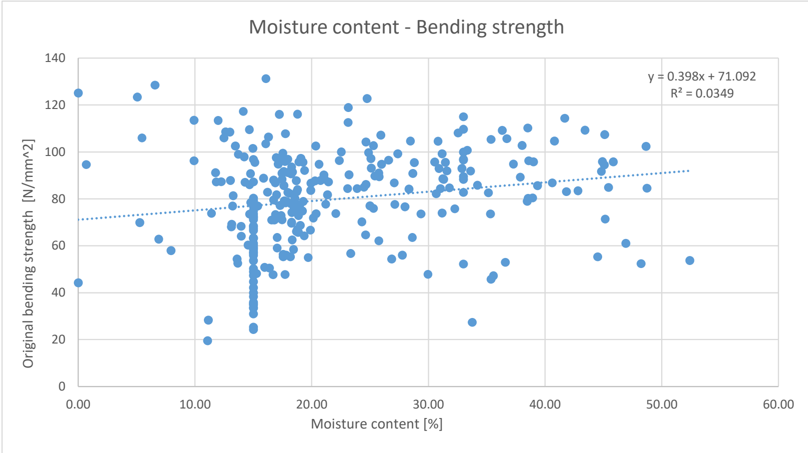

Figure 5.11: Moisture content vs. Original bending strength

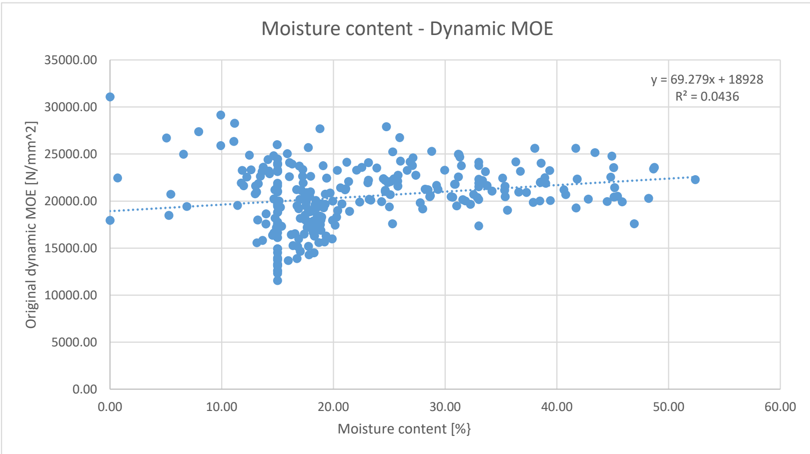

Figure 5.12: Moisture content vs. Original dynamic MOE

5.4. The 5th percentile characteristic values of Okan based on available dataset

In Chapter 4, a statistical method to determine the 5^{th} percentile value is elaborated. In this section, characteristic values were firstly calculated by the method[27] introduced in Section 4.4, based on the first group data. Okan could be assigned to **D35** with $37.12N/mm^2$ bending strength. Apparently, the weakest sample determines the final grading resultant. The detailed computational process of population value could be checked in Appendix A.

According to EN384 Clause 5.5.2[23], all data was manipulated. The final mechanical and physical characteristic values shows in Tab.5.4. For the sake of missing data in some samples, the non-parametric method was applied to all data (samples 1 to 10), see Tab.5.5. Only first group data (samples 1 to 6) was calculated by the parametric method, see Tab.5.6. **D35** is determined with $37.12N/mm^2$ bending strength for the non-parametric method for the population, see Tab.5.4. **D30** is determined with $32.30N/mm^2$ bending strength for the parametric method for the first group.

Table 5.4: Characteristic value

Characteristic value							
	Sample	Strength class	$1,2f_{05,i,min}$	$\frac{\sum_{i=1}^{ns} n_i f_{05,i}}{n}$	kn	f_k	Strength class requirement
Non-parametric method	1 to 6	**D35**	37.12	47.90	1.00	**37.12**	35
			$1,1\bar{E}_{i,\mathrm{min}}$	$\frac{\sum_{i=1}^{ns} n_i \bar{E}_i}{n}$	kn	$E_{0,\mathrm{mean}}$	Strength class requirement
			20435	22147.00	1.00	**21507**	10100
			$1,1\rho_{05,i,\mathrm{min}}$	$\frac{\sum_{i=1}^{ns} n_i \rho_{05,i}}{n}$	kn	ρ_k	Strength class requirement
			786	842.00	1.00	**786**	540
	Sample	Strength class	$1,2f_{05,i,min}$	$\frac{\sum_{i=1}^{ns} n_i f_{05,i}}{n}$	kn	f_k	Strength class requirement
Non-parametric method	1 to10	**D35**	37.12	51.92	1.00	**37.12**	35
			$1,1\bar{E}_{i,\mathrm{min}}$	$\frac{\sum_{i=1}^{ns} n_i \bar{E}_i}{n}$	kn	$E_{0,\mathrm{mean}}$	Strength class requirement
			20435	21550.00	1.00	**20435**	10100
			$1,1\rho_{05,i,\mathrm{min}}$	$\frac{\sum_{i=1}^{ns} n_i \rho_{05,i}}{n}$	kn	ρ_k	Strength class requirement
			693	809.00	1.00	**693**	540
	Sample	Strength class	$1,2f_{05,i,min}$	$\frac{\sum_{i=1}^{ns} n_i f_{05,i}}{n}$	kn	f_k	Strength class requirement
Parametric method	1 to 6	**D30**	32.30	50.97	1.00	**32.30**	30
			$1,1\bar{E}_{i,\mathrm{min}}$	$\frac{\sum_{i=1}^{ns} n_i \bar{E}_i}{n}$	kn	$E_{0,\mathrm{mean}}$	Strength class requirement
			20435	22147.00	1.00	**21507**	9200
			$1,1\rho_{05,i,\mathrm{min}}$	$\frac{\sum_{i=1}^{ns} n_i \rho_{05,i}}{n}$	kn	ρ_k	Strength class requirement
			723	792.00	1.00	**723**	530

*Strength in N/mm^2, Dynamic MOE in N/mm^2 Density in kg/m^3

Table 5.5: Basic test data by non-parametric method

Non-parametric method			Adjusted bending strength/ [N/mm^2]			Adjusted MOE/ [N/mm^2]		Adjusted density/ [kg/m^3]			Slope of grain		Knot ratio	
Sample	Source	Size	Mean	Cov	$f_{05,i}$	**E-mean**	Cov	Mean	Cov	**rho05,i**	Mean	COV	Mean	COV
1	/	54	92.80	0.305	**38.29**	**24786**	0.138	960	0.146	**805**	\	\	\	\
2	Ghana	42	81.70	0.157	**59.51**	**19210**	0.098	962	0.084	**839**	\	\	\	\
3	Cameroon	44	60.20	0.303	**30.93**	**18577**	0.210	1043	0.053	**966**	0.337	0.688	0.081	0.536
4		50	77.70	0.227	**48.33**	**20338**	0.161	921	0.157	**714**	0.214	0.520	0.147	0.912
5	Gabon	48	103.90	0.191	**64.41**	**24703**	0.085	932	0.114	**799**	0.159	0.766	\	\
6		50	98.70	0.185	**71.85**	**24258**	0.086	1030	0.058	**948**	0.233	0.530	\	\
Total		**288**	**79.90**	**0.262**		**22147**	**0.176**	**973**	**0.118**		**0.227**	**0.692**	**0.089**	**0.688**
7	Cameroon	104	107.80	0.190	**67.70**	**22534**	0.060	1005	0.040	**915**				
8		62	87.10	0.270	**41.10**	**20005**	0.170	933	0.140	**630**				
9		53	89.50	0.260	**48.20**	**20566**	0.160	954	0.110	**678**				
10		52	75.20	0.280	**35.60**	**19118**	0.160	951	0.090	**758**				
Total		**559**	**89.70**			**21550**		**971**						

Table 5.6: Basic test data by parametric method

Parametric method			Adjusted bending strength/ [N/mm^2]			Adjusted MOE/ [N/mm^2]		Adjusted density/ [kg/m^3]		
Sample	Source	Size	Mean	Cov	$f_{05,i}$	E-mean	Cov	Mean	Cov	rho05,i
1	/	54	92.80	0.305	41.47	24786	0.138	960	0.146	707
2	Ghana	42	81.70	0.157	58.28	19210	0.098	962	0.084	813
3	Cameroon	44	60.20	0.303	26.92	18577	0.21	1043	0.053	941
4		50	77.70	0.227	45.61	20338	0.161	921	0.157	657
5	Gabon	48	103.90	0.191	67.7	24703	0.085	932	0.114	738
6		50	98.70	0.185	65.57	24258	0.086	1030	0.058	922
Total		**288**	**79.90**	**0.262**		**22147**	**0.176**	**973**	**0.118**	

*The characteristic value is defined as: -for the bending strength the 5% fractile at 12% m.c., 150mm; - for the MOE the mean value at 12% m.c., 150mm; -for the density the 5% fractile at 12% m.c., 150mm

5.5. The 5th percentile characteristic values from different regions

Those samples from the existing dataset grew up in West Africa but different regions including Ghana, Cameroon, and Gabon whose locations are indicated in the Fig.5.13. From a botanical point of view, varying soil, climate, the natural environment could bring different results on the timber quality. The number of each region samples in the existing dataset are uneven, it is hard to conduct a rigorous derivation that which region has the best Okan growing environment. Besides, the timber quality also associated with the forest environment which might vary a lot even in the same region.

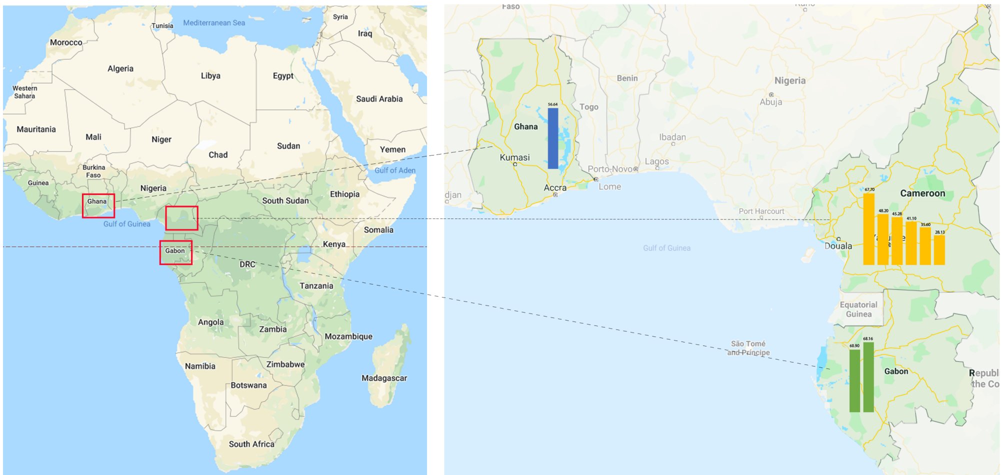

Figure 5.13: Sources of Okan in existing dataset

In this section, only a rough conclusion with respect to regions is given. However, the conclusion just gives out insight and does not mean the timber quality has an absolute relationship with regions. Fig.5.14 presents the 5-percentile characteristic value of adjusted bending strength distribution among the three countries mentioned above. According to NEN-EN 384[23] 5.5.2, The highest bending strength, up to D55, occurs in samples from Gabon. In the existing dataset, Cameroon sample has the lowest stiffness batch which just satisfies the D35. In the first group data, the average value of the population excluding sample 1 (sample 1 does not have region information) is 50.19 N/mm^2. Cameroon samples are below the average level with a large deviation. By contrast, Ghana's sample is slightly higher than the average value, but its sample number is too limited to represent Ghana and could be assigned to D40. There are 2 samples from Gabon, both meeting the standard requirement, namely D40, even reaching up to D55. Roughly speaking, Gabon tends to have a relatively high bending strength level with an average value of 68.13 N/mm^2.

In conclusion, with regard to Okan batches from a particular source, the higher class could be achieved instead of D30-D40.

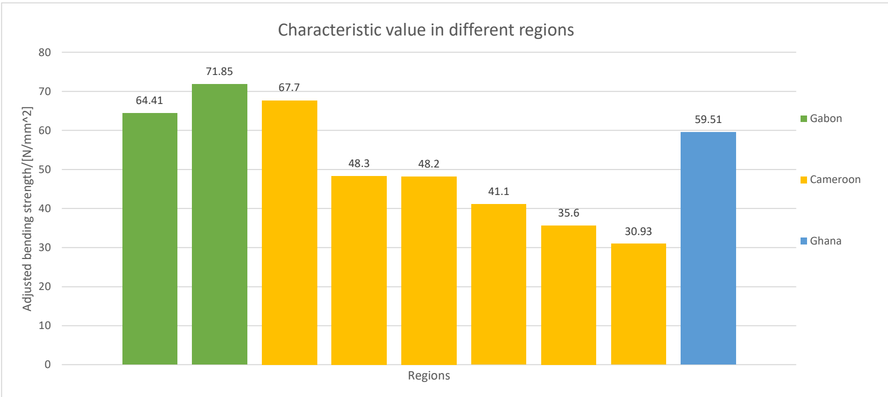

Figure 5.14: 5-percentile characteristic value in different African regions

* Calculated based on non-parametric methods

5.6. The 5th percentile characteristic values after screening

The above outcome of characteristic value is the first-hand experimental data and reflects all Okan samples' properties only with pre-selection but without proper screening and classification of their source, producers, etc. To verify the significance and economical efficiency of visual inspection during grading, the failed samples were selected out before calculating characteristic value.

According to NEN5493[20], compression failure is not permitted[20]. Sample 1 was analyzed with screening out samples with compression failure. Moreover, in section 5.1 and section 5.2, it is mentioned that to achieve a higher class, the slope of grain limitation could be promoted to around 0.3-0.4. In this section, the failed sample is defined as the slope of grain is above 0.3, conservatively, for sample 3,4,5,6 (sample number could be checked in Tab.5.1). In Tab.5.7 and Tab.5.8, 0.3 for the threshold of the slope of grain and the 0.2-knot ratio was set.

Compared sample 1 in Tab.5.9 to Tab.5.6 and Tab.5.5, after removing compression failure samples, all indicators have dramatic improvements. In Tab.5.6 and Tab.5.5, it is easy to find out, sample 3 is the governing sample for the Okan population, which determines the final first group data's characteristic value. The same circumstance happens in samples 3 to 6. That phenomenon makes the characteristic before and after screening comparable. After enhancing the slope of grain threshold to 0.3, the Okan could be assigned to **D45** instead of D35 in terms of the non-parametric method and **D35** instead of D30 in terms of the parametric method. Furthermore, the large portion of statistical indicators in light of covariance has a slight improvement as well. In other words, the scattering of those samples drops.

Theoretically speaking, the proper screening process gives better classification outcome but also sacrifice the pass rate in practice. In the following assessment, threshold 0.3 will be applied to analyze the grading procedure.

Table 5.7: Characteristic values of Sample 3,4,5,6 data after screening at 0.3 slope of grain by non-parametric method

Non-parametric method			Adjusted bending strength/[N/mm^2]			Adjusted MOE/[N/mm^2]		Adjusted density/ [kg/m^3]			Slope of grain		Knot ratio	
Sample	Failed Ratio	Size	Mean	Cov	$f_{05,i}$	E-mean	Cov	Mean	Cov	rho05,i	Mean	Cov	Mean	Cov
3	0.32	30	64.91	0.240	**39.88**	19565	0.202	1050	0.044	**966**	0.184	0.346	0.083	0.575
4	0.24	38	80.49	0.220	**56.92**	20606	0.154	929	0.154	**686**	0.158	0.373	0.069	0.011
5	0.15	41	103.95	0.200	**62.92**	25014	0.083	925	0.106	**796**	0.121	0.644	\	\
6	0.3	35	94.69	0.200	**64.89**	24098	0.093	1032	0.060	**941**	0.18	0.569	\	\
Total	**0.25**	**144**	**87.37**	**0.270**		**22493**	**0.163**	**978**	**0.115**		**0.156**	**0.530**	**0.081**	**0.542**
Characteristic value														
Strength			$1,2f_{05,i,min}$	47.86	$\frac{\sum_{i=1}^{ns} n_i f_{05,i}}{n}$		57.02	kn	0.95	f_k	**45.47**	**D45**		
MOE			$1,1\bar{E}_{i,\min}$	21522	$\frac{\sum_{i=1}^{ns} n_i \bar{E}_i}{n}$		22967	kn	0.97	$E_{0,\text{mean}}$	**22967**			
Density			$1,1\rho_{05,i,\min}$	755	$\frac{\sum_{i=1}^{ns} n_i \rho_{05,i}}{n}$		838	kn	0.97	ρ_k	**813**			

Table 5.8: Characteristic values of Sample 3,4,5,6 data after screening at 0.3 slope of grain by parametric method

Parametric method			Adjusted bending strength/[N/mm^2]			Adjusted MOE/[N/mm^2]		Adjusted density/ [kg/m^3]			Slope of grain		Knot ratio	
Sample	Failed Ratio	Size	Mean	Cov	$f_{05,i}$	E-mean	Cov	Mean	Cov	rho05,i	Mean	Cov	Mean	Cov
3	0.32	30	64.91	0.240	**32.50**	19565	0.202	1050	0.044	**943**	0.184	0.346	0.083	0.575
4	0.24	38	80.49	0.220	**45.40**	20606	0.154	929	0.154	**642**	0.158	0.373	0.069	0.011
5	0.15	41	103.95	0.200	**63.30**	25014	0.083	925	0.106	**730**	0.121	0.644	\	\
6	0.3	35	94.69	0.200	**56.60**	24098	0.093	1032	0.06	**908**	0.180	0.569	\	\
Total	**0.25**	**144**	**87.37**	**0.270**		**22493**	**0.163**	**978**	**0.115**		**0.156**	**0.530**	**0.081**	**0.542**
Characteristic value														
Strength			$1,2f_{05,i,min}$	39.00	$\frac{\sum_{i=1}^{ns} n_i f_{05,i}}{n}$		50.53	kn	0.95	f_k	**37.05**	**D35**		
MOE			$1,1\bar{E}_{i,\min}$	21522	$\frac{\sum_{i=1}^{ns} n_i \bar{E}_i}{n}$		22967	kn	0.97	$E_{0,\text{mean}}$	**22967**			
Density			$1,1\rho_{05,i,\min}$	706	$\frac{\sum_{i=1}^{ns} n_i \rho_{05,i}}{n}$		794	kn	0.97	ρ_k	**684**			

Table 5.9: Characteristic values of Sample 1 after removing compression failure samples

Deleting compression failure			Adjusted bending strength/ [N/mm^2]			Adjusted MOE/ [N/mm^2]		Adjusted density/ [kg/m^3]		
Sample	method	Size	Mean	Cov	$f_{05,i}$	**E-mean**	Cov	Mean	Cov	rho05,i
1	Non-parametric	44	103.20	0.179	**59.28**	24960	0.135	969	0.141	**941**
1	Parametric				**88.83**					**969**

5.7. Conclusion

1. The regression coefficient between basic data and the mechanical parameter is not very high (<0.5). One possible reason is different samples had different visual inspection precision, which makes samples are incomparable.
2. The linear regression result of modulus of elasticity and bending strength is more preferable than density and bending strength.
3. From those data, there is a statistical relationship between the moisture content and bending strength, but the correlation is blurring and hard to conclude from an existing dataset. The customed experimental procedure is needed for further study.
4. Proper pre-visual inspection can mitigate the negative influence of low tile samples and scattering. Therefore, there is room for promoting the limitation of the slope of grain in order to have a more fitting and economical model.
5. The dataset after screening out shows the D35-D45 grading result compared to D30-D35 from original dataset, meaning that it is possible to grade specific batch more economically when narrowing down the Okan source with adequate samples and applying proper visual grading process.

6

Laboratory testing procedure

6.1. Non-destructive testing

Before conducting the destructive experimental testing, some pre-processing work and preparation need to be done. Thanks to producer, testing timber was **sawn, preselected and planned** properly. Thus, concisely, there are three steps to follow for now. First of all, according to plan, testing timber is suppose to be **divided into two groups**, namely wet and dry group. To achieve the high moisture content for the wet group setting, half of those materials were **conditioned** in a wet chamber room with 20 degree Celsius (± 2) and a relative humidity of 65% (± 5). Then, after **numbering and marking** all beams, physical properties (including weight, dimension, moisture content, dynamic modulus of elasticity) and strength-reducing properties (including knots, slope of grain, fissures, wane, distortion and compression failure, etc.) should be **measured and assessed**. Some equipment needs to be **calibrated** beforehand. Table 1 lists the necessary tools for basic parameter measurement. All of the data(including destructive testing data) are recorded in the Table shown in Appendix B.

6.1.1. Numbering and marking

Group number: To discriminate the dry group from the wet group, the label Dxx indicates the dry group timber and the label Wxx indicates the wet group timber. The label of dry group timber goes from D1 to D30 and the label of wet group timber goes from W31 to W60.

Beam face: A beam consists of six faces and numbered A through F. An indication is shown in the below figure.

Figure 6.1: Indication of numbering

6.1.2. Measurement and assessment overview

Basic physical parameters and their corresponding measuring tools are shown in the below table. For more accurate results, dimensions and moisture content should be recorded as the average of three separate measurements taken at different positions on the length of each piece.[23] Each parameters' measurement details are articulated in the following sections.

According to EN1309-3[26], the strength-reducing properties measurement will be carried out.

Table 6.1: Parameters and measurement tools

Parameters	**Tools**	**Remark**	**Measurement error**
Weight	Electronic scale		0.001kg
Dimensions	Tape measure – length	Length	1.0mm
	Vernier capiler – height & width	Width / Height	0.01mm
Moisture content-ω	Capacitance moisture meters	Calibration before testing	
	Oven dry method		
Eigenfrequency-f_e[Hz]	Brookhuis © MTG handheld timber grader		
Density	Weight/volume		

6.1.3. Knot

Knot, defined as the portion of a branch embedded in wood referring to NEN-EN 844-9, in sawn timber will be quantified in terms of their position, size, and shape. In this thesis, size is formulated according to EN1309-3[26] clause 5.1.1 as a percentage of a dimension of the surface where the knot occurs or in millimeters.

Several related symbols are defined as follows:

d: the size, in millimeters;

a: the width on the minor axis, in millimeters;

b: the width on the major axis, in millimeters.

Forms of knots are various, but basically, the size could be indicated as the arithmetic average value of minor axis (a) and major axis (b) of the knot, which could be formulated as d=(a+b)/2. The knot ratio, according to the literature [27], is indicated as follows Eq.6.1:

$$\text{Group knot ratio } (\mathrm{GKR}) = \max\left(\frac{d_1 + d_2 + \cdots + d_i}{2\hbar + 2t} \text{ over } 150\mathrm{mm} \text{ length}\right) \tag{6.1}$$

6.1.4. Determination of growth ring angle

Different from temperate trees, in tropical areas, some tropical hardwood including Okan don't experience extreme seasonal variation like the transition between spring and summer. However, those kinds of trees do have their own grow ways happen via seasonal changes, like rainy seasons versus dry seasons. Usually, under tropical climate, trees could manage to create a dozen very thin rings without a certain tendency. Another special property of Okan is the interlocked grain caused by trees growing with grain with spiral-like circling the trunk[1]. Consequently, the growth ring structure is indistinct and hard to distinguish them layer by layer with naked eyes[5].

In this section, observed in the transverse direction, even though the boundary of the growth ring layer is blurring, the rough orientation patterns still could be identified by naked eyes, see Fig.6.2. Therefore, the growth ring is defined as the angle between the tangent line of the ribbon stripe and edge side in the bottom face see Fig.6.3. In this measurement, the growth ring angle is denoted as θ. Because the E/F faces have checks and rough saw notch, it is more convenient to use an angulometer to measure them manually.

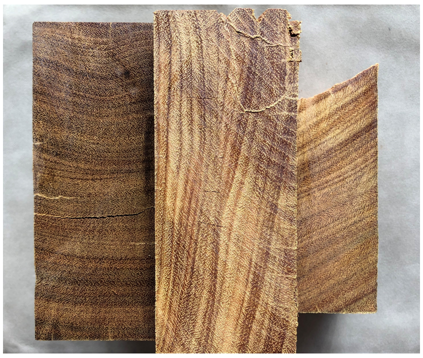

Figure 6.2: Cross-sections of Okan beams

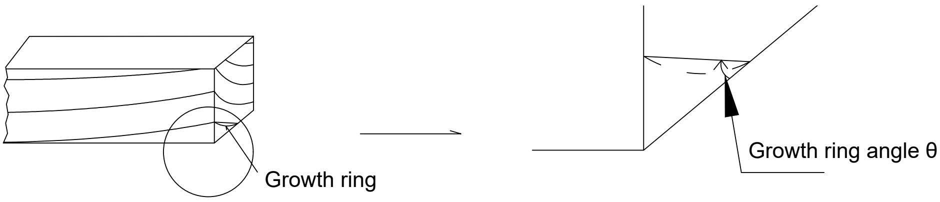

Figure 6.3: Angle ring orientation indication

6.1.5. Determination of SOG by manual check based on image processing

In this and the following section, two new methods based on image processing technology are proposed and articulated.

The slope of grain, defined as divergence of the direction of the fiber from the longitudinal axis of the piece according to NEN-EN 844-9, is derived from the x/y and expressed as a ratio[25]. Usually, recording the slope of grain always comes with human error, to decrease which, a scribe is used to assist the location of the slope. Several related symbols are defined as follows and a corresponding indication shows in Fig.6.4. However, it is important to be aware of that this method might ignore some local fiber deviations for structural size beams when measuring the slope of grain.

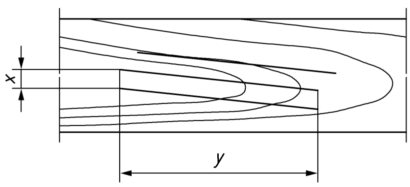

Figure 6.4: The slope of grain formula indication

where:

x: the deviation of the grain, in millimeters;

y: the length over which the measurement is taken, in millimeters.

Apart from the above-mentioned method which is the only approach regulated in the current standards, several systems, including tracheid effect, microwave measurement, electrical field strength measurement, and image analysis technique, are widely used for grain angle determination of softwood and European softwood, which could offer some associated reference[10]. Among four non-destructive methods, except the outcome of the image analysis technique, the remaining three approaches could barely guarantee the precision and certainty on grain angle of tropical hardwood species for the sake of lacking data to back. As for the image analysis technique, it relies on the geometrical input instead of mathematical transformation based on other physical parameters, which is corresponding to current standards[10].

In practice, the inaccuracy of grain angle determination has to be attributed to the subjective factor (naked-eye inspection error) and objective factors (uneven grain pattern, interlocked grain, existence of local grain in the vicinity of knots, and 3D effect, etc.)

To overcome subjective factor in the grain angle determination process that, especially, the human eyes cannot distinguish the grain pattern from the surrounding fiber, and promote the efficiency in the lab, the half-automated analysis based on image processing comes into play. Diagram 6.5 presents the workflow of the grain angle determination taking the beam NO.3 as an example.

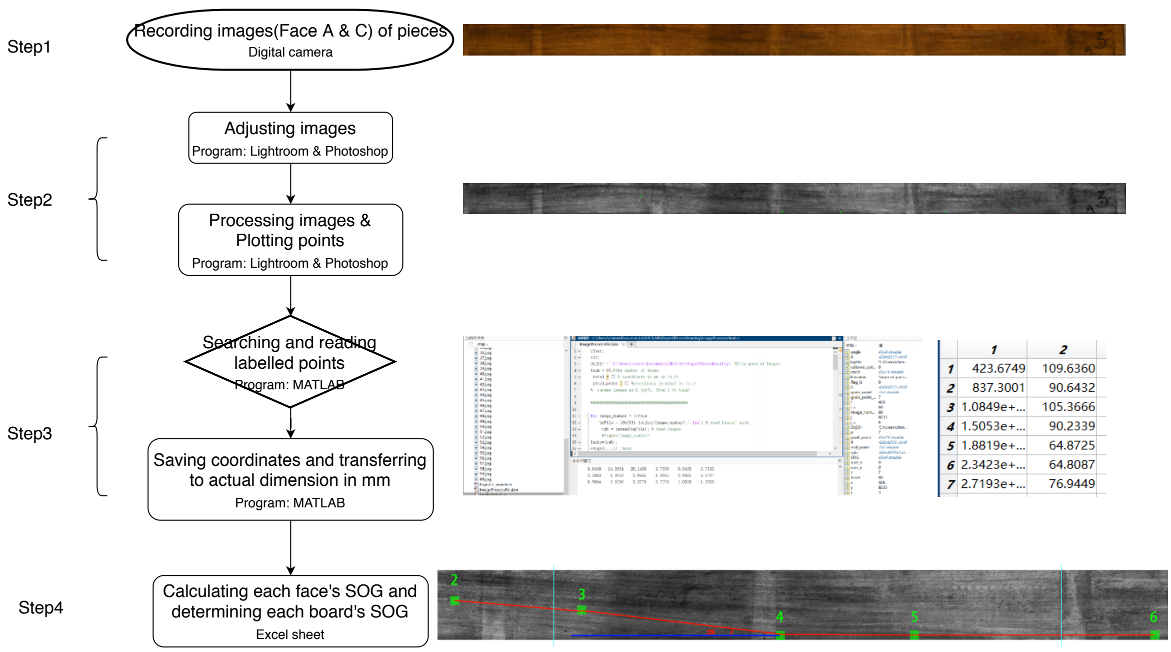

Figure 6.5: workflow of determination of SOG

- **Step1: Capturing the image of the beam.**

  Devices applied in the capturing process include a camera, tripod and marking tools. The Canon EOS 5DS lens was used to capture images. All four faces of the timber beams were photographed labeled as beam number *-A (B, C, D)*, for example, *15A*, see Fig.6.6.

Figure 6.6: Preliminary image of face A of a beam

- **Step2: Processing of the images**

  Those images were processed by the program *Lightroom* for problems caused by lens distortion. To better identify and quantify the grain in the image, those images were **cropped** to beam size and **adjusted to black and white**. Black and white picture is more naked-eyes friendly for distinguishing grain direction. The green dots in Fig.6.7 were **plotted** conservatively along the course of the grain over the entire length manually and subjectively by *Photoshop*. Two adjacent dots could describe one small area's grain orientation. To make the results more precise in the *Matlab*, the dot size is quite small with 10 to 20 pixels. For the reason that in this experiment set-up, the bending crack most likely happens in the mid-span where dots would be more concentrated than the two sides, the slope of grain of large portion of beams would be determined according to the mid-span dots of face A and C.

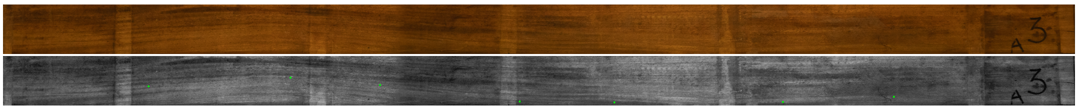

Figure 6.7: The course of grain plot

- **Step3: Processing of the data**

  The position of those dots would be **searched and read** by MATLAB and output in the form of coordinate in pixel. The principle behind it is that the *imread()* function could read image data in forms of RGB value from graphics files (.jpg format) into MATLAB workspace. The green dot has different RGB composition from black and white background characterized by R=G=B, according to which, each green dot's position is identified and located by reaching every pixel point of this image. Then, the coordinates in pixel of all green dots would be **transferred** proportionally into millimeters according to the real size of the beam which would be written into the excel sheet. The calculation of transfer use Eq.6.2 - Eq.6.3. It is important to note that, in the proportional transfer process, beam size is assumed as 3005mm * 150mm * 60mm. The MATLAB code of this process is presented in Appendix C.

$$x_m = \frac{\text{Length}_{m\_\text{Xtotal}}}{\text{Length}_{p\_,\text{Xtotal}}} * x_p \quad (6.2)$$

$$y_m = \frac{\text{Length}_{m\_\text{Ytotal}}}{\text{Length}_{p\_\text{Ytotal}}} * y_p \quad (6.3)$$

x_m: the actual x coordinate in millimeters

y_m: the actual y coordinate in millimeters

x_p: x coordinate in pixel

y_p: y coordinate in pixel

$Length_{(m\_Xtotal)}$: The actual total length of the beam in x-direction which is 150mm.

$Length_{(m\_Ytotal)}$: The actual total length of the beam in y-direction which is 3005mm.

$Length_{(p\_Xtotal)}$: the total length of the beam in x-direction in pixel.

$Length_{(p\_Ytotal)}$: the total length of the beam in x-direction in pixel.

- **Step4: Calculating the slope of grain**

  Based on the NEN-EN 1309-3[26], the principle behind the measurement is finding out the deviation of the grain, indicated as x in millimeters and the length over which the measurement is taken, indicated as y in millimeters. Then the result is expressed as a proportion by the formula x/y, see Section.6.1.5. In this case, the same principle is applied by identifying the coordinates of each dot in the MATLAB.

  For the majority of beams, seven dots were plotted, three in the mid-span and two on each side, respectively, which almost could cover the whole length slope course. The large portion of timber beams could be classified into two types. One is the slope of grain grows in one single direction in the mid-span, either going upwards or going downwards, the maximum slope could be regarded as the slope of grain. The other one case is that the grain slope goes down and up, showing as a wavy line, the maximum absolute value is determined as the slope of grain of this beam. The following formula Eq.6.4 shows the logic based on the indication in Fig.6.8.

  To avoid wrong judgment, those data are recorded and documented digitally. if the failure does not happen in the mid-span, the grain in other locations could still be rechecked.

$$\text{The slope of grain } = \max\left[\frac{x2-x3}{y2-y3}|,|\frac{x3-x4}{y3-y4}|,|\frac{x5-x6}{y5-y6}|,|\frac{x6-x7}{y6-y7}|\right] \tag{6.4}$$

xi: the x-coordinate of the point i

yi: the y-coordinate of the point i

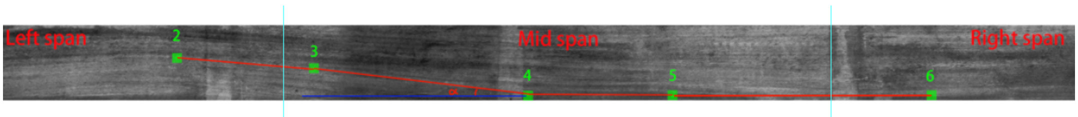

Figure 6.8: The indication of slope of grain

Reflection

- Advantages

1. All images' information is documented digitally and is easy to check anytime.
2. The image processing method is naked-eyes friendly. When plotting the dot, the image could be zoomed in to improve the identification of grain orientation, which is constrained by naked eyes.
3. There is no one-by-one manual measurement in site which is time-consuming and infeasible in practice.
4. There is no error created during scribing and manual measurement.
5. The principle of this method still follows the NEN-EN 844-9[25] but has more mechanical meanings.

- Disadvantages & Constrains

1. This method is still manual check based on subjectivity and naked-eye judgment.
2. In Step 3, the beam size is assumed 3005mm * 150mm * 60mm, which is actually based on the in-site measurement. However, the size varies from beam to beam slightly, which might bring error.
3. There is no denying the fact that there are potentials to optimize the capturing process in terms of the machine and the set-up to decrease the image distortion and improve the pixel.

6.1.6. Determination of SOG by automation method

To enhance the efficiency of visual inspection and assessment process, the process of determination of SOG based on the image processing is possible to be optimized by automation. Automation fully relies on the image features, for example color information, lines, brightness, etc. to identify characteristics of objects, like pits, fibers without the assistance of naked eyes. The key point of the automation of visual inspection is to find the corresponding correlation between representative image features and object characteristics.

Several conclusions from previous researches with regard to the fiber direction recognition were drawn. Firstly, for Okan, a dominating crack develops along the corridors formed by fiber and growth rings together. Secondly, grain patterns at the wide face(A/C face) could be captured by digital devices, which is also slightly visible to the pure naked eye by distinguishing the color variance. Based on those conclusions, the strong indicator of estimation of fiber direction relies on the image information difference between useful information (fiber line) and extraneous surrounding image interference (the image information that does not represent fiber).

To sum up, the core question for this chapter is how to define and extract the image feature which could represent fiber line mechanically and distinguish the “useful information” and “extraneous information”.

6.1.6.1. Principle

Technical speaking, in image processing, The definition of ”feature” is that, a piece of information to tackle the computational task related to a certain application[7]. On that basis, feature descriptors function as a series of numerical “fingerprint” which is the medium to differentiate one feature from another by encoding interesting information[2] .

In this case, the HOG feature descriptor is used, which extracts and computes the distribution (histograms) of directions of gradients (orientated gradients) as features. The gradient calculation (Eq.6.5 & Eq.6.6) could help filter a lot of non-essential information (e.g.constant colored flat region). For color images, each pixel is equipped with three channels. The magnitude of gradients is the maximum of the magnitude of gradients among the three channels and the angle(θ) is in line with the angle of the maximum gradient. In Fig.6.9, the middle RGB patch in the red box illustrates the corresponding relation, in the form of the vector arrow, whose direction and length indicate the direction of the gradient and the magnitude, respectively. The right two boxes listed all raw numbers of gradient calculations of this patch.

For Okan, the magnitude of gradients at a pixel is large around edges, occurring crossing the constant flat region and fiber line, where abrupt intensity changes happen.

$$g = \sqrt{g_x^2 + g_y^2} \tag{6.5}$$

$$\theta = \arctan \frac{g_y}{g_x} \tag{6.6}$$

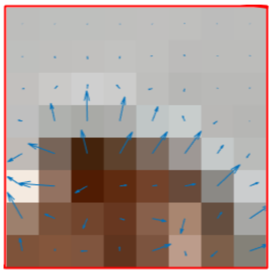

2	3	4	4	3	4	2	2
5	11	17	13	7	9	3	4
11	21	23	27	22	17	4	6
23	99	165	135	85	32	26	2
91	155	133	136	144	152	57	28
98	196	76	38	26	60	170	51
165	60	60	27	77	85	43	136
71	13	34	23	108	27	48	110

Gradient Magnitude

80	36	5	10	0	64	90	73
37	9	9	179	78	27	169	166
87	136	173	39	102	163	152	176
76	13	1	168	159	22	125	143
120	70	14	150	145	144	145	143
58	86	119	98	100	101	133	113
30	65	157	75	78	165	145	124
11	170	91	4	110	17	133	110

Gradient Direction

Figure 6.9: Indication of gradient magnitude and gradient direction[2]
(Notice that the direction of arrows points to the direction of change in intensity and the magnitude shows how big the difference is.)

Usually, a full image is divided into several patches to assure that the feature descriptor contains a compact representation. Each patch contains a certain amount of pixel values, each of which has two values, magnitude, and direction. The reason for the division is that, compared to calculating every single pixel's gradient, manipulation for a patch could make the output less sensitive to noise and more robust to noise. Abstracted from the above explanation, the total information values for every single patch is pixel number in one patch * channel numbers in each pixel (3) * two values (magnitude and direction). To archive that image information, X bins are created (here X = 9 is used as an example) in the histogram, which is corresponding to angles 0, 20, 40 … 160. The gradient magnitude values are assigned to each bin according to the gradient direction by weight, see Figure 6.10. To decrease the negative impact of lighting variations, normalization is done for removing the scale of the histogram. In this histogram, the angle corresponding to the maximum value is recorded, representing this orientation makes the biggest contribution within the histogram. In other words, in this direction, the gradient magnitude has the most intense change. Ideally, the edge directions, which, are the slope of grain directions in timber inspection, are normal to the gradient directions.

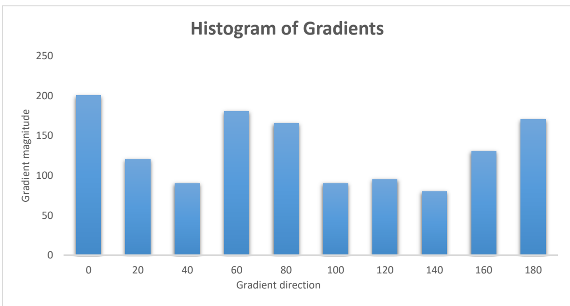

Figure 6.10: Histogram of Gradients

6.1.6.2. Image processing

To intensify the fiber edge and keep the image informative as much as possible, the color information is preserved, and the sharpen image is conducted. The margin of the beam is cropped out for the sake of site background noise.

Abstracted from the last section, the threshold of determination is the gradient magnitude change. Therefore, the precise outcome requests the input image has uniform brightness, a clear boundary between fiber and flat region, a clear surface without visible fungi, no water stain, and no dirt. For example, Figure 6.11 is not a suitable input for the sake of water stain and mold. Figure 6.12 was joined by two images with different brightness which might bring interference in terms of color information. To avoid the error introduced by noise and mitigate the inaccuracy, the patch with low Coefficient of Variation in terms of angle is removed.

Figure 6.11: Example of board with water stain and mold

Figure 6.12: Example of brightness problem

6.1.6.3. Judgment condition

After manipulation articulated in Section Principle 6.1.6.1 and Image Processing 6.1.6.2, an angle matrix comes out and indicates every patch's edge direction, see Fig.6.13. Plotting that matrix in the form of the line with angle displays the edge orientation, see Fig.6.14. Statistically, the angles of an image distribute normally, see Figure 6.15. Thus, from the global perspective, the middle region at the X-axis in the Angle – Number histogram, namely, the mode, could roughly represent the global slope of grain range. In this example, [-1,7] is the global slope of grain range.

Mechanically, the sensitivity to grain angle deviation varies from position to position determined by the loading effect. Diagrams 6.16 and 6.17 present the loading effect of the four-bending test. Given that each patch has its own properties, the difference between resistance and loading effect could be calculated. Resistance formula refers to Hankinson formula Eq.3.3. In the loading process, elastic-plastic behavior and pure elastic behavior can occur.[27] In either case, the compression side is more ductile and the critical crack more likely happens in the tension side. Even though, when a failure occurs, the neural axis is not the middle axis anymore and moves down a bit, to simplify the algorithm, the value of the difference between resistance and loading on the bottom half is kept and displayed as Fig.6.18. However, the diagram only could give an insight that the possible critical spot instead of quantifying the stress.

From the above, the conclusion is that the smaller difference between resistance and loading effect, the patch is more likely to fail in the beginning, the grain angle deviation in which is more important. Thus, the patch with a high difference of resistance and loading effect should be assigned with a high weight factor calculated as Eq.6.7. With the weight value, and the global slope of grain range is [1,9]. To obtain the local slope of grain the critical zone, the blue zone in Fig.6.18, and the surrounding area could be cropped and repeated the algorithm without considering the loading effect. For safety consideration, in the following chapters, the automation output is the highest grain angle within the critical zone output range.

All code could be check in Appendix D.

$$\text{Weight}(x,y) = \frac{\mathrm{Max}(\text{Delta}[]) - \mathrm{Delta}(x,y)}{\mathrm{Max}(\text{Delta}[]) - \mathrm{Min}(\text{Delta}[])} \tag{6.7}$$

where:

$Delta[]$: the matrix of difference between resistance and the loading effect

x, y: the coordination of patch

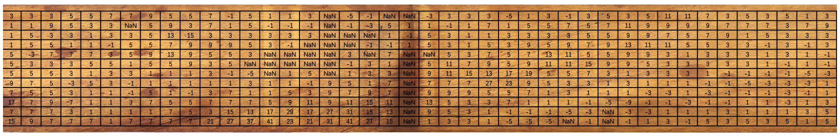

Figure 6.13: Image with its corresponding angle matrix

Figure 6.14: Visualization of edge direction

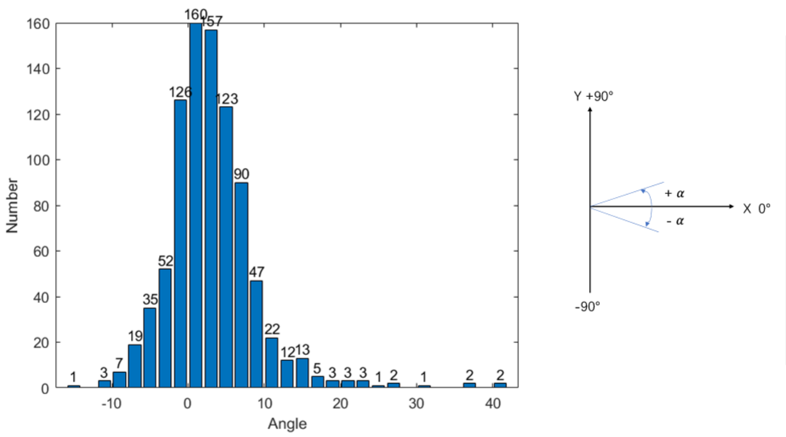

Figure 6.15: Histogram of angle distribution

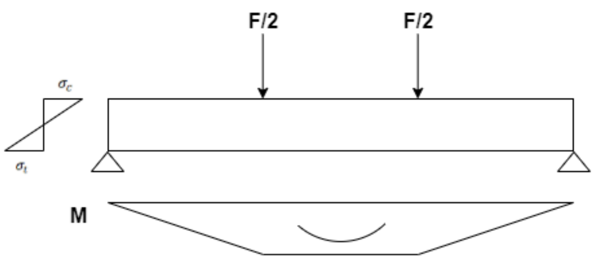

Figure 6.16: Schematic of loading effect of four-point bending test

Figure 6.17: Colored stress patterns of four-point bending test [negative sign indicates tension, positive sign indicates compression.

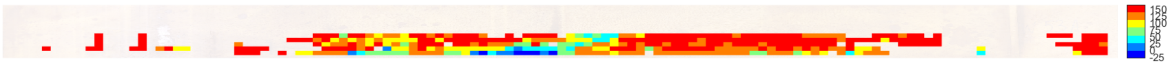

Figure 6.18: Rough indication of dangerous spots

6.1.6.4. Accuracy analysis

Thomas Ehrhart[10] proposed an automated visual method and the algorithm could identify the fiber direction clear with the black and white image information. The method proposed in this section could process images with color information and put the mechanical meaning to each small block. It could predict the most dangerous spot under different loading cases eventually.

However, this method is not applicable to all Okan timber beams and its accuracy is impacted by a few factors listed as follows.

Interlocked grain

The interlocked grain is a negative impact on the recognition. In a small block, fibers do not grow in a unified direction, see Fig.6.19, which brings deviation to the output. In this case, the algorithm can assess the dominant grain angle direction.

Figure 6.19: Interlocked grain example: flat cut sections of a piece of ipe[3]

Growth ring

Ideally, beams are produced by cutting parallel through the log, namely, plainsawn, see Figure 6.20. This cutting approach yields distinctive figures on the face of the beam, see Figure 6.21. Usually, the pattern caused by growth rings has relatively apparent color variation, which makes more contribution to the gradient magnitude. Therefore, the final output is closer to the pattern caused by growth ring's orientation, which deviates from the fiber direction.

Figure 6.20: Sawning method[4]

Figure 6.21: Features caused by plainsawn

3D deviation

In tangential- longitudinally face, the fiber goes with the longitudinal direction. However, when the cutting face is not parallel to the fiber direction plane, the 3D deviation between the face of the beam and fiber occurs.

Stain

Visible fungi, water stain, dirt, and other external substances could bring the noise to image identification.

6.1.7. Other strength-reducing properties

In the non-destructive measurement phase, those characteristics listed below will be recorded as well. All definitions refer to NEN 5493-2010[20] and NEN-EN 844-9[25].

1. Fissure, check: Longitudinal separation of fibers
2. Resin pocket: Fissure along a growth ring in which an excessive resin deposit, respectively calcium deposit, has taken place
3. Bark pocket: Small pieces of bark, overgrown completely during the thickness growth by the newly formed timber
4. Bore holes
5. Heart: Primary tissue around which the growth rings are formed
6. Compression failure: Fracture running through the timber perpendicular to the fiber direction
7. Wane: Natural rounded surface of a log still presents on sawn and/or processed timber
8. Fungal decay: Deterioration of timber caused by fungi
9. Sapwood: Outer zone of wood that, in the growing tree, contains living cells

6.1.8. Dynamic Modulus of Elasticity (MOE)

In practice, the more efficient and quicker dynamic MOE measurement in a non-destructive way has been widely applied based on the relationship between vibration and its corresponding response. In this thesis, this approach will be used for machine grading procedure. MTG handheld from Brookhuis Micro Electronics is going to be the tool for measuring the dynamic modulus of elasticity.

The principle is indicated in Fig.6.22. First of all, by a stroke, a longitudinal vibration is activated. Then, a vibration signal is accepted and analyzed by the sensor, see the signal in Fig.6.23 left image. Then the first natural frequency f_m (highest peak in the right image in Fig.6.23) is determined from a Fast Fourier Transformation(FFT). The dynamic MOE could be calculated by the Eq.6.8:

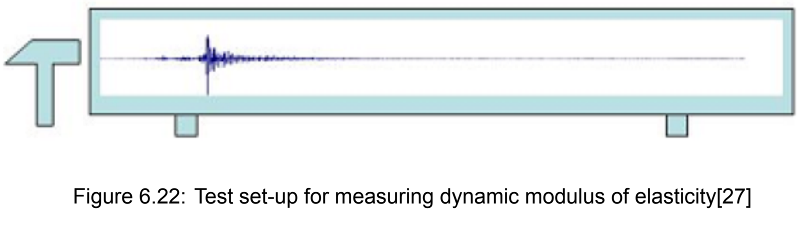

Figure 6.22: Test set-up for measuring dynamic modulus of elasticity[27]

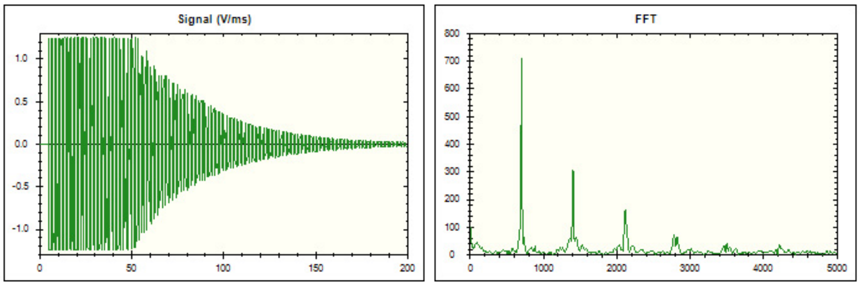

Figure 6.23: Diagrams of MTG handheld grader (left is the signal of the acceleration of a beam end in time, right is the FFT diagram)

$$E_{\mathrm{L}} = 4L^2 f_{\mathrm{m}}^2 \rho / m^2 \tag{6.8}$$

where:

E_L: longitudinal dynamic MOE $[GPa]$

L: length of timber $[m]$

f_m: longitudinal resonant frequency $[Hz]$

ρ: density $[kg * m^{-3}]$

m: the harmonic frequency, in this case, $m = 1$

6.2. Destructive testing

After recording all basic parameters and physical features by words and images, other mechanical and physical properties will be determined by the four-point bending test. This type of testing is prescribed in EN384[23]. In this section, more detailed mechanical parameters will be measured and checked including bending strength, MOEs, density and moisture content from the defect-free slice, the fiber orientation after failure and corresponding failure mechanism. During destructive testing, digital image correlation (DIC) will be included for a better understanding of the failure mechanism.

6.2.1. Bending strength test set-up

The test piece shall be symmetrically loaded and simply supported as shown in Fig.6.24. Besides, lateral restraint will be provided to avoid lateral buckling in two loading points. A small steel plate in a certain size inserted between the piece and the loading head (or support) is going to be applied for mitigating the local indentation. Load will be imposed at constant speed so that the failure happens within five minutes (±120s) under the maximum load (F_{max}).The bending strength could be determined by the Eq.6.9:

$$f_m = \frac{3Fa}{bh^2} \tag{6.9}$$

Several related symbols are defined as follows:

a: distance between a loading position and the nearest support in a bending test, in millimeters;

b: width of cross section in a bending test, or the smaller dimension of the cross section, in millimeters;

h: depth of cross section in a bending test, or the larger dimension of the cross section, or the test piece height in perpendicular to grain and shear tests, in millimeters;

F_{max}: maximum load, in newtons;

f_m: bending strength, in newtons per square millimeter

It is important to note that, in this step, only first-hand data without adjustment will be recorded, meaning that the bending strength is not going to be adjusted by the size effect and reference moisture content.

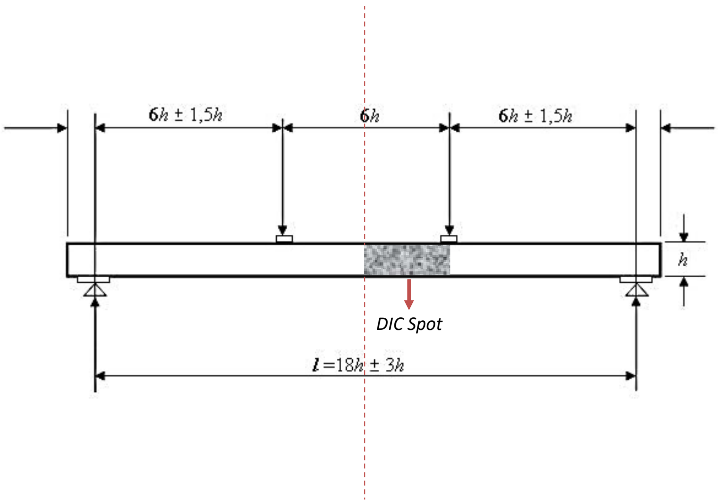

Figure 6.24: Test arrangement for measuring bending strength[24]

6.2.2. (Static) Modulus of Elasticity (MOE) measurement set-up

During four the bending test, the global and local modulus of elasticity could be calculated according to EN384[23]. It is the same as bending strength derivation that no size effect and moisture content adjustment will be expected in this section.

Local Modulus of Elasticity The principle of local modulus of elasticity derivation is based on the average deformation in a limited part, namely at the center of a central gauge. Corresponding load/deformation graph will be plotted and among this range, two points are picked out for regression analysis (see Fig.6.26). The measured deformation range is shown below(See Fig.6.25).

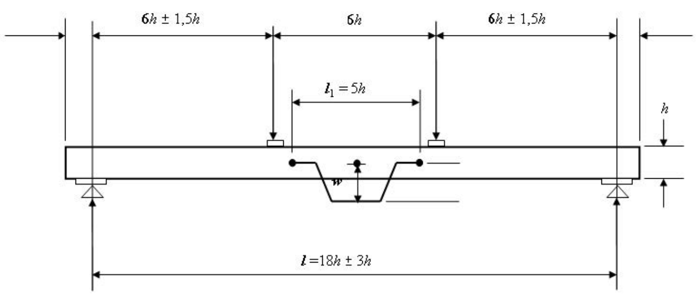

Figure 6.25: Test arrangement for measuring local modulus of elasticity in bending[24]

Local modulus of elasticity is formulated as follow Eq.6.10[24]:

$$E_{m,l} = \frac{a l_1^2 \,(F_2 - F_1)}{16I\,(w_2 - w_1)} \tag{6.10}$$

$F_2 - F_1$: an increment of load in newtons on the regression line with a correlation coefficient of 0.99 or better

$w2 - w1$: the increment of deformation in millimeters corresponding to $F_2 - F_1$

l_1: gauge length for the determination of modulus of elasticity or shear modulus, in millimeters

F_1 and F_2 usually happen between 0.1 to 0.4 maximum load which could be obtained either from appropriate existing test data or tests on at least ten pieces.

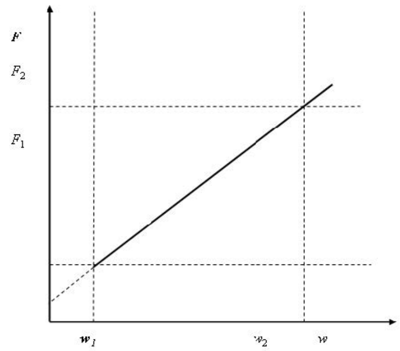

Figure 6.26: Load-deformation graph within the range of elastic deformation[24]

Global Modulus of Elasticity

The deformation measurement approach differs from local modulus of elasticity, which shall be measured at the center of the span from the tension edge, namely the bottom side by optical laser, see Fig.6.27.

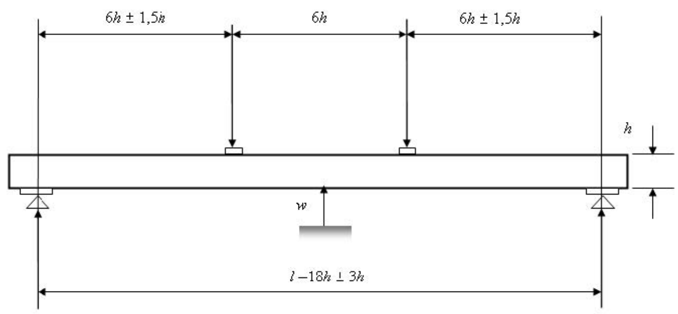

Figure 6.27: Test arrangement for measuring global modulus of elasticity in bending[24]

The computation principle and symbols are similar to the Local modulus of elasticity. Thus, global modulus of elasticity is formulated as follow (Eq.6.11[24]):

$$E_{\mathrm{m,g}} = \frac{3al^2 - 4a^3}{2bh^3\left(2\frac{w_2-w_1}{F_2-F_1} - \frac{6a}{5Gbh}\right)} \tag{6.11}$$

In this case, shear modulus should be taken as infinite according to EN384, which means shear deformation is neglected.

6.2.3. Moisture content

Before testing, this batch of Okan has been stored in the certain climate condition for more than two weeks. After destructive testing, the moisture content will be determined by the oven-dry method in accordance with EN13183-1[21]. Basically, a slice near the major fracture of full cross section free from defects with a length of 25mm will be cut out and weighed indicated as m_1 in grams before being dried at 103°C (± 2). When the moisture content is nearly 0%, technically, constant mass occurs, the dry mass could be weighed indicated as m_0 in grams.

The moisture content by the oven-dry method could be expressed as follows (Eq.6.12[21]):

$$\omega = \frac{m_1 - m_0}{m_0} \times 100 \tag{6.12}$$

6.2.4. Fracture measurement

In the non-destructive test phase, the slope of grain normally will be different from the real crack angle. Thus, the crack pattern of each face and will be observed and the main crack angle will be measured after the destructive test by cutting beams in the main fracture spot,

6.2.5. Digital image correlation

Digital image correlation is an optical method. It has been commonly applied for measuring deformation, displacement, and strain by matching speckle images on the test specimen before and after deformation to track the movement of points on the surface. The schematic illustration is shown in Fig.6.28. Via corresponding algorithm in software GOM Correlate, the relationship between displacement field and strain field could be manipulated[6]. The location of speckle in the four-point bending test is indicated in Fig.6.24.

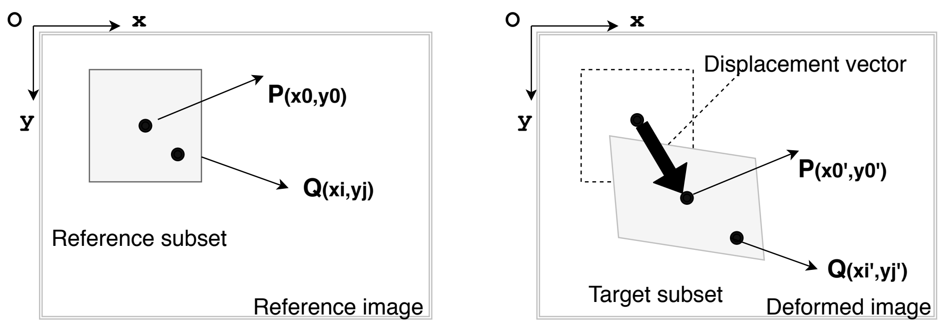

Figure 6.28: Schematic illustration of points tracking and movement

7

Experimental results

7.1. Description of batch

7.1.1. Size & weight

Wet group and dry group consist of 10 samples, respectively with length 3005mm, with width within the range from 148mm to 151mm. The dry group has apparent shrink in the depth direction. The depth of the dry group's beams from 58mm to 61mm. By contrast, the range of depth in the wet group varies from 59mm to 64mm.

7.1.2. Checks

Checks occur across or through the growth ring pattern and occur when drying stresses during seasoning is larger than the tensile strength perpendicular to the grain, especially at the surface and two ends. Surface develops firstly for the reason that it dries more quickly than the inside. In addition, the ends of boards dry faster than the middle board, which leads to the stress developing at the ends. NEN-5493-2010[20] C3 STH regulates the surface checks are permitted. Checks images could be checked in the Appendix E.

The dry group

Each end of the wood, namely E, F faces have varying degrees of checks. In A, C faces, on average, each end has two to three 5cm length longitudinal checks along the fiber direction at the surface. Above 50% checks are 0-5cm. Just a few boards have checks whose length exceeds 10cm. There are no boards without end checks. In addition, around 30% of samples have obvious surface checks uniformly distributing in A, C face.

The wet group

End check occurs in every wet sample. However, visually, the end check of the wet group looks more shallow than that in the dry group because of the higher moisture content. Similar to the dry group, around 30% of samples have surface checks in A, C faces.

7.1.3. Warp

Due to the pre-selection by the producer, the warp in this batch of timber is within the acceptable range.

7.1.4. Knots

In this batch of Okan, knots are rare and small. In the destructive test, the main fracture and mechanism do not have a clear association with knots. The vicinity of knots does not cause an extreme slope of grain deviation. Hence, knots will not be taken into account in the prediction model.

7.2. Basic test results

In table 7.1, the tested parameters are shown. The qualified data are available when the denotation is 'Y' in the cell. The visual assessment method could be referred to as Section 6.1. Half of the tested beams were tested dry (15% moisture content) and the other half was tested above fiber saturation point (25%) moisture content. The slope of grain and growth ring angle is measured after test based on the failure crack.

Table 7.1: Information of experimental outcome overview

Group	Source	Number	Density	m.c.	MOEdyn	MOEloc	MOEglob	Slope of grain	Ring angle	Knot ratio	Max Load
Dry	√	√	√	√	√	√	√	√	√		√
Wet	√	√	√	√	√	√	√	√	√		√

In table 7.2, the mean and standard deviations for the mechanical and physical properties are presented. Among all samples, knot ratios are either zero or approximate to zero. Therefore, knots are not taken in to account in the following assessment. All MOE values are rounded to $1N/mm^2$, all density values to $1kg/m^3$. All bending strength values and moisture content values are kept in one decimal place. The same holds for angle measurements.

Table 7.2: Basic result overview

Sample	size	Density		m.c.		Slope of grain		Ring angle	
		$\bar{x}$	s	$\bar{x}$	s	$\bar{x}$	s	$\bar{x}$	s
Dry	10	1064	59	17.5	3.5	9.0	5.0	50.0	32.8
Wet	10	1101	46	32	8.5	11	8.1	43.5	24.8
		Dynamic MOE		Global MOE		Local MOE		Bending strength	
		$\bar{x}$	s	$\bar{x}$	s	$\bar{x}$	s	$\bar{x}$	s
Dry	10	20493	1273	21687	1012	21076	1443	91.8	13.3
Wet	10	20309	1413	17822	2112	19672	3067	83.6	18.2

*the slope of grain is measured after test

7.2.1. Digital image correlation check

6 out of 20 beams were validly recorded in terms of the crack angle by the DIC technique. In the early stage of crack development, the angle of initiating crack could be measured in the tensile side stress concentration spot where is in the vicinity of the major crack. Table 7.3 compares the outcome of DIC

to the actual fiber grain angle measured after test. The in-site measurement, namely the actual fiber grain angle, perfectly matches the DIC angle measurement tool, but the low-value range shows high sensitivity. Generally speaking, the after-test in-site measurement of the actual slope of grain is valid. Images of angle measurement of the major crack in DIC could be checked in Appendix F.

Table 7.3: Verification of actual grain angle by DIC

Number	Autual	DIC
4	8	8
5	15	12
6	1	4.5
9	10	10
18	5	4.3
24	5	6.2

* unit: degrees

7.3. Relationship between unadjusted properties

In this section, the basic linear correlation between measured parameters is manipulated by the least-square regression, see Fig.7.1. In each typical scatterplot, the equation of the linear regression line and the coefficient of determination r^2 are indicated. Also, the details of equations could be checked in Tab. 7.4 (the regression lines between MOE are forced through the origin).

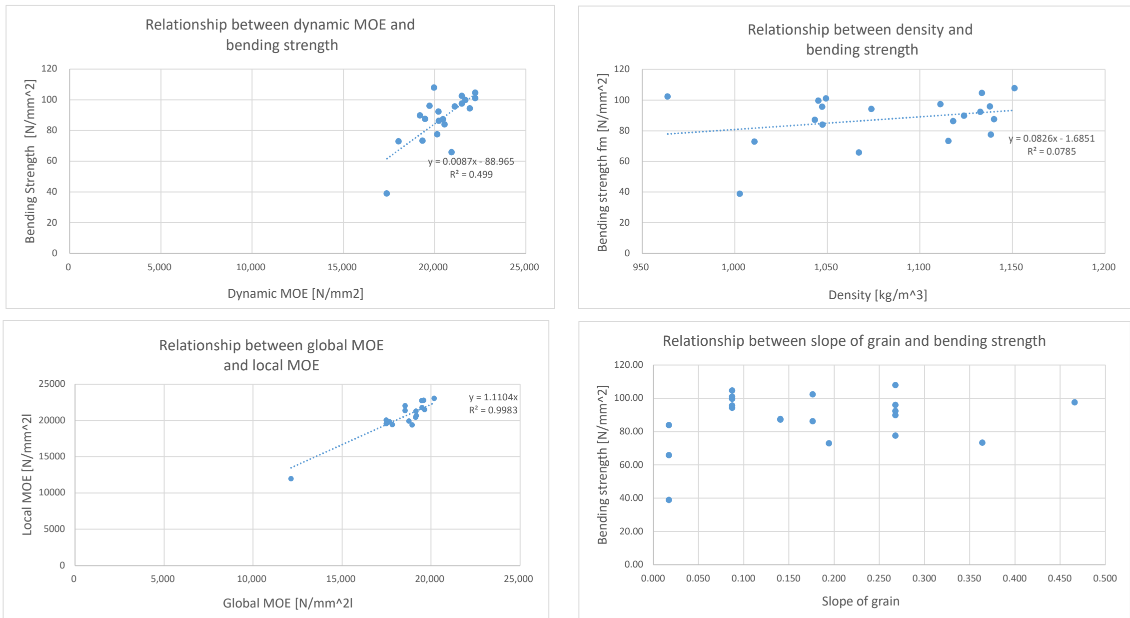

Figure 7.1: Basic correlation of original data
***up left: Dynamic MOE vs. Bending strength up right: Density vs. Bending strength
bottom left: Global MOE vs. Local MOE bottom right: Slope of grain vs. Bending strength

The variability of density shows no clear trend with the change of bending strength with R^2 less than 0.1. The same weak relationship happens between density and other mechanical properties. Even though, the mechanical properties increase with increasing density. Modulus of Elasticity is a strong indicator for the bending strength. Local MOE exhibited a nearly perfect linear relationship with global MOE and dynamic MOE agrees well with static MOE. Therefore, MOE is a good indicator for predicting static MOE with a preferable linear regression model and will be used as a grading parameter. From bottom right in Fig.7.1, it is scattering in the correlation between slope of grain measured after test and mechanical properties. The same circumstance occurs in the 3D fiber orientation scatterplot, see Fig.7.2.

Table 7.4: Linear correlation overview

y\x	content	Edyn	Eglo	Eloc	Density	Bending strength
Edyn	Equation	y=x	y=1.11x	y=0.997x	y=0.16x+20230	y=57.63x+15347
	r^2	1.000	0.997	0.992	0.000	0.499
Eglo	Equation	y=0.901x	y=x	y=0.899x	y=5.01x+12953	y=80.90x+11278
	r^2	0.997	1.000	0.998	0.027	0.604
Eloc	Equation	y=0.996x	y=1.11x	y=x	y=12.13+7310	y=112.01x+10501
	r^2	0.993	0.998	1.000	0.075	0.599
Density	Equation	y=0.0003x+1077	y=0.0053+985	y=0.006x+951.5	y=x	y=0.95x+999
	r^2	0.000	0.023	0.075	1.000	0.079
Bending strength	Equation	y=0.0087x-90.0	y=0.0075x-49.4	y=0.0053x-20.7	y=0.083x-1.7	y=x
	r^2	0.499	0.604	0.599	0.079	1.000

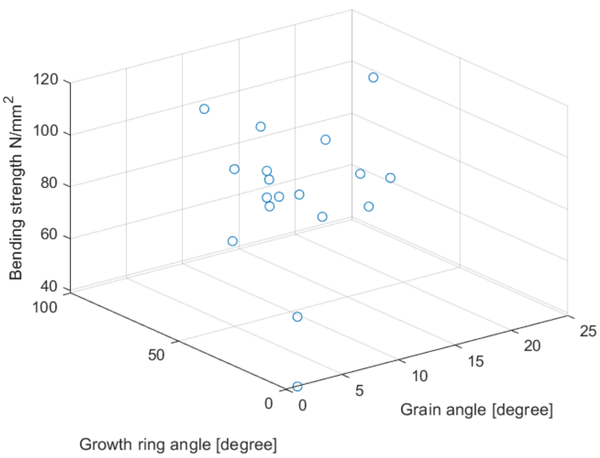

Figure 7.2: Bending strength plotted against the 3D fiber orientation
*the grain angle and growth ring angle are measured after test

7.4. Verification of visual inspection

In this section, two methods proposed for predicting the slope of grain in A/C face in Section 6.1 are verified by the experimental outcome, denoted as the actual slope of grain determined based on the major fracture line after destructive bending test and regarded as a reference in following sections.

Generally speaking, the outcome of the automation method (proposed in 6.1.6) has higher precision than the manual check method (proposed in 6.1.5).

7.4.1. Manual check

This method, which is based on human judgment and subjective thinking with computer assistance, is similar to the approach regulated in the current code. The output of the manual check method gives a close but unstable prediction of A, C face's slope of grain. The difference between the actual number and the predicted number (manual check outcome) is shown in Fig.7.3 and Fig.7.4. To make the comparison more direct, the slope of grain is transferred to grain angle in degree. The instability has to be attributed to the difference between the global fiber angle (manual check result) and the local fiber angle (actual slope of grain). Because inspectors could not predict where the critical spot is and give the corresponding local slope of grain.

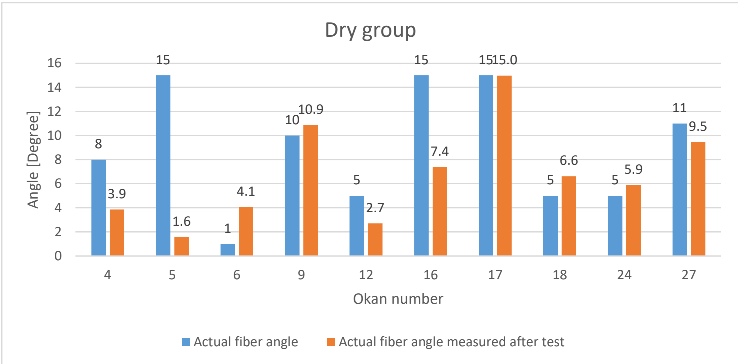

Figure 7.3: Comparison between manual check outcomes and actual grain angle [dry group]

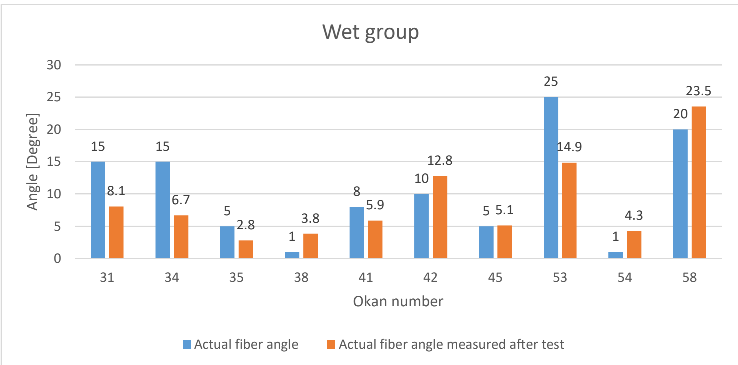

Figure 7.4: Comparison between manual check outcomes and actual grain angle [wet group]

7.4.2. Automation

This method fully relied on the image information and could indicate the most dangerous local spot and gives the angle of the possible fracture line. Take the No.58 beam as an example, the algorithm indicates the possible failed spot in the blue zone (bottom diagram in Fig.7.5), which perfectly predicts the actual fracture location as the actual image in Fig.7.5 shows. The failed location could be retrieved in the Fig.7.6. In Fig.7.7, the output of the automation method almost perfectly matches the actual slope of grain.

An indicator is introduced and defined in Eq.7.1 to quantify the precision based on the mean arithmetic square deviation between actual values and expected values. p_{manual} is 24 which is higher than the p_{auto} 14, meaning that automation method has a better prediction resultants.

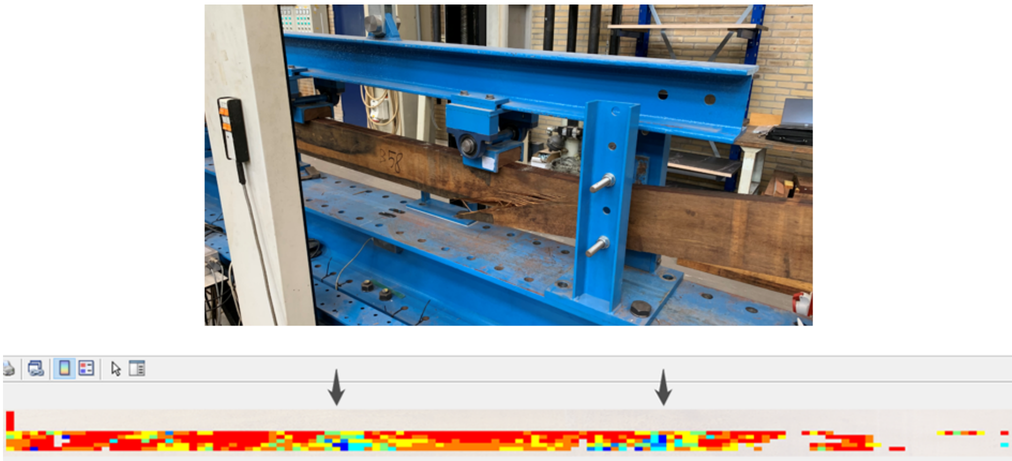

Figure 7.5: Prediction of dangerous spot

*black arrows indicate two jack loading spots

Figure 7.6: Complete failed beam

*black arrows indicate the right side jack loading spot

this image is a bit distorted and without correct ratio

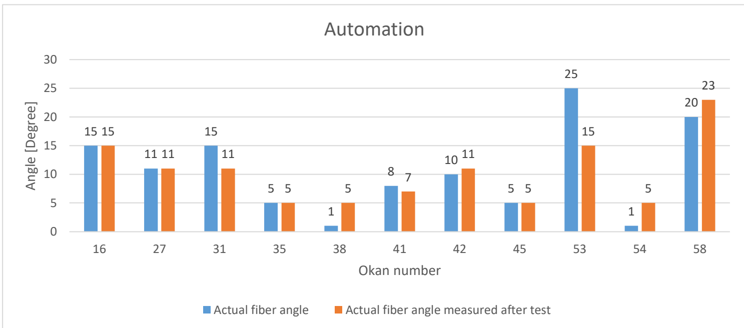

Figure 7.7: Comparison between automation method outcomes and actual grain angle

$$p=\frac{\sum_{i=1}^{n}\left(\alpha_{\text{actual },i}-\alpha_{\text{expected },i}\right)^{2}}{n} \tag{7.1}$$

7.4.3. Compression failure check

After the four-point test, the failure mechanism of beam NO.54 is classified as a compression failure, see Fig.7.8, which should have been removed from the grading process due to visual inspection. However, the automation algorithm did not tell any abnormity. The explanation might be the feature of compression failure shown in Fig.7.9 is identified as noises like water stain or dirt and the range of this feature is too local to recognize. In practice, this type of image feature is more stereoscopic and friendly to in-site inspection.

To tackle this bug, the solution is engaging the machining grading by the grader. When a relatively low dynamic MOE is tested, a more detailed visual inspection is supposed to come into play. In the following chapters, the threshold of dynamic MOE for the second visual inspection will be studied.

Figure 7.8: Compression failure example [Okan 54]

Figure 7.9: The feature of compression failure beam

7.5. Observation of the fracture section

Okan is featured by the spiral or diving grain, which means the final fracture develops in the form of 3D and the fiber is not parallel to the beam axis. To observe the inside fiber angle, beams are cut in the main fracture spot after the destructive testing, see the cutting indication Fig.7.10.

The indication of surface number could be checked in Fig.6.1. The determination of growth ring angle could be checked in the section 6.1.4. In the A/C face, the fracture develops along the fiber direction and fiber angles in A and C surface are approximately symmetry. In the B/D face, due to the narrow area, the crack does not develop with the fiber direction and goes with the fracture section determined by the growth ring angle and slope of grain in wide face. Consequently, the slope of grain in B/D faces is not the dominant indicator. In the E/F face, the fracture develops along the growth ring pattern. Moreover, it is easy to find out that in each beam, the angle of ring pattern is almost constant along the longitudinal direction by observing the cross-sections in different spots.

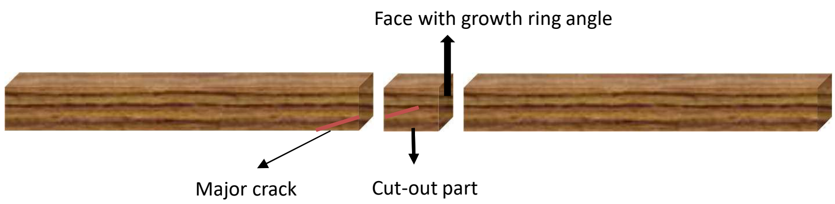

Figure 7.10: Cutting indication

From the observation of 20 damaged beams, three fracture-section forms in the cut-out part are concluded. All types of figure 7.11 could match the actual images, see Fig.7.12. Other detail of the fracture could be checked in the Appendix H.

Ring angle = 0 (load applied parallel to longitudinal – radial face): When the growth ring angle is close to zero and almost flat, the fracture would directly cross the edge side and develop along the fiber direction in the wide face, see Fig.7.11 a.

Ring angle = 90 (load applied parallel to longitudinal – tangential face): The initiating fracture starts from the tangential direction and then develops radially, see Fig.7.11 b.

Ring angle between 0 and 45 degrees: The peeling off part is like a tetrahedron comprised of the slope of grain, ring angle, and bottom surface, see Fig.7.11 c.

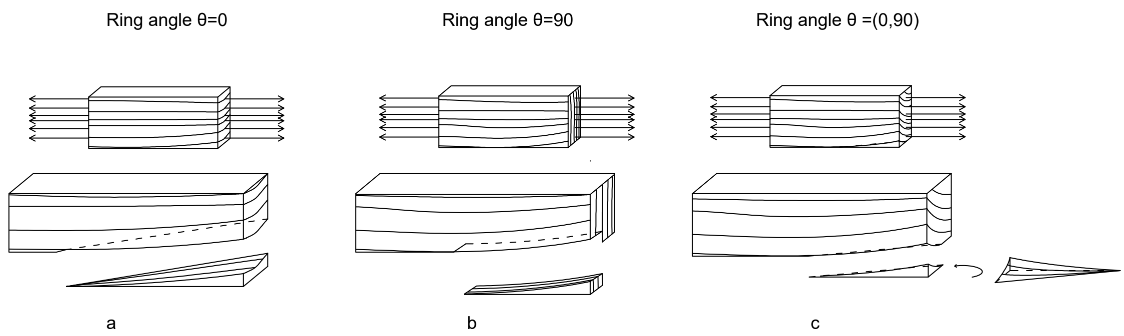

Figure 7.11: Three types of fracture sections of cut-out part

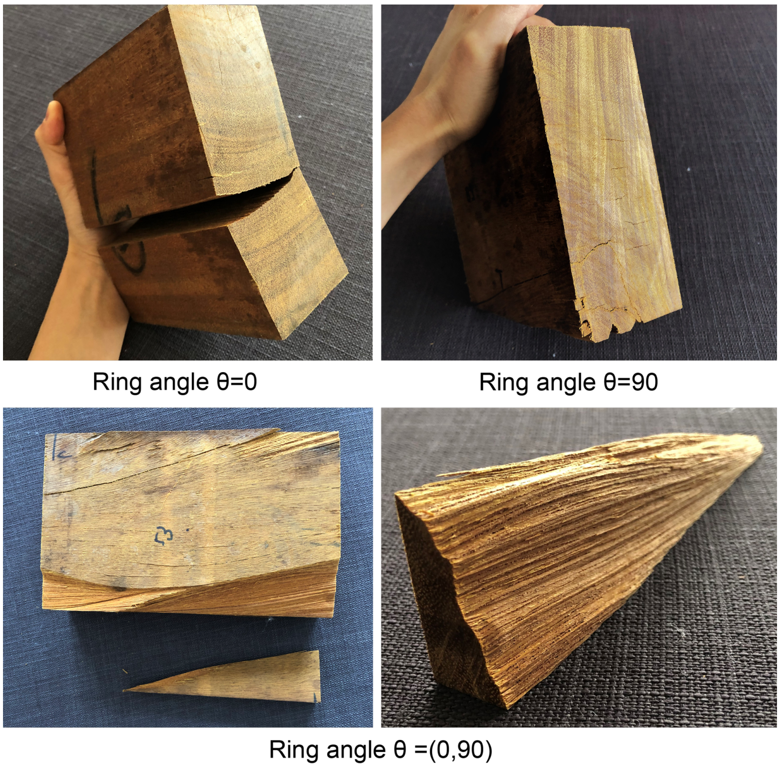

Figure 7.12: Real images of fracture sections

The fracture section consists of the fiber angle in the wide face and the growth ring angle. In the peeling off part, all fiber start from the E/F face (two-side edge faces), grow along the longitudinal direction, and end in pointed spot, see Fig.7.13, which means the combination of growth ring angle and outside fiber grain direction is a good predictor for the main fracture form.

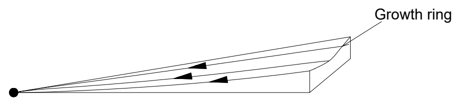

Figure 7.13: Fiber orientation displayed in 3D

It is clear that the growth ring pattern has an impact on the fracture section. However, from the current experimental outcome, it is still hard to conclude that the growth ring angle has strong mathematical relationship with the bending strength and stiffness. Despite the contribution of the growth ring angle to the fracture section, literature still shows that longitudinal stiffness and stiffness perpendicular to the grain are still dominated factors of bending strength.

7.6. Moisture content

The effect of moisture content is studied in this section. The current standard regulates a reference moisture content 12% is used for characteristic values calculation. Therefore, to obtain the characteristic value, the test results have to be adjusted to 12%.

7.6.1. Influence of moisture content on mechanical properties

The moisture content is determined by the material's structure (microsystem and macrosystem) and environmental humidity. Wood is a capillary-porous material with a hygroscopic cavity system which could adsorb airborne moisture and transport liquid water. For the majority of timber species, more moisture content brings lower strength because of the decline of molecular binding forces and weaker hydrogen bonds to the cell wall together[9]. Timber tends to be more malleable above fiber saturation point where only free water could be absorbed further. Generally, in tropical hardwood, high moisture content adversely affects the mechanical performance. Drying fibers usually are equipped with higher stiffness which offers more resistance to the external force.

In practice, to assess the effect of moisture content, experiments should control variables to make the outcome comparable. However, it is impossible to have a beam with the same density and fiber orientation. In this thesis, two groups stored in dry and wet conditions, respectively, are observed.

In Fig.7.14, the bending strength of the wet group and moisture content are inversely proportional. The dry group holds the same trend but with less determination of coefficient. (It is important to aware that, beams stored in the wet condition not necessarily with a moisture content higher than 25%.) However, previous studies show mechanical properties generally decrease remarkably with increasing moisture content only below the fiber saturation point. Beyond the fiber saturation point, further absorption of free water has no significant influence on mechanical properties, see Fig.7.15. Some reasons could explain these incompatible phenomena in this experiment. Firstly, the conclusion of the previous study is based on species-level equipped with similar physical properties (density, fiber saturation point, etc.). By contrast, in this batch of Okan, differences among each individual are non-negligible. Especially, in the wet group, under the same high environmental humidity far beyond the ordinary timber's fiber saturation point, the more porous the timber leads to the higher saturation point, the higher possibility to have higher moisture content and lower stiffness. In other words, in a humid environment, porous samples' mechanical properties are more sensitive to the moisture content. Secondly, the sample size of this experiment is too small to eliminate errors caused by individual differences including fiber deviation and fiber length, etc. When the tested sample is grouped properly and large enough, the error might be mitigated. In right diagram of figure 7.14, the dynamic modulus of elasticity decreases with increasing moisture content without apparent fluctuation.

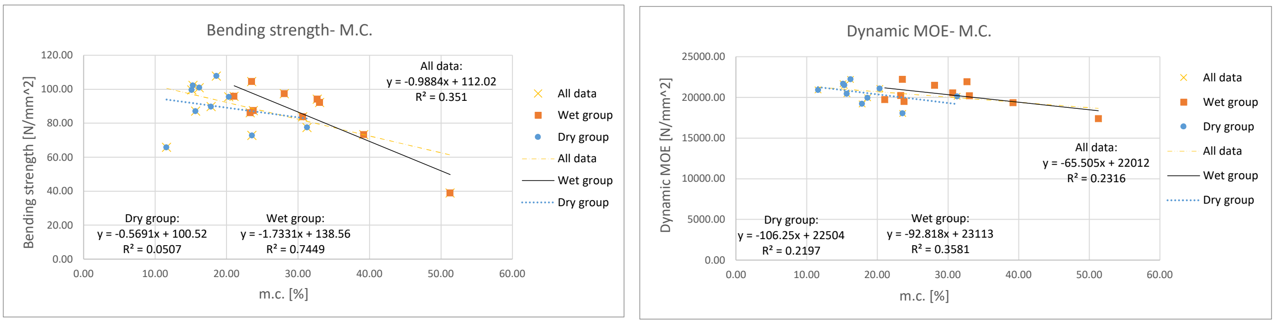

Figure 7.14: Correlations between moisture content and mechanical properties

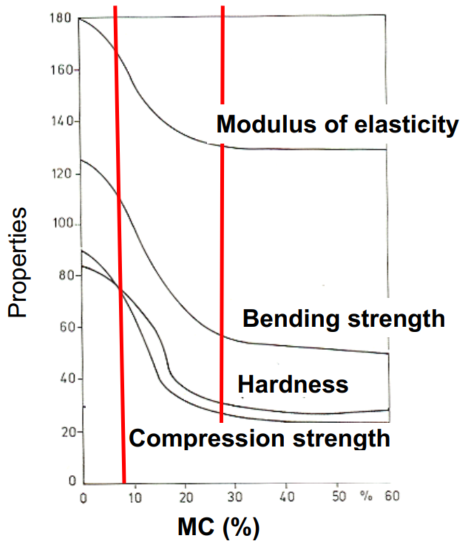

Figure 7.15: Relationship between mechanical properties and moisture content [9]

7.6.2. Adjustment to the reference moisture content

To eliminate the error introduced by fiber deviation, mechanical properties against moisture content are divided into three groups according to the fiber grain angle (measured after test). Two out of the three groups are valid. Grouped data are plotted in up diagrams and all data are plotted in bottom diagrams in Fig.7.16 as references. It is clear to observe the linear correlation. Thus, linear interpolation equations 7.2 and 7.3[27] are used for adjustment. $k_{mc} = 0.13$ for bending strength is found, for $k_{mc} = 0.05$ is found for dynamic modulus of elasticity. Both values are close to the experimental results in the literature[27].

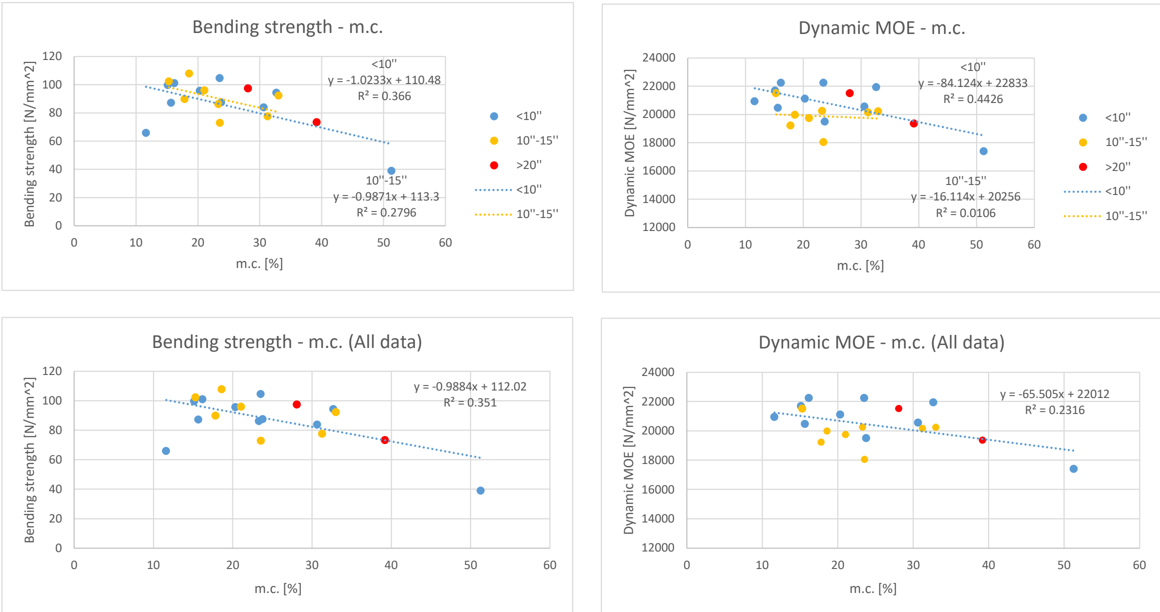

Figure 7.16: Relationship between mechanical properties and moisture content grouped by the grain angle
** Up: Mechanical properties plotted against moisture content grouped by the grain angle
** Bottom: Mechanical properties plotted against moisture content grouped

$$f_{m,12\%} = f_{m,mc} / \left(1 - k_{b,mc} \frac{\min(m \cdot c; 25.0) - 12}{13}\right) \tag{7.2}$$

$$MOE_{dyn,12\%} = MOE_{dyn,mc} / \left(1 - k_{mc} \frac{\min(m \cdot c; 25.0) - 12}{13}\right) \tag{7.3}$$

In conclusion, under the same high humidity environment, high porosity is often accompanied by high moisture content. Therefore, the higher proportion of cell walls would link with water via hydrogen bonds and molecular binding force becomes weaker. Consequently, bending strength decline remarkably, which explains why the tendency of the experiment differs from previous researches. Furthermore, the experimental results show a similar linear correlation similar to the literature. For a more detailed correlation, further testing with more samples needs to be tested. Equation 7.2 and 7.3 are used for the adjustment to reference moisture content. Diagram 7.17 shows the cumulative distribution function of bending strength value before and after adjustment to 12% moisture content.

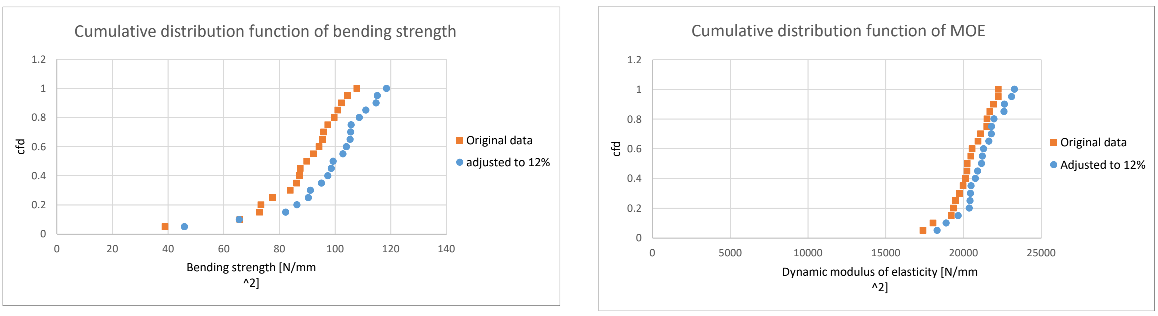

Figure 7.17: Cumulative distribution function of bending strength

7.7. Characteristic value

In this section, the characteristic values of all tested beams which are pre-selected by the producer and inspected by a combination of visual and machine grading are calculated. EN384[23] regulates the depth of beams 150 mm and corresponding test set-up both of which are met by the experiment of this thesis. Thus, only the moisture content adjustment but no size adjustment will be conducted.

The calculation method is already explained in Chapter 5. Because only 20 beams were tested, the parametric method is used to calculate characteristics values. Density is adjusted according to equation 7.4 with a coefficient of volumetric shrinkage $\beta_v = 0.61\%$ [27].

$$\rho_{12\%} = \rho_{\mathrm{m.c}} \frac{(1 + 0,01 * \beta_{v^*}(\min(m \cdot c; 25.0) - 12))}{(1 + 0,01 * (m \cdot c - 12))} \tag{7.4}$$

The coefficient of variation of three parameters all meets the EN14358 Clause 5. Table 7.5 lists characteristic values and corresponding numerical values. Based on 20 beams, this batch of Okan could be graded to D40, see in the Tab.7.5. However, NO.54 is the beam with compression failure and beam NO.53 and NO.58's SOG is over 0.3, which are supposed to be excluded in the grading procedure. Thus, after screening this failed sample, D50 is achieved, see Tab.7.6.

Table 7.5: Characteristic values after adjustment

	Mean	Sta.	COV	f05,i	kn	Characteristic value	
Bending strength	97.20	17.43	0.179	63.56	0.70	f_k	44.49
Density	1020	79	0.078	867	0.88	ρ_k	763
MOE(dynamic)	21135	1299	0.061	/	0.88	$E_{0,\mathrm{mean}}$	18599

*kn is taken from Table 1 in EN384[23]

Table 7.6: Characteristic values after adjustment and screening

	Mean	Sta.	COV	f05,i	kn	Characteristic value	
Bending strength	99.83	12.88	0.129	75.04	0.70	f_k	52.53
Density	1037	54	0.052	933	0.88	ρ_k	821
MOE(dynamic)	21334	1152	0.054	/	0.88	$E_{0,\mathrm{mean}}$	18774

*kn is taken from Table 1 in EN384[23]

7.8. Study of the slope of grain threshold

Section 5.2 advised that 0.3 for the threshold of the slope of grain could be considered in the testing program. In this section, the theoretical slope of grain of experimental data is calculated with inputting the experimental bending strength and the density. The calculation method could be checked in Section 5.2. The degree of overlapping between theoretical slope of grain and theoretical Hankinson formula will be checked.

In figure 7.18, a perfect overlapping occurs, meaning formula 5.2 works well for tested beams and 0.3 is a reasonable range for D40 Okan species pre-selection. However, to achieve the higher-grade assignment, the stricter threshold for the slope of grain is supposed to come into play. Fig.7.18 shows that, in light of the theoretical Hankinson, 0.23 slope of grain corresponds to $50N/mm^2$. The theoretical slope of grain up to 0.24 could make this batch of Okan from Gabon pass the D50 in terms of the 5-percentile characteristic value.

Therefore, to check if 0.2 is a suitable threshold for higher classification, D50, 0.2 was set for the slope of grain under the following two circumstances: 1. Sample 3,4,5,6 in the first group (sample number could be checked in Tab.5.1). 2. Okan from Gabon including sample 5,6 and the experimental 20 beams. Tab.7.9 concludes the classification of whole dataset and Okan fram Gabon, respectively.

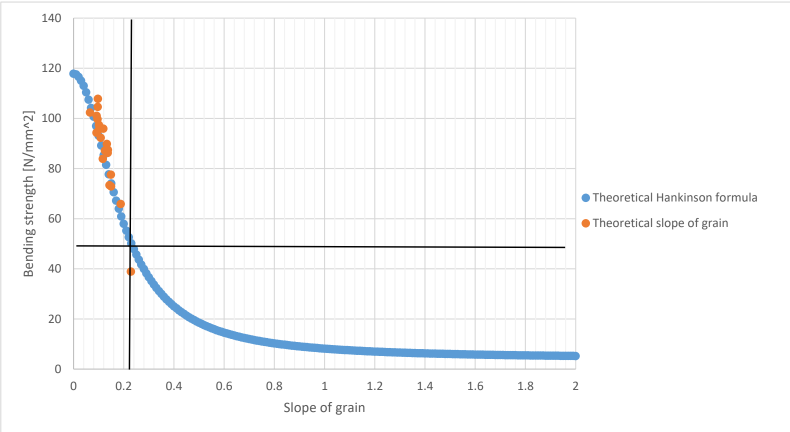

Figure 7.18: Bending strength against the theoretical slope of grain derived from experimental results and the theoretical Hankinson line drawn according to formula 5.1[30]

1. **Sample 3,4,5,6 in the first group**

   Compared to the Tab.7.7 and 7.8 to Tab.5.7 and 5.8. In terms of the non-parametric method, the classification D45 does not change, the dominant sample is still the weakest sample 3. In terms of the parametric method, the outcome is improved from D35 to D40. Generally, the classification is just promoted slightly and sacrifice the pass ratio. Moreover, threshold 0.2 can't help the Okan achieve the D50.

2. **Okan from Gabon including sample 5,6 and the new 20 beams**

   Those three samples could represent better quality Okan compared to other samples in the dataset. Originally, it could be assigned D55 without any screening, see Tab.7.10. However, Tab.7.11 shows that the 0.3 threshold does not bring too much positive influence on the outcome. By contrast, Tab.7.12 suggests that the 0.2 threshold makes the final classification decrease a bit. The possible reason might be when the threshold of the slope of grain becomes stricter, the more beams are screened out, consequently, the factor of characteristic value decreases, which brings more reduction for the final result. Moreover, better quality timber might be less influenced by the low range slope of grain.

0.3 threshold works for the whole dataset and it could improve the classification. 0.2 is too strict for the Okan and the impact of the reduction factor determined by the number of beams makes a big contribution to the strength loss. In light of the Okan from Gabon with better quality, 0.3 does not bring obvious change to the outcome. 0.2 is not a good option and the same reason as it happens in the whole dataset analysis.

Table 7.7: Characteristic values of Sample 3,4,5,6 data after screening at 0.2 slope of grain by non-parametric method

Non-parametric method			Adjusted bending strength/[N/mm^2]			Adjusted MOE/[N/mm^2]		Adjusted density/ [kg/m^3]			Slope of grain	
Sample	Failed Ratio	Size	Mean	Cov	$f_{05,i}$	E-mean	Cov	Mean	Cov	rho05,i	Mean	Cov
3	0.36	28	66.15	0.232	39.88	19856	0.195	1053	0.044	981	0.171	0.320
4	0.34	33	81.75	0.213	56.92	20807	0.152	942	0.150	714	0.144	0.329
5	0.29	34	103.39	0.194	62.41	25107	0.085	939	0.102	796	0.102	0.556
6	0.66	17	101.30	0.192	49.86	23418	0.082	1002	0.064	941	0.095	0.883
Total	**0.42**	**112**	**87.39**	**0.269**		**22219**	**0.163**	**978**	**0.112**		**0.126**	**0.518**
Characteristic value												
Strength			$1,2f_{05,i,min}$	47.86	$\frac{\sum_{i=1}^{ns} n_i f_{05,i}}{n}$	53.26	kn	0.95	f_k	45.46	D45	
MOE			$1,1\bar{E}_{i,\min}$	21841	$\frac{\sum_{i=1}^{ns} n_i \bar{E}_i}{n}$	22271	kn	0.97	$E_{0,\text{mean}}$	21186		
Density			$1,1\rho_{05,i,\min}$	785	$\frac{\sum_{i=1}^{ns} n_i \rho_{05,i}}{n}$	840	kn	0.97	ρ_k	762		

Table 7.8: Characteristic values of Sample 3,4,5,6 data after screening at 0.2 slope of grain by parametric method

Parametric method			Adjusted bending strength/[N/mm^2]			Adjusted MOE/[N/mm^2]		Adjusted density/ [kg/m^3]			Slope of grain	
Sample	Failed Ratio	Size	Mean	Cov	$f_{05,i}$	E-mean	Cov	Mean	Cov	rho05,i	Mean	Cov
3	0.36	28	66.15	0.232	37.44	19856	0.195	1053	0.044	966	0.171	0.320
4	0.34	33	81.75	0.213	49.52	20807	0.152	942	0.150	681	0.144	0.329
5	0.29	34	103.39	0.194	66.22	25107	0.085	939	0.102	762	0.102	0.556
6	0.66	17	101.30	0.192	63.42	23418	0.082	1002	0.064	877	0.095	0.883
Total	**0.42**	**112**	**87.39**	**0.269**		**22219**	**0.163**	**978**	**0.112**		**0.126**	**0.518**
Characteristic value												
Strength			$1,2f_{05,i,min}$	44.92	$\frac{\sum_{i=1}^{ns} n_i f_{05,i}}{n}$	53.68	kn	0.95	f_k	42.68	D40	
MOE			$1,1\bar{E}_{i,\min}$	21841	$\frac{\sum_{i=1}^{ns} n_i \bar{E}_i}{n}$	22967	kn	0.97	$E_{0,\text{mean}}$	22967		
Density			$1,1\rho_{05,i,\min}$	749	$\frac{\sum_{i=1}^{ns} n_i \rho_{05,i}}{n}$	806	kn	0.97	ρ_k	727		

Table 7.9: Classification conclusion

	Method	Parametric		Non-parametric
	Population	Sample:3456	Gabon	Sample:3456
Threshold for slope of grain	All	D30	D55	D35
	0.3	D40	D55	D45
	0.2	D40	D50	D45

Table 7.10: Characteristic values of sample from Gabon by parametric method

All beams			Adjusted bending strength/ [N/mm^2]			Adjusted MOE/ [N/mm^2]		Adjusted density/ [kg/m^3]			Slope of grain	
Sample	Source	Size	Mean	Cov	$f_{05,i}$	E-Mean	Cov	Mean	COV	rho05,i	Mean	COV
5	Gabon	48	103.90	0.191	**67.70**	**24703**	0.085	932	0.114	**738**	0.159	0.766
6		50	98.70	0.185	**65.57**	**24258**	0.086	1030	0.058	**922**	0.233	0.530
new		20	97.20	0.179	**63.56**	**21135**	0.061	1020	0.078	**867**	0.174	0.695
Characteristic value												
Strength			$1,2f_{05,i,min}$	76.27	$\frac{\sum_{i=1}^{ns} n_i f_{05,i}}{n}$		66.10	kn	0.90	f_k	**59.49**	**D55**
MOE			$1,1\bar{E}_{i,\min}$	23248	$\frac{\sum_{i=1}^{ns} n_i \bar{E}_i}{n}$		23910	kn	0.94	$E_{0,\text{mean}}$	**21853**	
Density			$1,1\rho_{05,i,\min}$	812	$\frac{\sum_{i=1}^{ns} n_i \rho_{05,i}}{n}$		838	kn	0.94	ρ_k	**763**	

Table 7.11: Characteristic values of Sample from Gabon after screening at 0.3 slope of grain by parametric method

Threshold: 0.3			Adjusted bending strength/ [N/mm^2]			Adjusted MOE/ [N/mm^2]		Adjusted density/ [kg/m^3]			Slope of grain	
Sample	Failed Ratio	Size	Mean	Cov	$f_{05,i}$	E-Mean	Cov	Mean	COV	rho05,i	Mean	COV
5	0.15	41	103.95	0.200	**63.30**	**25014**	0.083	925	0.106	**730**	0.121	0.644
6	0.30	35	94.69	0.200	**56.60**	**24098**	0.093	1032	0.060	**908**	0.180	0.569
new	0.15	17	99.83	0.129	**75.04**	**21334**	0.054	1037	0.052	**933**	0.169	0.699
Characteristic value												
Strength			$1,2f_{05,i,min}$	67.92	$\frac{\sum_{i=1}^{ns} n_i f_{05,i}}{n}$		62.92	kn	0.90	f_k	**56.63**	**D55**
MOE			$1,1\bar{E}_{i,\min}$	23467	$\frac{\sum_{i=1}^{ns} n_i \bar{E}_i}{n}$		23997	kn	0.94	$E_{0,\text{mean}}$	**22059**	
Density			$1,1\rho_{05,i,\min}$	803	$\frac{\sum_{i=1}^{ns} n_i \rho_{05,i}}{n}$		834	kn	0.94	ρ_k	**755**	

Table 7.12: Characteristic values of Sample from Gabon after screening at 0.2 slope of grain by parametric method

Threshold: 0.2			Adjusted bending strength/ [N/mm^2]			Adjusted MOE/ [N/mm^2]		Adjusted density/ [kg/m^3]			Slope of grain	
Sample	Failed Ratio	Size	Mean	Cov	$f_{05,i}$	E-Mean	Cov	Mean	COV	rho05,i	Mean	COV
5	0.29	34	103.39	0.194	**62.41**	**25107**	0.085	939	0.102	**796**	0.102	0.556
6	0.66	17	101.30	0.192	**49.86**	**23418**	0.082	1002	0.064	**941**	0.095	0.883
new	0.40	12	98.44	0.14	**70.24**	**21524**	0.057	1022	0.052	**915**	0.105	0.571
Characteristic value												
Strength			$1,2f_{05,i,min}$	59.83	$\frac{\sum_{i=1}^{ns} n_i f_{05,i}}{n}$		60.51	kn	0.90	f_k	**53.85**	**D50**
MOE			$1,1\bar{E}_{i,\min}$	23676	$\frac{\sum_{i=1}^{ns} n_i \bar{E}_i}{n}$		23969	kn	0.94	$E_{0,\text{mean}}$	**22256**	
Density			$1,1\rho_{05,i,\min}$	876	$\frac{\sum_{i=1}^{ns} n_i \rho_{05,i}}{n}$		858	kn	0.94	ρ_k	**807**	

8
Strength modelling

In this chapter, the failure mode for typical flexural timber beams with grain angle deviation will be studied, based on which the strength modeling will be derived step by step and extended from 2D to 3D.

8.1. Failure mechanism and failure criterion

In this section, how the timber beam fails is presented. Few assumptions are given. The timber beam is simulated as the Bernoulli-Euler beam which has characteristics that the plan sections remain plane and any section of a beam is perpendicular to the neutral axis. In the elastic range, for stresses and strains relationship, Hooke's law works. Elastic range and brittle failure could happen in the tension zone and bi-linear stress-strain relation is considered in the compressive zone. Equation 3.1 is used for calculating the bending strength of a four-point test. Before the failure happens, the full section modulus of the beam is used with neglection of the existence of knots and inhomogeneity of cross-section caused by grain angle deviation.

8.1.1. Failure mode

From Fig. 8.1 to 8.2, actual failure patterns and corresponding mechanical diagrams are displayed. All beams except the NO.58 beam have tension failures. In other words, beams failed when the maximum tensile strength was reached at the tension side (bottom). From the load-displacement diagram and the time-crack diagram measured by digital image correlation (DIC), either the elastic-plastic behavior or elastic behavior could be seen. Properties of fiber including length, angle, homogeneity, etc. contribute to the type of behavior. When the beam is in the elastic stage, the elongations in the tensile side are equal to the shortenings in the compressive zone. Meanwhile, the neural plane lies in the middle. Within the plastic phase, gradually, the fiber in the compressive zone starts failing from the upper side with the increasing load. To achieve the balance, the neutral plane must sink to the tensile side and the bottom fibers are pulled by remarkable tension, see the scheme 8.3. During the loading process, small cracks might occur before the main fracture happens. The ultimate failure occurs in the tensile side, which is a brittle failure.

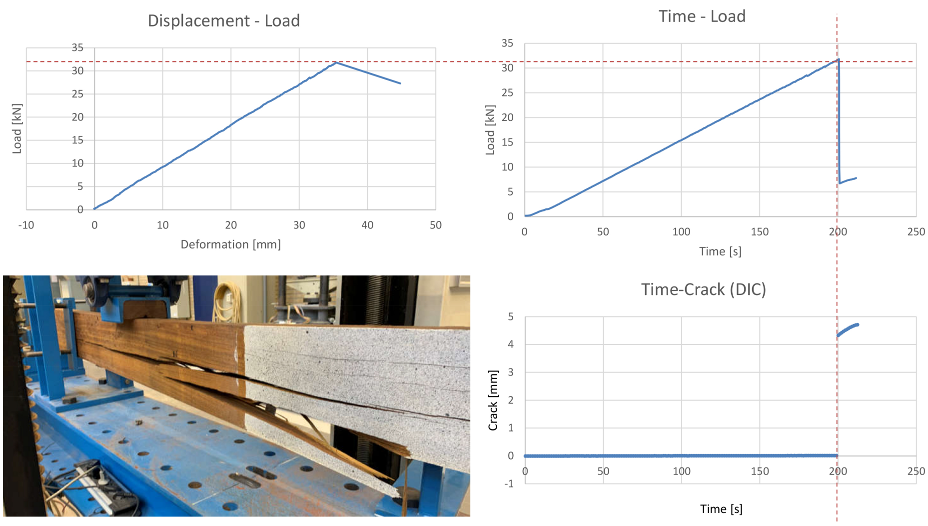

Figure 8.1: Mechanical diagrams of beam with elastic behavior

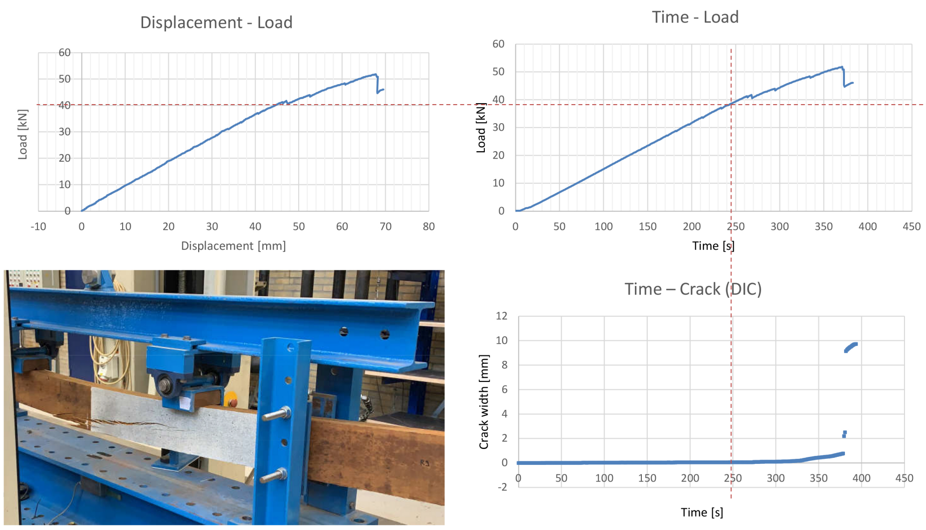

Figure 8.2: Mechanical diagrams of beam with elastic-plastic behavior

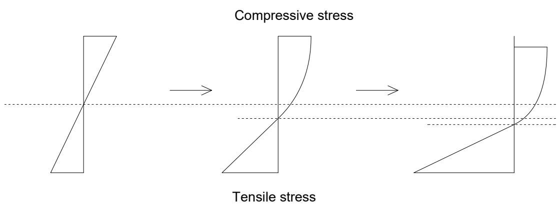

Figure 8.3: Stress distribution during loading

8.1.2. The impact of the fiber (2D)

In the section 7.5, the influencing factors of the fracture section are concluded. Apparently, the governing fiber section is not parallel to the longitudinal direction resulting in that the normal stress might be perpendicular to the fiber direction and shear stress parallel to the fiber direction.

The well-known Hankinson formula describes the correlation between tensile strength and grain angle (denoted as α), presented in Equation 3.3 and repeated in the form of generalized formula Eq. 8.1, in which n is from 1.5 to 2. The unadjusted mean bending strength value of tested Okan is around 90MPa. According to the literature[19], k = 28 is assumed. $f_{m.0}$ will be derived by curve fitting of 20-beams test results. Fig.8.4 displays the fitting effect of generalization of Hankinson formula with several typical exponents. The expected value is calculated from the Eq.8.1 with inputting the actual slope of grain.

Summarized from Fig.8.4, Hankinson formula is too conservative for the actual experimental outcome. All of the coefficients of determination (R^2) of expected value and actual value are below 0.2 which means grain angle deviation (slope of grain) is not a good sole stiffness predictor by the Hankinson formula. The same trend happens for modulus of elasticity against the grain angle.

$$f_{m,\alpha} = \frac{f_{m,0}}{\frac{f_{m,0}}{f_{m,90}} \sin^n(\alpha) + \cos^n(\alpha)} \tag{8.1}$$

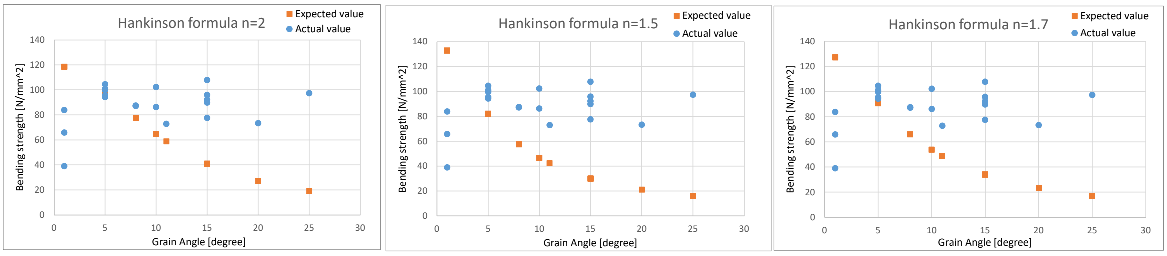

Figure 8.4: Hankinson formula curves with different exponents

The possible reasons for scattering are that Hankinson formula only takes superficial grain angle deviation instead of spiral angle into account and the natural variability of wood affects a lot. Moreover, theoretically speaking, one species timber is supposed to have a certain $f_{m,0}$ in the Hankinson formula model. However, in practice, each beam has its own composition and physical properties leading to various bending strength parallel to the grain, namely $f_{m,0}$.

8.2. Prediction model for bending strength

In this section, a new strength predicting model is proposed, combined with two existing models, namely Hankinson formula and linear correlation with MOE.

In the section 7.3 and section 8.1.2, two models to predict the bending strength by inputs from the non-destructive test were presented respectively. The first one is the linear correlation based on the dynamic MOE measured by the handheld grader, and dynamic MOE is available as an input. The second prediction based on the Hankinson formula fully replies on the fiber deviation via the visual inspection outcome, and the slope of grain is available as inputs. Each approach could involve few properties of Okan into the mechanical model but both have its own restrictions. To be specific, the linear model does not take the grain angle information into account, which is indispensable in the hardwood grading process. In terms of the 2D modified Hankinson formula, it is assumed that every beam has the same bending strength parallel to the grain which is investigated from tons of data by statistical method, denoted in the red circle in figure 8.5. The value makes statistical sense to one species but individuals. Hence, to play their own strength, the combination of machine grading and visual inspection in the predicting model is necessary.

$$f_{t,\alpha} = \frac{f_{t,0} \cdot f_{t,90}}{f_{t,0} \cdot \sin^2\alpha + f_{t,90} \cdot \cos^2\alpha} = \frac{f_{t,0}}{\frac{f_{t,0}}{f_{t,90}} \cdot \sin^2\alpha + \cos^2\alpha}$$

Figure 8.5: Hankinson formula

Based on sections in this chapter and Chapter 5, the following assumptions are made:

1. This model only focuses on 2D fiber deviation.
2. Structural timber is modeled as clear wood but with mechanical property reducing characteristics.
3. The presence of knots is negligible and the reduction caused by knots is not considered into the model.
4. Each beam at each angle has its bending strength $f_{i,\alpha}$ and modulus of elasticity $MOE_{i,\alpha}$.
5. Each beam's MOE is linearly related to the bending strength.
6. Hankinson formula(2D) could cover the reduction from fiber angle deviation. Exponent n=2 is the optimal option.
7. Each batch of Okan has constant $f_{m,0}/f_{m,90}$ and $MOE_{m,0}/MOE_{m,90}$.

According to assumption 5, a linear equation could be formulated:

$$f_{i,\alpha} = k_\alpha * MOE_{i,\alpha} + b_\alpha \tag{8.2}$$

$$f_{i,0} = k_0 * MOE_{i,0} + b_0 \tag{8.3}$$

where i is the number of beams.

Combined with assumption 4, the modified Hankinson formula is :

$$f_{i,\alpha} = \frac{f_{i,0}}{\frac{f_{m,0}}{f_{m,90}} \sin^2\alpha + \cos^2\alpha} \tag{8.4}$$

$$\mathrm{MOE}_{i,\alpha} = \frac{MOE_{i,0}}{\frac{MOE_{m,0}}{MOE_{m,90}} \sin^2\alpha + \cos^2\alpha} \tag{8.5}$$

Substituting the $f_{i,0}$ in Eq.8.4 for Eq.8.3. Equation 8.4 could be rewritten as

$$f_{i,\alpha} = \frac{k_0 * MOE_{i,0} + b_0}{\frac{f_{m,0}}{f_{m,90}} \sin^2\alpha + \cos^2\alpha} \tag{8.6}$$

Substituting the $MOE_{i,0}$ in Eq.8.6 for equation 8.7

$$MOE_{i,0} = MOE_{i,\alpha} * (\frac{MOE_{m,0}}{MOE_{m,90}} \sin^2\alpha + \cos^2\alpha) \tag{8.7}$$

gives,

$$f_{i,\alpha} = \frac{k_0 * \left(MOE_{i,\alpha} * \left(\frac{MOE_{m,0}}{MOE_{m,90}} \sin^2 \alpha + \cos^2 \alpha\right)\right) + b_0}{\frac{f_{m,0}}{f_{m,90}} \sin^2 \alpha + \cos^2 \alpha} \tag{8.8}$$

Simplifying the equation,

$$f_{i,\alpha} = k_0 * \gamma * MOE_{i,\alpha} + b_\alpha \tag{8.9}$$

or

$$f_{i,\alpha} = k_\alpha * MOE_{i,\alpha} + b_\alpha \tag{8.10}$$

Where

$$k_\alpha = k_0 * \gamma \tag{8.11}$$

$$\gamma = \frac{\frac{MOE_{m,0}}{MOE_{m,90}} * \sin^2 \alpha + \cos^2 \alpha}{\frac{f_{m,0}}{f_{m,90}} * \sin^2 \alpha + \cos^2 \alpha} \tag{8.12}$$

$$b_\alpha = \frac{b_0}{\frac{f_{m,0}}{f_{m,90}} * \sin^2 \alpha + \cos^2 \alpha} \tag{8.13}$$

Among those, constant $f_{m,0}/f_{m,90}$ and $MOE_{m,0}/MOE_{m,90}$ are determined as 28 and 15, respectively from the literature[19]. k_0 and b_0 are supposed to be obtained by a clear wood experiment. In this thesis, they are obtained from a regression. $k_0 = 0.00972$, $b_0 = -120.4$ are found with 95% confidence bounds by the Matlab curve fitting tool. The corresponding scatterplot and residual of new model are shown in Diagram 8.6.

Applying this model to experimental data. In Tab.8.1, compared to the linear correlation model and Hankison formula, the combined model has an optimized coefficient of determination (R^2 = 0.685). It is important to aware that, factor k and b of Okan vary from batch to batch.

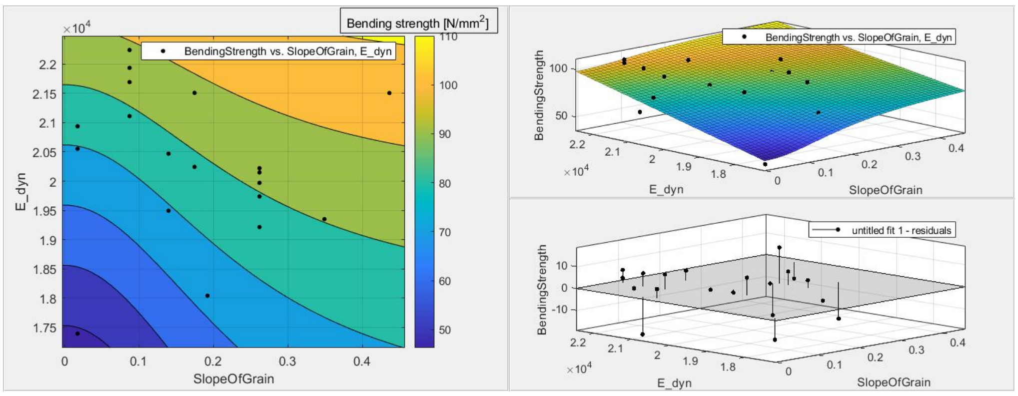

Figure 8.6: Scatter plot of new strength model

Table 8.1: Comparison among strength models

Model	Input	Type	R^2
Machining grading	E_dyn	Linear regression	0.499
Visual grading	Slope of grain	Hankinson model	<0.2
Combined method	E_dyn & Slope of grain	Linear+Hankinson	0.685

8.3. Application to dataset

To verify the generalization of predicting strength model, four samples, sample 3,4,5,6 from the dataset were studies. Samples' information can be checked in Chapter 5. According to section 8.2, inputs for this model are dynamic MOE and slope of grain measured after test. Beams with the slope of grain exceeding 0.3 were screened out first.

Figure 8.7 shows the cumulative distribution function curve of the original strength value, the expected value and the expected value with reduction factor. In the low tile range, the expected bending strength (yellow curve) is more conservative than the actual bending strength (orange curve) and provides the same 5 percentile characteristic value $52N/mm^2$. In the middle range, the predicting model gives a slightly higher bending strength value than the actual number which might cause safety issues in practice. The possible reason is that the constant value k_0 and b_0 are derived from an experiment in which this batch of Okan has better quality. Thus, to tackle this problem, a safety factor is introduced, γ . When $\gamma = 0.9$ is applied, the cumulative distribution function (blue curve) shows a safer result with $47N/mm^2$ 5 percentile characteristic value.

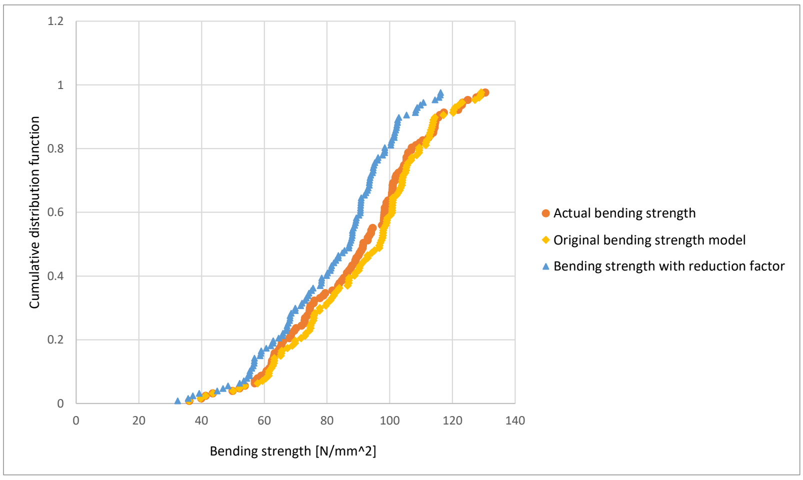

Figure 8.7: Cumulative distribution function of bending strength at 12% moisture content.

8.4. Find the threshold for dynamic MOE

In section 7.4.3, the weakness of automation visual inspection was discussed. To solve this issue that some types of compression failure could be found, the combination of machine grading is important. In the figure 8.6, the contour of D40 falls in $17500N/mm$ for dynamic modulus of elasticity, meaning that when the dynamic modulus of elasticity is less than $17500N/mm^2$, the sample is more likely to be graded less than D40. Given that the influence of moisture content, to make the threshold in the safer side, $18500N/mm^2$ at 12% is considered as the threshold.

In the sample 1, there is a beam with similar failure with Fig.7.8, see the failure pattern in Fig.8.8. The corresponding dynamic MOE at 12% m.c. is $16035N/mm^2$ and bending strength is $39N/mm^2$, which could be identified by the proposed judgment condition.

Figure 8.8: Compression failure happens in Sample 1 beam NO.28

To sum up, the grading procedure should start with conducting automation visual inspection for quantifying the slope of grain, subsequently, dynamic MOE measurement follows for double-checking. If the dynamic MOE is lower than $18500N/mm^2$ at 12% moisture content, then the sample should be visually checked again.

8.5. The impact of the fiber (3D)

In the last section, the strength model has been optimized but without including the influence of the 3D-effect. Consequently, the precision might deviate. In this section, the 3D-effect including effects of the slope of grain (α) and growth ring angle (θ) are studied. Figure 8.9 is the indication of two indicators (α and θ) in timber's space coordination.

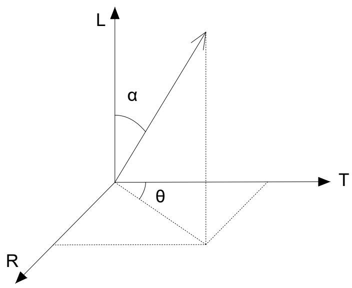

Figure 8.9: The coordination of timber
L: Longitudinal T: Tangential R: Radial

As Fig.6.20 shows, it is assumed that the beam is sawn straightly from the stem and parallel to the stem axis. In terms of growth ring orientation, researches [14] states when growth ring orientation is lower than 45 degrees, the increasing growth ring angle has negative impacts on the strength and stiffness. At a higher angle, compression properties are promoted by the increasing angle slightly. However, the detail of the growth ring angle's effect is still without proof. In terms of bending, studies about hardwood Robinia and southern pines found that the MOE of beams with a zero-degree growth ring angle is closed to the MOE of beams with a 90-degree growth ring angle. In other words, with the constant slope of grain and increasing growth ring angle, the bending strength value will drop when the growth ring angle is less than 45 degrees, and then it will rise back to the starting point. It is worth noting that the influence might be species dependently and only could be determined by the experiment.

Currently, some models describe the influence of the growth ring angle and slope of grain. Szalai (1994) proposed an approach (Eq.8.14) that could be derived from the four-dimensional strength tensor by transforming the first element of a tensor with 6 strength values which needs to be decided by experiment[8].

$$\begin{aligned}\frac{1}{\hat{\sigma}_{\alpha}^{\theta}} = \frac{1}{\sigma_L}\cos^4\alpha + \frac{1}{\sigma_R}\sin^4\alpha\sin^4\theta + \frac{1}{\sigma_T}\sin^4\alpha\cos^4\theta \\ + \left(\frac{4}{\sigma_{90^\circ}^{45^\circ}} - \frac{1}{\sigma_R} - \frac{1}{\sigma_T}\right)\sin^4\alpha\sin^2\theta\cos^2\theta \\ + \left(\frac{4}{\sigma_{45^\circ}^{0^\circ}} - \frac{1}{\sigma_L} - \frac{1}{\sigma_T}\right)\cos^2\alpha\sin^2\alpha\cos^2\theta \\ + \left(\frac{4}{\sigma_{45^\circ}^{90^\circ}} - \frac{1}{\sigma_L} - \frac{1}{\sigma_R}\right)\cos^2\alpha\sin^2\alpha\sin^2\theta\end{aligned} \tag{8.14}$$

Where:

$\hat{\sigma}_{\alpha}^{\theta}$: the predicted strength at grain angle α and growth ring angle θ

α: the longitudinal grain angle

θ: the growth ring angle

Bodig, J. and B. A. Jayne (1982) based on 2D compressive Hankinson formula proposed a model by substituting strength at 90° grain angle and ring angle θ for tensile strength perpendicular to the grain, see Eq.8.15. This model is an empirical approach without firm orthotropic tensor theory but the Hankinson formula has been applied for a long time. In the following section, the trend will be studied.

$$\hat{\sigma}_{\alpha}^{\theta} = \frac{\sigma_L \hat{\sigma}_{90^\circ}^{\theta}}{\sigma_L \sin^2\alpha + \hat{\sigma}_{90^\circ}^{\theta}\cos^2\alpha} \tag{8.15}$$

Where:

$\hat{\sigma}_{90^\circ}^{\theta}$: the predicted strength at $90°$ grain angle and ring angle θ

To obtain $\hat{\sigma}_{90^\circ}^{\theta}$, equation 8.14 is used for derivation. It is assumed that in tropical hardwood Okan,$\sigma_R = \sigma_L$. One experimentally determined value k is supposed to obtain from the experiment.

Thus,

$$\sigma_{90}^{\theta} = \sigma_R * \frac{1}{1 + A * \sin^2 2\theta} \tag{8.16}$$

Where:

$\sigma_R = \sigma_{90}^{90}$

$\sigma_T = \sigma_{90}^{0}$

$A = \frac{4*\sigma_R}{\sigma_{90}^{45}} - 2$ - empirical constant value

Diagram 8.10 displays the changing trend of σ_{90}^{θ} with the ring angle, which is congruent with the literature mentioned above. With the constant longitudinal grain angle and increasing growth ring angle, the bending strength value will drop when the growth ring angle is less than 45 degrees, and then it will rise back to the starting point. The ratio between σ_R and σ_{90}^{45} determines the importance of the growth ring angle. As the ratio increases, the lower the valley of the curve means the greater the influence of the growth ring angle on the strength.

Replace σ_{90}^{θ} with equation 8.16 and modify it, the bending strength at any longitudinal grain angle and growth ring angle could be obtained by the equation 8.17 derived from Eq.8.15. The correlation between bending strength and fiber 3D orientation is presented in Fig.8.11. This model is intended for grading with simple inputs without destructive testing, leading to inevitable model simplifications and assumptions. However, more experiments still need to be conducted to verify its precision. Once constant B is determined, the model could be inserted into the combined model in the section Prediction model for bending strength.

$$f_{m,\alpha}^{\theta} = \frac{f_{m,0}^{0}}{B * \frac{f_{m,0}^{0}}{f_{m,90}^{90}} \sin^2(\alpha) + \cos^2(\alpha)} \tag{8.17}$$

Where: $B = 1 + A * \sin^2 2\theta$

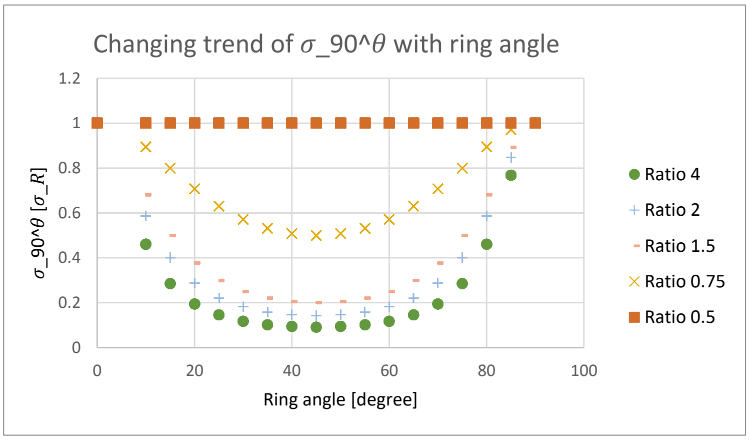

Figure 8.10: Scatter plot of σ_{90}^{θ} against θ

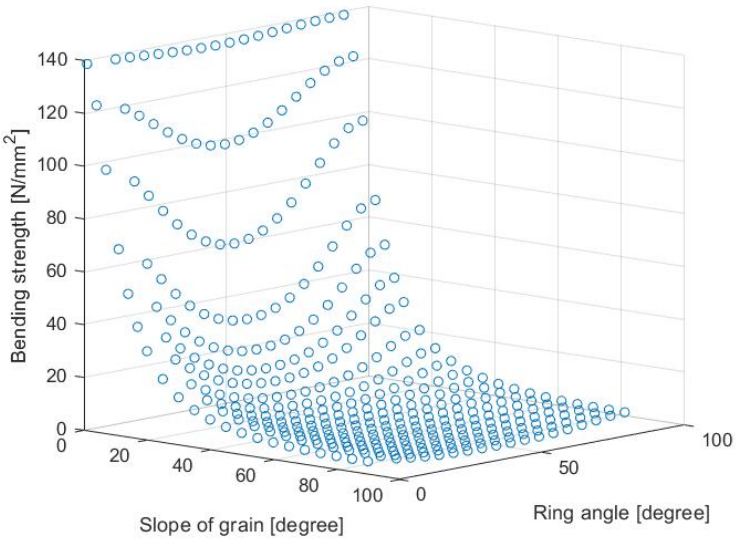

Figure 8.11: The correlation between bending strength against the grain angle and the growth ring angle

9

Conclusions and recommendations

9.1. Conclusions

In this thesis, the associated influencing factors of mechanical properties and characteristic calculation methods have been investigated. The correlation between the influencing factors and the bending strength has been established. Destructive tests have been conducted on 20 beams. The main questions and sub-questions proposed in Section 2.2 are summarized and answered here. Some recommendations come after the summary.

Main questions

- **Which influencing factors could be correlated to the Okan's mechanical properties?**

  Geographically speaking, climate, precipitation, soil quality, water source etc. could be classified into different levels, bring varying degrees of impacts.

  Individually speaking, fiber orientation (slope of grain & ring angle), moisture content, density, modulus of elasticity (dynamic, static) are important factors.

- **What relationship between those influencing factors and Okan's mechanical properties?**

  Knots have a negligible influence on the stiffness.

  Hankinson formula does not provide a good correlation between the **slope of grain** and the bending strength, which is too sensitive when the slope of grain is small and is easy to deviate.

  The **moisture content** is linear inversely proportional to the stiffness and strength.

  The **growth ring angle** has an impact on the fracture section form. However, from the current experimental outcome, it is still hard to conclude that the growth ring angle has a clear numerical relationship with the bending strength and stiffness.

  Density is not an efficient sole grading parameter and positively correlates with mechanical properties with only a low coefficient of determination.

  A good positive linear correlation was found between the **dynamic modulus of elasticity** and the bending strength.

  In the combination of those correlations, a new strength prediction model could be established as Eq. 8.8 without taking 3D fiber deviation into account. Some theoretical models considering the 3D fiber orientation are given out but still needs further experimental proof.

Sub questions

- **How physical features (fiber orientation, knots, etc.) of Okan by visual grading could be quantified and simplified during measurement?**

  EN1309-3 and NEN-EN 844-9 regulate methods to measure and quantify timber surface defects. In terms of the slope of grain, image processing methods mentioned in Section 6.1.6 are efficient and more precise than traditional inspection before the destructive testing.

- **What is the relationship between parameters including machine grading (modulus of elasticity, density) and visual grading (knots, slope of grain)?**

  The density at the certain moisture content is decided by timber composition including the knot ratio, fiber length, fiber density, etc., but without strong mathematical relationship.

  Fiber orientation will have an effect on the modulus of elasticity. 2D Hankinson formula is the most common model to describe their correlation, but with an unpredictable scattering.

- **What is the best mathematical way to adjust testing data to reference moisture content and the size?**

  Moisture content is reversely linear correlated to bending strength and modulus of elasticity which are grouped by the slope of grain to eliminate the irrelevant errors.

  The increasing size of a beam is more likely to bring more defects. Subsequently, strength might decrease with the existence of potential failure points. In this thesis, all tested beams conform to the standard. Thus, no size adjustment was conducted.

- **What is the fitting effect of final predicting models?**

  The final predicting model refers to the one derived in Section 8.2. with a preferable coefficient of determination (R^2) = 0.685. Compared to the common linear regression and Hankinson formula, the new model has a remarkable optimization.

- **What are the most suitable thresholds of those influencing factors in the view of producer?**

  In light of the Okan, to achieve the objective D40 or higher classification economically, the limit of slope of grain could be increased up to 0.3 rather than 0.1. Further promotion to 0.2 doesn't improve the outcome and even worsen it.

- **Is the current class D40 as defined in NEN-EN 338(2016) a suitable assignment for this batch of Okan from Gabon?**

  This batch of Okan from Gabon could be conservatively graded into D55 which is better than the overall Okan's classification D40.

- **What could be added or improved for current grading method (procedure) for Okan?**

  This thesis proposes a new visual inspection approach based on the image processing method via Matlab, which could replace the manual check by naked-eye and greatly improve the accuracy of identifying the slope of grain on the beam's surface. This approach could also highlight the critical spot where the major crack occurs, which might offer designers a reference. However, this method could hardly identify the compression failure. To avoid the existence of compression failure, beams with the dynamic modulus of elasticity less than $18500 N/mm^2$ are supposed to be checked again by the inspector. Moreover, to avoid certain fracture forms, the growth ring angle recording is supposed to come into inspection.

9.2. Recommendations

In this thesis, the theory that the growth ring angle might bring influences on mechanical properties is proposed without experimental investigation. It is highly recommended that other researchers could customize the testing procedure to quantify its impacts on the stiffness. Same recommendation for the observation of moisture content's influence.

Inspection of the surface slope of grain should be done at the beginning of manufacture so that the grain pattern would not be covered or contaminated by external substances.

The machine grading result fluctuates less and gives a higher strength grade. If the producer has to pick one of the grading methods, machine grading is a recommended option.

A

Determination the 5th percentile value

Determination the 5th percentile value Descriptive statistics for Sample 1 to Sample 6

Sample ID	mean	s.d.	n	k	fm 0.05
1	92.8	28.3	54	1.81	41.47
2	81.7	12.8	42	1.83	58.28
3	60.2	18.2	44	1.83	26.92
4	77.7	17.6	50	1.82	45.61
5	103.9	19.9	48	1.82	67.71
6	98.7	18.2	50	1.82	65.57

Step 1. fm_{mean} of samples is 86.3N/mm^2

	O	E	$(O-E)^2/E$
1	29.630	49.034	7.7
2	64.286	49.034	4.7
3	95.455	49.034	43.9
4	66.000	49.034	5.9
5	20.833	49.034	16.2
6	18.000	49.034	19.6
Z			98.1
sig			1.33E-19

Step 2. fm_{mean} of the remaining samples is 83.0N/mm^2

	O	E	$(O-E)^2/E$
1	25.9	47.745	10.0
2	47.6	47.745	0.0
3	93.2	47.745	43.2
4	56.0	47.745	1.4
6	16.0	47.745	21.1
Z			75.7
sig			1.39E-15

Step 3. fm_{mean} of the remaining samples is 78.8N/mm^2

	O	E	$(O-E)^2/E$
1	25.9	48.338	10.4
2	33.3	48.338	4.7
3	84.1	48.338	26.4
4	50.0	48.338	0.1
Z			41.6
sig			5.00E-09

Step 4. fm_{mean} of the remaining samples is 73.3N/mm^2

	O	E	$(O-E)^2/E$
2	26.2	47.548	9.6
3	70.5	47.548	11.0
4	46.0	47.548	0.1
Z			20.7
sig			1.23E-04

Step 5. fm_{mean} of the remaining samples is 69.5N/mm^2

	O	E	$(O-E)^2/E$
3	63.6	49.818	3.8
4	36.0	49.818	3.8
Z			7.7
sig			0.0216

Now Sample 3 and Sample 4 are regarded as the weakest samples for determining the characteristic values.

The minimum number of pieces is Sample 3, for which k=1.83 (look up the Tab.4.5)

Then by

$$k_{N,n} = z_p + \frac{(k - z_p)}{\sqrt{N}} \tag{A.1}$$

$$\mathrm{k_{N,n}} = 1.78 \tag{A.2}$$

The average of the means of the bending strength of Sample 3 and 4 is 68.93N/mm^2.

The average of the standard deviations of the bending strength of Sample 3 and 4 is 17.93 N/mm^2.

The 5th percentile value of bending strength of this population is: 68.93-1.78*17.93=**37.01** N/mm^2.

The average of the means of the MOE of Sample 3 and 4 is: (18577+20338)/2=**19457.5**N/mm^2.

The average of the means of the density of Sample 3 and 4 is 982.15 kg/mm^3

The average of the standard deviations of the bending strength of Sample 3 and 4 is 99.95 kg/mm^3

The 5th percentile value of density of this population is: 982.15-1.78* 99.95=**804.24** kg/mm^3

B

Experimental results (data)

		Full-length							a [mm]		900		l1 [mm]		750 l [mm]		2700	
Dry	M [kg]	Freq [Hz]	L [mm]	B [mm]	D [mm]	I [mm4]	Max load	Date	rho [kg/m3]	rho12	Edyn	Edyn12	Eglob	Eglob12	Eloc	Eloc12	fm	fm-12
4	27.700	737	3005	149.5	59.1	16456210	42.6444	5/29/2020	1043.29	1024.85	20468.71	21247.33	19180.527	19910.15	20623.057	21407.55	87.17	90.41
5	30.000	700	3005	149.4	58.7	16312054	37.6269	5/11/2020	1138.38	1016.50	20148.05	23158.68	18694.753	21488.22			77.54	91.13
6	27.900	737	3005	150.0	58.0	16312500	31.8234	5/29/2020	1067.19	1069.30	20937.48	20905.70	19133.224	19057.91	20385.776	20305.53	65.84	65.58
9	26.500	786	3005	149.5	61.2	17040948	51.8469	5/29/2020	963.85	948.42	21508.14	21785.34	18751.954	19393.54	19872.698	20552.63	102.34	105.75
12	27.700	766	3005	149.9	58.6	16448309	49.2543	5/29/2020	1049.39	1028.31	22240.40	22604.29	20181.507	21063.12	23008.657	24013.77	101.00	105.39
16	30.300	693	3005	148.7	58.9	16138641	52.0092	5/29/2020	1151.26	1115.64	19970.42	20490.22	19471.375	20846.32	22689.454	24291.64	107.82	115.18
17	29.500	688	3005	148.3	58.9	16008753	43.0911	5/29/2020	1123.88	1092.90	19215.29	19656.43	17999.396	19114.75			89.82	95.11
18	27.800	758	3005	149.5	59.2	16484054	48.8486	5/29/2020	1045.29	1029.37	21693.26	21958.64	19631.281	20268.16	21469.256	22165.77	99.68	102.83
24	27.200	747	3005	149.0	58.0	15988420	45.5788	5/13/2020	1047.39	1007.13	21110.59	21809.17	19588.776	21368.38	22734.423	24799.80	95.57	104.08
27	26.700	703	3005	149.0	59.0	16264083	35.3567	5/13/2020	1010.71	958.36	18042.14	18881.42	17819.916	20148.46	19395.931	21930.42	72.88	82.27
Wet																		
31	30.980	693	3005	151.0	60.0	17214755	48.5969	6/15/2020	1137.91	1090.72	19738.95	20450.43	17479.063	19217.36	19506.636	21446.58	95.91	105.62
34	30.840	703	3005	151.0	60.0	17214755	46.7647	6/15/2020	1132.77	996.81	20220.94	23242.46	17572.404	20198.17	19679.407	22620.01	92.29	108.76
35	28.750	752	3005	151.0	59.0	16927842	46.9691	6/15/2020	1073.90	947.67	21935.58	25213.31	19159.952	22022.93	21248.463	24423.52	94.27	111.09
38	29.040	737	3005	150.0	61.5	17296875	42.9852	6/15/2020	1047.58	940.31	20552.74	23623.84	18549.22	21320.94	22004.268	25292.26	83.87	98.67
41	31.560	688	3005	151.0	61.0	17501668	45.0568	6/17/2020	1140.21	1080.21	19494.48	20418.15	17657.561	20011.27	19783.45	22420.53	87.47	99.29
42	30.440	708	3005	151.0	60.0	17214755	43.6872	6/17/2020	1118.08	1061.24	20243.59	21164.83	18542.335	20908.57	21348.306	24072.62	86.22	97.39
45	31.480	737	3005	151.5	61.0	17676102	54.2245	6/15/2020	1133.57	1075.00	22239.84	23271.28	19489.138	22027.55	21716.557	24545.09	104.57	118.48
53	31.260	732	3005	151.0	62.0	17788580	50.9972	6/17/2020	1111.16	1019.30	21505.37	24718.82	18929.968	21758.58	19348.746	22239.94	97.40	114.78
54	29.120	693	3005	151.0	64.0	18362405	21.0367	6/17/2020	1002.74	766.78	17394.24	19993.38	12134.927	13948.19	11917.786	13698.60	38.92	45.87
58	32.180	693	3005	150	64	18000000	39.1216	6/17/2020	1115.50	933.89	19350.21	22241.62	17492.794	20106.66	19996.875	22984.91	73.35	86.30

	Cut-out					After testing			Manual Visual inspection			Automation		
Dry	Width	Weight [g]	dry-date	dry-weight	m.c	SOG	DIC	Fiber angle	Ring angle	Fiber Angle	SOG	knot [number]	Global sog range	Critical angle
4	25	219.3	6/2/2020	189.6	15.66	0.140	8	8	25	3.9	0.067			
5	25.2	249.6	6/2/2020	189.5	31.27	0.262	12	15	40	1.6	0.028			
6	25.7	213.5	6/2/2020	191.3	11.60	0.017	1	1	0	4.1	0.071			
9	25.4	220.7	6/2/2020	191.4	15.31	0.175	10	10	90	10.9	0.192			
12	25.2	225.4	6/2/2020	194	16.19	0.087		5	20	2.7	0.047			
16	25.8	244.9	6/2/2020	206.5	18.60	0.262		15	/	7.4	0.129		[1,9] 5	15
17	25.4	228.6	6/2/2020	194	17.84	0.262		15	90	15.0	0.268	2.000		
18	25.1	226.6	6/2/2020	196.8	15.14	0.087	5	5	50	6.6	0.116			
24	25.6	227.3	6/2/2020	188.9	20.33	0.087	5	5	/	5.9	0.103			
27	25.5	237.6	6/2/2020	192.3	23.56	0.192		11	65	9.5	0.167	1.000	[1,7] 1	11
Wet														
31	25	266.3	20-Jul	220.0	21.05	0.262		15	60	8.1	0.14		[1,7] 1	11
34	25	259.4	20-Jul	195.0	33.03	0.262		15	30	6.7	0.12			
35	25	232.2	20-Jul	175.0	32.69	0.087		5	35	2.8	0.05		[1,7] 3	5
38	25	241.7	20-Jul	185.0	30.65	0.017		1	30	3.8	0.07		[1,5] 1	5
41	25.00	259.90	20-Jul	210.0	23.76	0.140		8	45	5.9	0.11		[1,5] 5	7
42	26.20	252.80	20-Jul	205.0	23.32	0.175		10	60	12.8	0.23		[1,5] 5	11
45	25.00	259.40	20-Jul	210.0	23.52	0.087		5	35	5.1	0.09		[1,5] 1	5
53	26.00	262.60	20-Jul	205.0	28.10	0.436		25	90	14.9	0.27		[5,11] 5	15
54	25.50	249.60	20-Jul	165.0	51.27	0.017		1	0	4.3	0.07		[1,5] 1	5
58	25.50	264.50	20-Jul	190.0	39.21	0.349		20	70	23.5	0.44		[1,3] 1	23

C

Matlab (Manual check)

```
clear;
clc;
ObjDir = 'F:\Backup0609\MATLAB\SlopeOfGrainReading\';%file path of images
tnum = 1;%the number of image
 excel = [] % coordinate in mm in (x,y)
 pixel_point = [] %coordinate in pixel in (x,y)
% rename images as:i.jpg(i: from 1 to tnum)

%%%%%%%%%%%%%%%%%%%%%%%%%%%%%%%%%%%%%%%%%%%%%%%%%%%%%%%%%%%%%

for image_number = 1:tnum
     bgFile = [ObjDir,int2str(image_number),'.jpg'];% read images' path
      rgb = imread(bgFile); % read images
      %figure(image_number);
imshow(rgb);
R=rgb(:,:,1); %red
G=rgb(:,:,2); %green
B=rgb(:,:,3); %blue
[x,y,z]=size(rgb);
grain_point = []; %define the marked point coordinates
grain_point_counter=0;

flag_G = 0;

sum_x=0;
sum_y=0;

for j=1:y % loop starts with vertical line
     colored_column=false; % Logical identifier to check if current column contains ...
         colored pixels
     for i=1:x

          % &&
          if (abs(R(i,j)-B(i,j))+abs(G(i,j)-B(i,j))+abs(R(i,j)-G(i,j)) >0) % make sure ...
              its not b&w
              sum_x=sum_x+i;% calculate sum of x coordinates of colored pixels
              sum_y=sum_y+j;% calculate sum of y coordinates of colored pixels
              colored_column=true;
              flag_G=flag_G+1;
          end

     end
     if colored_column==false && flag_G≠0
        grain_point_counter=grain_point_counter+1;%
        grain_point(grain_point_counter,1)=sum_x/flag_G;%calculate average value of the ...
            x coordinates of the dot
```

```
        grain_point(grain_point_counter,2)=sum_y/flag_G;%calculate average value of the ...
            y coordinates of the dot

        sum_x=0; % restore sum of x coordintates for next colored dot
        sum_y=0; % restore sum of x coordintates for next colored dot
        flag_G=0; % restore the counter of colored pixels for next dot
    end

end


%export real point to excel sheet in the real dimension
%grain point's coordination is (x,y) - match the definition of SOG
real_point = []

for p = 1:grain_point_counter

        real_point(p,1)= 150*grain_point(p,1)/x ;
         real_point(p,2)= 3005*grain_point(p,2)/y   ;

end

%write in this image's coordinates

    for t=1:grain_point_counter
        excel(image_number,2*t-1)=real_point(t,1);
        excel(image_number,t*2)=real_point(t,2);
        pixel_point(image_number,2*t-1) = grain_point(t,1);
        pixel_point(image_number,2*t) = grain_point(t,2);
    end

end

% write it into excel sheet
filename = 'slope of grain.xlsx';
writematrix(excel,filename,'Sheet',1,'Range','B3');

%calculate slope of grain
SOG=[];
for i_s = 1: image_number
    for j_s = 1: (grain_point_counter-1)
    SOG(i_s,j_s) = ...
        abs((excel(i_s,2*j_s-1)-excel(i_s,2*j_s+1))/(excel(i_s,2*j_s)-excel(i_s,2*j_s+2)))
    end
end
filename = 'slope of grain.xlsx';
writematrix(SOG,filename,'Sheet',2,'Range','B3')

%inverse tangent in degrees
angle=[];
angle = atand(SOG);
filename = 'slope of grain.xlsx'
writematrix(angle,filename,'Sheet',3,'Range','B3')
```

D
Matlab (Automation)

```
% this file invokes functions extractHOGFeatures_xy.m and Visualization.m
% which are changed based on the Matlab function library.
clear;
close all;
clc;


% ---------------------------------------------------------------
% File location
% ---------------------------------------------------------------
ObjDir = 'C:\Users\chenx\Documents\MATLAB\Automation\';%file path of images
tnum = 60;%the number of image
excel_angle=[];
weight_angle=[];
% ---------------------------------------------------------------
% Define image parameters
% ---------------------------------------------------------------
for image_number = 1
%
%     TimberImg = [ObjDir,int2str(image_number),'A.png'];% read images' path
%   img = imread(TimberImg);
      img = imread('C:\Users\chenx\Documents\MATLAB\Automation\24A.png');%test1.jpg

% Input
BinsNum=90;

SizeCell=32; %32 %16 for small images
% Size of image
[H,W,z]=size(img);

% ---------------------------------------------------------------
% (Pre-process)  Mitigate peripheral noise, cut off the corner information and sharpen
% ---------------------------------------------------------------
Height=round(H*9/10);
Width=round(W);
targetSize = [Height Width];
% targetSize = [H-40 W-40]
r = centerCropWindow2d(size(img),targetSize);
Final_img = imcrop(img,r);

% Final_img=img;

% sharpen the image
w=fspecial('laplacian',0);
g1=imfilter(Final_img,w,'replicate');
```

```
Final_img=Final_img-g1;

% ---------------------------------------------------------------------
% Extract image feature
% ---------------------------------------------------------------------
[ThisHog, visualization] = ...
    extractHOGFeatures_xy(double(Final_img),'CellSize',[SizeCell,2*SizeCell],'BlockSize',[2,2],'NumBin

% free them
figure;
imshow(Final_img);
hold on
visualization.plot; %plot(visualization)



% ---------------------------------------------------------------------
% Extract Histogram matrix
% ---------------------------------------------------------------------
nBins   = visualization.NumBins;
numHOGs       = size(visualization.Feature,1);
featureClass = class(visualization.Feature);
avgHogs = zeros([floor(visualization.WindowSize./visualization.CellSize) nBins ...
    numHOGs], featureClass);
for idx = 1:numHOGs
    avgHogs(:,:,:,idx) = averageHOGs(visualization,idx); %averageHOGs() is a function ...
        shown below
end




% ---------------------------------------------------------------------
% Find each cell's maximum angle value (Judgement condition)
% ---------------------------------------------------------------------

% MaxLocation is page number(val)
% f_x/y is the number of feature in x/y direction
A=visualization.WindowSize./visualization.CellSize ;
avgHogs_x =floor(A(1,2)); % Column number
avgHogs_y= floor(A(1,1)); % Row number

% Creat matrixs
MaxAngleFeature=zeros(avgHogs_y,avgHogs_x);
MaxLocation=zeros(avgHogs_y,avgHogs_x);
MaxAngleValue=zeros(avgHogs_y,avgHogs_x);
Loading=zeros(avgHogs_y,avgHogs_x);
Resistance=zeros(avgHogs_y,avgHogs_x);
Redundancy=zeros(avgHogs_y,avgHogs_x);
Weight=zeros(avgHogs_y,avgHogs_x);

% Calculate the max angle matrix and loading matrix
for i=1:avgHogs_y
    Loading_Cross = (-2*i+1+avgHogs_y)/(1-avgHogs_y);% Assumption: linear stress ...
        distribution
    for j=1:avgHogs_x
        [M, Location_val] = max(avgHogs(i,j,:)); % Find at which page, the cell has max ...
            angle
        MaxAngleFeature(i,j)=M; % MaxAngleFeature stores the max angle information in ...
            the form of feature
        MaxLocation(i,j)=Location_val; % MaxLocation stores at which page the max angle ...
            occurs

        % Loading is calculated according to stress (loading effect matrix)
        if j≥0 && j/avgHogs_x < 1/3
        Loading(i,j)=Loading_Cross* 3*(j-1)/(avgHogs_x-3);
        else if j/avgHogs_x ≥ 1/3 && j/avgHogs_x ≤ 2/3
                Loading(i,j) =Loading_Cross * 1;
            else Loading(i,j) = Loading_Cross*(-3*j/avgHogs_x+3);
            end
        end
```

```

    end

end



% (ÉÏÃæavghogsÖÐµÄ½Ç¶ÈÊÇÒÔyÖáÕýÏòÎª0¶ÈÆðÊ¼¼ÆËã£¬ÏÖÔÚ×ªÎª−90ÖÁ90¶È£¬²Î¿¼xÖáÕýÏòÎª0£¬ ...
    ÄæÊ±ÕëÎªÕý£¬Ë³Ê±ÕëÎª¸º)
AngleList=zeros(BinsNum,2);
for k=1:BinsNum
    AngleList(k,1)=180/BinsNum/2+(k−1)*(180/BinsNum)−90; % Transfer angle to normal ...
        coordination
end

% Calculate effect angle and the redundancy matrix
for i=1:avgHogs_y
    for j=1:avgHogs_x
         Cov = std(avgHogs(i,j,:))/mean(avgHogs(i,j,:));
        if Cov > 0.4
        MaxAngleValue(i,j)=AngleList(MaxLocation(i,j),1);
        al= MaxAngleValue(i,j);
        %f%
        Resistance(i,j)= 166/(33.1*sin(al/180*pi)^2+cos(al/180*pi)^2);
         %f%
        else
            MaxAngleValue(i,j)=NaN;
            %f%
            Resistance(i,j)=NaN;
            %f%
        end
%               Calculate the Redundancy
            if Loading(i,j)<0
                Redundancy(i,j) = 20*Loading(i,j)+Resistance(i,j);%NaN;%( ...
                    20*Loading(i,j)+Resistance(i,j));        compressive
            else if Loading(i,j)≥0
                    Redundancy(i,j) = Resistance(i,j)−20*Loading(i,j);   % tensile
                end
            end
%f%
    end
end

% Creat Weight matrix according to the Redundancy
if numel(find(isnan(MaxAngleValue)))<avgHogs_x*avgHogs_y*0.7

        max_r=  max(max(Redundancy));
        min_r= min(min(Redundancy));
        for i=1:avgHogs_y
            for j=1:avgHogs_x
                    Weight(i,j)=(max_r−Redundancy(i,j))/(max_r−min_r);
                if ¬isnan(Weight(i,j))
                    Order = ((MaxAngleValue(i,j)+90)* BinsNum + 90)/180;
                    AngleList(Order,2)= AngleList(Order,2)+Weight(i,j);
                end
            end
        end

        % −−−−−−−−−−−−−−−−−−−−−−−−−−−−−−−−−−−−−−−−−−−−−−−−−−−−−−−−−−−−−−−−
        % Visuailization
        % −−−−−−−−−−−−−−−−−−−−−−−−−−−−−−−−−−−−−−−−−−−−−−−−−−−−−−−−−−−−−−−−
        % draw line
        [cellCentersXY, cIdx] = computeCellCenters(visualization);
        cellCentersXYangle=reshape(transpose(MaxAngleValue),[],1); % Transfer matrix to ...
            vector

        % free them
            figure;
            imshow(Final_img);
            alpha(0.1);
             hold on
```

```

        for pt = 1:avgHogs_y*avgHogs_x
            if ¬isnan(cellCentersXYangle(pt,1))
            pt_xleft=cellCentersXY(pt,1)-SizeCell/2*cos(cellCentersXYangle(pt,1)/180*pi);
            pt_xright=cellCentersXY(pt,1)+SizeCell/2*cos(cellCentersXYangle(pt,1)/180*pi);
            pt_yleft=cellCentersXY(pt,2)+SizeCell/2*sin(cellCentersXYangle(pt,1)/180*pi);
            pt_yright=cellCentersXY(pt,2)-SizeCell/2*sin(cellCentersXYangle(pt,1)/180*pi);
        % free them
             line([pt_xleft,pt_xright],[pt_yleft,pt_yright],'Color','black','LineWidth',1);
            end
        end

        % Draw stress contour/ load effect

        % free them
        figure;
        imshow(Final_img);
        alpha(0.1);
        hold on
        pcolor(reshape(cellCentersXY(:,1),[avgHogs_x,avgHogs_y])',reshape(cellCentersXY(:,2),[avgHogs_
        shading interp;
        colorbar;
        shading flat;

        % Draw Redundancy matrix --- Delta = R-E (resistance - loading effect/weight)
        % Critical spot detection
        %f5

        % free them
        figure;
        imshow(Final_img);
        alpha(0.1);
        hold on
        pcolor(reshape(cellCentersXY(:,1),[avgHogs_x,avgHogs_y])',reshape(cellCentersXY(:,2),[avgHogs_
        colormap(jet(7));
        colorbar('Ticks',[-25,0,25,50,75,100,125,150]);
        shading flat;

        % xx=reshape(cellCentersXY(:,1),[avgHogs_x,avgHogs_y])';
        % yy=reshape(cellCentersXY(:,2),[avgHogs_x,avgHogs_y])';
        % xx=cellCentersXY(:,1);
        % yy=cellCentersXY(:,2);
        % xxm=max(xx);
        % yym=max(yy);
        % [xq,yq] = meshgrid(0:2:xxm, 0:2:yym);
        % [XX,YY,ZZ]=griddata(xx,yy,reshape(transpose(Redundancy),[],1),xq,yq,'v4');
        % ...
            contourf(reshape(cellCentersXY(:,1),[avgHogs_x,avgHogs_y])',reshape(cellCentersXY(:,2),[av
        % pcolor(XX,YY,Redundancy)



        %f%

        % ----------------------------------------------------------------
        % Output
        % ----------------------------------------------------------------

        % Count frequency of each angle and plot (global_maximum value)

        tb = tabulate(cellCentersXYangle);
        tbc = num2cell(tb);
        t = cell2table(tbc,'VariableNames', ...
          {'Value','Count','Percent'});
%         % free them
        figure;
        b=bar(t.Value,t.Count);
        xlabel('Angle');
        ylabel('Number');
        xtips1 = b.XEndPoints;
        ytips1 = b.YEndPoints;
```

```
        labels1 = string(b.YData);
        text(xtips1,ytips1,labels1,'HorizontalAlignment','center',...
            'VerticalAlignment','bottom');

        [B,I]=sort(t.Count,'descend');
        excel_angle(image_number,1) = tb(I(1,1),1);
        excel_angle(image_number,2) = tb(I(2,1),1);
        excel_angle(image_number,3) = tb(I(3,1),1);
        excel_angle(image_number,4) = tb(I(4,1),1);
        excel_angle(image_number,5) = tb(I(5,1),1);
        % [Ma,Id]=max(tb(:,2),[],1)
        % excel_angle(image_number,1) = tb(Id,1)

        % Count frequency of each angle and plot (Number * Weight value - maximum value)
        % Find max
        [Bi,In]=sort(AngleList(:,2),'descend');
        weight_angle(image_number,1) = AngleList(In(1,1),1);
        weight_angle(image_number,2) = AngleList(In(2,1),1);
        weight_angle(image_number,3) = AngleList(In(3,1),1);
        weight_angle(image_number,4) = AngleList(In(4,1),1);
        weight_angle(image_number,5) = AngleList(In(5,1),1);

    else
        for fine=1:5
            weight_angle(image_number,fine) = NaN;
            excel_angle(image_number,fine) = NaN;
        end
    end
end


        % write it into excel sheet
        filename = 'Automation.xlsx';

        writematrix(excel_angle,filename,'Sheet',1,'Range','B3');

        writematrix(weight_angle,filename,'Sheet',1,'Range','G3');



% -----------------------------------------------------------------
% (Definition function)
% -----------------------------------------------------------------
% -----------------------------------------------------------------
% Average HOG cells across overlapping blocks(Definition function)
% -----------------------------------------------------------------
function hog = averageHOGs(this, idx)

    numCellsPerWindow = floor(this.WindowSize./this.CellSize);
    accum = zeros([numCellsPerWindow this.NumBins], 'single');
    count = zeros(numCellsPerWindow);

    hBlockSize = [this.NumBins this.BlockSize];

    numBlocks = single(vision.internal.hog.getNumBlocksPerWindow(this));

    % reshape features to simplify averaging
    features = reshape(this.Feature(idx,:), [prod(hBlockSize) numBlocks]);

    blockStep = this.BlockStepSize ./ this.CellSize;
    for j = 1:numBlocks(2)
        for i = 1:numBlocks(1)
            hBlock = reshape(features(:,i,j), hBlockSize);
            % offset for cells based on current block position
            ox = (j-1)*blockStep(2);
            oy = (i-1)*blockStep(1);
            for x = 1:this.BlockSize(2)
                for y = 1:this.BlockSize(1)
                    accum(oy+y, ox+x,:) = ...
                        squeeze(accum(oy+y,ox+x,:)) + hBlock(:,y,x);
                    count(oy+y, ox+x)   = count(oy+y, ox+x) + 1;
```

```
                    end
                end
            end
        end

        % average overlapping cells
        count = repmat(count,[1 1 this.NumBins]);
        hog   = accum./(count + eps);
end


        function [centers, indices] = computeCellCenters(this)
            cellSize = this.CellSize;
            winSize  = this.WindowSize - rem(this.WindowSize,this.CellSize);

            % cell centers in spatial coordinates
            [cx,cy] = ndgrid(0.5 + (cellSize(2)/2:cellSize(2):winSize(2)),...
                0.5 + (cellSize(1)/2:cellSize(1):winSize(1)));

            % cell centers in pixel coordinates
            numCells = floor(this.WindowSize./this.CellSize);
            [cxIdx,cyIdy] = ndgrid(1:numCells(2),1:numCells(1));

            centers = [cx(:) cy(:)];
            indices = [cxIdx(:) cyIdy(:)];
        end

%  for k = 1:numHOGs
%                    f = avgHogs(:,:,:,k);
%  end

%function extractHOGFeatures_xy


function [features, varargout] = extractHOGFeatures_xy(I,varargin)
%extractHOGFeatures Extract HOG features.
%  features = extractHOGFeatures(I) extracts HOG features from a truecolor
%  or grayscale image I and returns the features in a 1-by-N vector. These
%  features encode local shape information from regions within an image and
%  can be used for many tasks including classification, detection, and
%  tracking.
%
%  The HOG feature length, N, is based on the image size and the parameter
%  values listed below. See the <a ...
   href="matlab:helpview(fullfile(docroot,'toolbox','vision','vision.map'),'extractHOGFeatures')" ...
   >documentation</a> for more information.
%
%  [features, validPoints] = extractHOGFeatures(I, points) returns HOG
%  features extracted around point locations within I. The function also
%  returns validPoints, which contains the input point locations whose
%  surrounding [CellSize.*BlockSize] region is fully contained within I.
%  The input points can be specified as an M-by-2 matrix of [x y]
%  coordinates, SURFPoints, KAZEPoints, cornerPoints, MSERRegions,
%  ORBPoints or BRISKPoints. Any scale information associated with the
%  points is ignored. The class of validPoints is the same as the input
%  points.
%
%  [..., visualization] = extractHOGFeatures(I, ...) optionally returns a
%  HOG feature visualization that can be shown using plot(visualization).
%
%  [...] = extractHOGFeatures(..., Name, Value) specifies additional
%  name-value pairs described below:
%
%  'CellSize'     A 2-element vector that specifies the size of a HOG cell
%                 in pixels. Select larger cell sizes to capture large
%                 scale spatial information at the cost of loosing small
%                 scale detail.
%
%                 Default: [8 8]
%
%  'BlockSize'    A 2-element vector that specifies the number of cells in
```

```
%                  a block. Large block size values reduce the ability to
%                  minimize local illumination changes.
%
%                  Default: [2 2]
%
%  'BlockOverlap' A 2-element vector that specifies the number of
%                  overlapping cells between adjacent blocks. Select an
%                  overlap of at least half the block size to ensure
%                  adequate contrast normalization. Larger overlap values
%                  can capture more information at the cost of increased
%                  feature vector size. This property has no effect when
%                  extracting HOG features around point locations.
%
%                  Default: ceil(BlockSize/2)
%
%  'NumBins'       A positive scalar that specifies the number of bins in
%                  the orientation histograms. Increase this value to encode
%                  finer orientation details.
%
%                  Default: 9
%
%  'UseSignedOrientation' A logical scalar. When true, orientation
%                         values are binned into evenly spaced bins
%                         between -180 and 180 degrees. Otherwise, the
%                         orientation values are binned between 0 and
%                         180 where values of theta less than 0 are
%                         placed into theta + 180 bins. Using signed
%                         orientations can help differentiate light to
%                         dark vs. dark to light transitions within
%                         an image region.
%
%                         Default: false
%
% Class Support
% -------------
% The input image I can be uint8, int16, double, single, or logical, and it
% must be real and non-sparse. POINTS can be SURFPoints, KAZEPoints,
% ORBPoints, cornerPoints, MSERRegions, BRISKPoints, int16, uint16, int32,
% uint32, single, or double.
%
%
% Example 1 - Extract HOG features from an image.
% -----------------------------------------------
%
%    I1 = imread('gantrycrane.png');
%    [hog1, visualization] = extractHOGFeatures(I1,'CellSize',[32 32]);
%    subplot(1,2,1);
%    imshow(I1);
%    subplot(1,2,2);
%    plot(visualization);
%
% Example 2 - Extract HOG features around corner points.
% ------------------------------------------------------
%
%    I2 = imread('gantrycrane.png');
%    corners   = detectFASTFeatures(rgb2gray(I2));
%    strongest = selectStrongest(corners, 3);
%    [hog2, validPoints, ptVis] = extractHOGFeatures(I2, strongest);
%    figure;
%    imshow(I2); hold on;
%    plot(ptVis, 'Color','green');
%
% See also extractFeatures, extractLBPFeatures, detectHarrisFeatures,
% detectFASTFeatures, detectMinEigenFeatures, detectSURFFeatures,
% detectMSERFeatures, detectBRISKFeatures, detectORBFeatures

% Copyright 2012-2018 The MathWorks, Inc.
%
% References
% ----------
% N. Dalal and B. Triggs, "Histograms of Oriented Gradients for Human
```

```
% Detection", Proc. IEEE Conf. Computer Vision and Pattern Recognition,
% vol. 1, pp. 886-893, 2005.
%

%#codegen
%#ok<*EMCA>

notCodegen = isempty(coder.target);

[points, isPoints, params, maxargs] = parseInputs(I,varargin{:});

% check number of outputs
if notCodegen
    nargoutchk(0,maxargs);
else
    checkNumOutputsForCodegen(nargout, maxargs);
end

if isPoints

    [features, validPoints] = extractHOGFromPoints(I, points, params);

    if nargout ≥ 2
        varargout{1} = validPoints;
    end

    if notCodegen
        if nargout == 3
            params.Points = validPoints;
            varargout{2}  = Visualization(features, params);
        end
    end
else

    features = extractHOGFromImage(I, params);

    if notCodegen
        if nargout == 2
            varargout{1} = Visualization(features, params);
        end
    end
end

% -------------------------------------------------------------------------
% Extract HOG features from whole image
% -------------------------------------------------------------------------
function features = extractHOGFromImage(I, params)
[gMag, gDir] = hogGradient(I);

[gaussian, spatial] = computeWeights(params);

features = extractHOG(gMag, gDir, gaussian, spatial, params);

% -------------------------------------------------------------------------
% Extract HOG features from point locations
% -------------------------------------------------------------------------
function [features, validPoints] = extractHOGFromPoints(I, points, params)

featureClass = coder.internal.const('single');
uintClass    = coder.internal.const('uint32');

blockSizeInPixels = params.CellSize.*params.BlockSize;

% compute weights
[gaussian, spatial] = computeWeights(params);

if ¬isnumeric(points)
    xy = points.Location;
else
    xy = points;
end
```

```
featureSize = vision.internal.hog.getFeatureSize(params);

halfSize = (single(blockSizeInPixels) - mod(single(blockSizeInPixels),2))./2;

roi = [1 1 blockSizeInPixels]; % [r c height width]

numPoints       = cast(size(xy,1), uintClass);
validPointIdx   = zeros(1, numPoints , uintClass);
validPointCount = zeros(1, uintClass);

features = zeros(numPoints, featureSize, featureClass);
for i = 1:numPoints

    % ROI centered at point location
    roi(1:2) = cast(round(xy(i,[2 1])), featureClass) - halfSize;

    % only process if ROI is fully contained within the image
    if all(roi(1:2) ≥ 1) && ...
            roi(1)+roi(3)-1 ≤ params.ImageSize(1) && ...
            roi(2)+roi(4)-1 ≤ params.ImageSize(2)

        validPointCount = validPointCount + 1;

        [gMag, gDir] = hogGradient(I, roi);

        hog = extractHOG(gMag, gDir, gaussian, spatial, params);

        features(validPointCount,:) = hog(:);
        validPointIdx(validPointCount) = i; % store valid indices
    end

end

features = features(1:validPointCount,:);

validPoints = extractValidPoints(points, validPointIdx(1:validPointCount));

% -------------------------------------------------------------------------
% Extract HOG features given gradient magnitudes and directions
% -------------------------------------------------------------------------
function hog = extractHOG(gMag, gDir, gaussianWeights, weights, params)

if isempty(coder.target)
    hog = visionExtractHOGFeatures(gMag, gDir, gaussianWeights, params, weights);
else
    featureClass = 'single';

    if params.UseSignedOrientation
        % make gDir range from [0 360]
        histRange = single(360);
    else
        % convert to unsigned orientation, range [0 180]
        histRange = single(180);
    end

    % range of gDir is [-180 180], convert range to [0 180] or [0 360]
    negDir = gDir < 0;
    gDir(negDir) = histRange + gDir(negDir);

    % orientation bin locations for all cells
    binWidth = histRange/cast(params.NumBins, featureClass);
    [x1, b1] = computeLowerHistBin(gDir, binWidth);
    wDir = 1 - (gDir - x1)./binWidth;

    blockSizeInPixels = params.CellSize.*params.BlockSize;
    blockStepInPixels = params.CellSize.*(params.BlockSize - params.BlockOverlap);

    r = 1:blockSizeInPixels(1);
    c = 1:blockSizeInPixels(2);

```

```
    nCells   = params.BlockSize;
    nBlocks = vision.internal.hog.getNumBlocksPerWindow(params);

    numCellsPerBlock = nCells(1)*nCells(2);
    hog = coder.nullcopy(...
        zeros([params.NumBins*numCellsPerBlock, nBlocks],...
        featureClass));
    % scan across all blocks
    for j = 1:nBlocks(2)

        for i = 1:nBlocks(1)

            wz1 = wDir(r,c);

            w = trilinearWeights(wz1, weights);

            % apply gaussian weights
            m = gMag(r,c) .* gaussianWeights;

            % interpolate magnitudes for binning
            mx1y1z1 = m .* w.x1_y1_z1;
            mx1y1z2 = m .* w.x1_y1_z2;
            mx1y2z1 = m .* w.x1_y2_z1;
            mx1y2z2 = m .* w.x1_y2_z2;
            mx2y1z1 = m .* w.x2_y1_z1;
            mx2y1z2 = m .* w.x2_y1_z2;
            mx2y2z1 = m .* w.x2_y2_z1;
            mx2y2z2 = m .* w.x2_y2_z2;

            orientationBins = b1(r,c);

            % initialize block histogram to zero
            h = zeros(params.NumBins+2, nCells(1)+2, nCells(2)+2, featureClass);

            % accumulate interpolated magnitudes into block histogram
            for x = 1:blockSizeInPixels(2)
                cx = weights.cellX(x);
                for y = 1:blockSizeInPixels(1)
                    z  = orientationBins(y,x);
                    cy = weights.cellY(y);

                    h(z,   cy,   cx  ) = h(z,   cy,   cx  ) + mx1y1z1(y,x);
                    h(z+1, cy,   cx  ) = h(z+1, cy,   cx  ) + mx1y1z2(y,x);
                    h(z,   cy+1, cx  ) = h(z,   cy+1, cx  ) + mx1y2z1(y,x);
                    h(z+1, cy+1, cx  ) = h(z+1, cy+1, cx  ) + mx1y2z2(y,x);
                    h(z,   cy,   cx+1) = h(z,   cy,   cx+1) + mx2y1z1(y,x);
                    h(z+1, cy,   cx+1) = h(z+1, cy,   cx+1) + mx2y1z2(y,x);
                    h(z,   cy+1, cx+1) = h(z,   cy+1, cx+1) + mx2y2z1(y,x);
                    h(z+1, cy+1, cx+1) = h(z+1, cy+1, cx+1) + mx2y2z2(y,x);
                end
            end

            % wrap orientation bins
            h(2,:,:)     = h(2,:,:)     + h(end,:,:);
            h(end-1,:,:) = h(end-1,:,:) + h(1,:,:);

            % only keep valid portion of the block histogram
            h = h(2:end-1,2:end-1,2:end-1);

            % normalize and add block to feature vector
            hog(:,i,j) = normalizeL2Hys(h(:));

            r = r + blockStepInPixels(1);
        end
        r = 1:blockSizeInPixels(1);
        c = c + blockStepInPixels(2);
    end

    hog = reshape(hog, 1, [])
end
```

```
% ----------------------------------------------------------------------------
% Normalize vector using L2-Hys
% ----------------------------------------------------------------------------
function x = normalizeL2Hys(x)
classToUse = class(x);
x = x./(norm(x,2) + eps(classToUse)); % L2 norm
x(x > 0.2) = 0.2;                      % Clip to 0.2
x = x./(norm(x,2) + eps(classToUse)); % repeat L2 norm

% ----------------------------------------------------------------------------
% Compute the interpolation weights for the spatial histogram over cells
% ----------------------------------------------------------------------------
function weights = spatialHistWeights(params)
% 2D interpolation weights are computed for 4 points surrounding (x,y)
%
% (x1,y1) o---------o (x2,y1)
%         |         |
%         |  (x,y)  |
%         |         |
% (x1,y2) o---------o (x2,y2)
%
% (x,y) are the pixel centers within a HOG Block
%
% (x1,y1); (x2,y1); (x1,y2); (x2,y2) are cell centers within a block

width  = single(params.BlockSize(2)*params.CellSize(2));
height = single(params.BlockSize(1)*params.CellSize(1));

x = 0.5:1:width;
y = 0.5:1:height;

[x1, cellX1] = computeLowerHistBin(x, params.CellSize(2));
[y1, cellY1] = computeLowerHistBin(y, params.CellSize(1));

wx1 = 1 - (x - x1)./single(params.CellSize(2));
wy1 = 1 - (y - y1)./single(params.CellSize(1));

weights.x1y1 = wy1' * wx1;
weights.x2y1 = wy1' * (1-wx1);
weights.x1y2 = (1-wy1)' * wx1;
weights.x2y2 = (1-wy1)' * (1-wx1);

% also store the cell indices
weights.cellX = cellX1;
weights.cellY = cellY1;

% ----------------------------------------------------------------------------
% Compute tri-linear weights
% ----------------------------------------------------------------------------
function weights = trilinearWeights(wz1, spatialWeights)

% define struct fields before usage
weights.x1_y1_z1 = coder.nullcopy(wz1);
weights.x1_y1_z2 = coder.nullcopy(wz1);
weights.x2_y1_z1 = coder.nullcopy(wz1);
weights.x2_y1_z2 = coder.nullcopy(wz1);
weights.x1_y2_z1 = coder.nullcopy(wz1);
weights.x1_y2_z2 = coder.nullcopy(wz1);
weights.x2_y2_z1 = coder.nullcopy(wz1);
weights.x2_y2_z2 = coder.nullcopy(wz1);

weights.x1_y1_z1 = wz1 .* spatialWeights.x1y1;
weights.x1_y1_z2 = spatialWeights.x1y1 - weights.x1_y1_z1;
weights.x2_y1_z1 = wz1 .* spatialWeights.x2y1;
weights.x2_y1_z2 = spatialWeights.x2y1 - weights.x2_y1_z1;
weights.x1_y2_z1 = wz1 .* spatialWeights.x1y2;
weights.x1_y2_z2 = spatialWeights.x1y2 - weights.x1_y2_z1;
weights.x2_y2_z1 = wz1 .* spatialWeights.x2y2;
weights.x2_y2_z2 = spatialWeights.x2y2 - weights.x2_y2_z1;

% ----------------------------------------------------------------------------
```

```
% Compute the closest bin center x1 that is less than or equal to x
% --------------------------------------------------------------------------
function [x1, b1] = computeLowerHistBin(x, binWidth)
% Bin index
width    = single(binWidth);
invWidth = 1./width;
bin      = floor(x.*invWidth - 0.5);

% Bin center x1
x1 = width * (bin + 0.5);

% add 2 to get to 1-based indexing
b1 = int32(bin + 2);

% --------------------------------------------------------------------------
% Compute Gaussian and spatial weights
% --------------------------------------------------------------------------
function [gaussian, spatial] = computeWeights(params)
blockSizeInPixels = params.CellSize.*params.BlockSize;
gaussian = gaussianWeights(blockSizeInPixels);
spatial  = spatialHistWeights(params);

% --------------------------------------------------------------------------
% Gradient computation using central difference filter [-1 0 1]. Gradients
% at the image borders are computed using forward difference. Gradient
% directions are between -180 and 180 degrees measured counterclockwise
% from the positive X axis.
% --------------------------------------------------------------------------
function [gMag, gDir] = hogGradient(img,roi)

if nargin == 1
    roi = [];
    imsize = size(img);
else
    imsize = roi(3:4);
end

img = single(img);

if ndims(img)==3
    rgbMag = zeros([imsize(1:2) 3], 'like', img);
    rgbDir = zeros([imsize(1:2) 3], 'like', img);

    for i = 1:3
        [rgbMag(:,:,i), rgbDir(:,:,i)] = computeGradient(img(:,:,i),roi);
    end

    % find max color gradient for each pixel
    [gMag, maxChannelIdx] = max(rgbMag,[],3);

    % extract gradient directions from locations with maximum magnitude
    sz = size(rgbMag);
    [rIdx, cIdx] = ndgrid(1:sz(1), 1:sz(2));
    ind  = sub2ind(sz, rIdx(:), cIdx(:), maxChannelIdx(:));
    gDir = reshape(rgbDir(ind), sz(1:2));
else
    [gMag,gDir] = computeGradient(img,roi);
end

% --------------------------------------------------------------------------
% Gradient computation for ROI within an image.
% --------------------------------------------------------------------------
function [gx, gy] = computeGradientROI(img, roi)
img    = single(img);
imsize = size(img);

% roi is [r c height width]
rIdx = roi(1):roi(1)+roi(3)-1;
cIdx = roi(2):roi(2)+roi(4)-1;

imgX = coder.nullcopy(zeros([roi(3)    roi(4)+2], 'like', img)); %#ok<NASGU>
```

```
imgY = coder.nullcopy(zeros([roi(3)+2 roi(4)  ], 'like', img)); %#ok<NASGU>

% replicate border pixels if ROI is on the image border.
if rIdx(1) == 1 || cIdx(1)==1  || rIdx(end) == imsize(1) ...
        || cIdx(end) == imsize(2)

    if rIdx(1) == 1
        padTop = img(rIdx(1), cIdx);
    else
        padTop = img(rIdx(1)-1, cIdx);
    end

    if rIdx(end) == imsize(1)
        padBottom = img(rIdx(end), cIdx);
    else
        padBottom = img(rIdx(end)+1, cIdx);
    end

    if cIdx(1) == 1
        padLeft = img(rIdx, cIdx(1));
    else
        padLeft = img(rIdx, cIdx(1)-1);
    end

    if cIdx(end) == imsize(2)
        padRight = img(rIdx, cIdx(end));
    else
        padRight = img(rIdx, cIdx(end)+1);
    end

    imgX = [padLeft img(rIdx,cIdx) padRight];
    imgY = [padTop; img(rIdx,cIdx);padBottom];
else
    imgX = img(rIdx,[cIdx(1)-1 cIdx cIdx(end)+1]);
    imgY = img([rIdx(1)-1 rIdx rIdx(end)+1],cIdx);
end

gx = conv2(imgX, [1 0 -1], 'valid');
gy = conv2(imgY, [1;0;-1], 'valid');

% -------------------------------------------------------------------------
function [gMag,gDir] = computeGradient(img,roi)

if isempty(roi)
    gx = zeros(size(img), 'like', img);
    gy = zeros(size(img), 'like', img);

    gx(:,2:end-1) = conv2(img, [1 0 -1], 'valid');
    gy(2:end-1,:) = conv2(img, [1;0;-1], 'valid');

    % forward difference on borders
    gx(:,1)   = img(:,2)   - img(:,1);
    gx(:,end) = img(:,end) - img(:,end-1);

    gy(1,:)   = img(2,:)   - img(1,:);
    gy(end,:) = img(end,:) - img(end-1,:);
else
    [gx, gy] = computeGradientROI(img, roi);
end

% return magnitude and direction
gMag = hypot(gx,gy);
gDir = atan2d(-gy,gx);

% -------------------------------------------------------------------------
% Compute spatial weights for HOG blocks.
% -------------------------------------------------------------------------
function h = gaussianWeights(blockSize)

sigma = 0.5 * cast(blockSize(1), 'double');

```

```
h = fspecial('gaussian', double(blockSize), sigma);

h = cast(h, 'single');

% -----------------------------------------------------------------------
% Extract valid points
% -----------------------------------------------------------------------
function validPoints = extractValidPoints(points, idx)
if isnumeric(points)
    validPoints = points(idx,:);
else
    if isempty(coder.target)
        validPoints = points(idx);
    else
        validPoints = getIndexedObj(points, idx);
    end
end

% -----------------------------------------------------------------------
% Input parameter parsing and validation
% -----------------------------------------------------------------------
function [points, isPoints, params, maxargs] = parseInputs(I, varargin)

notCodegen = isempty(coder.target);

sz = size(I);
validateImage(I);

if mod(nargin-1,2) == 1
    isPoints = true;
    points = varargin{1};
    checkPoints(points);
else
    isPoints = false;
    points = ones(0,2);
end

if notCodegen
    p = getInputParser();
    parse(p, varargin{:});
    userInput = p.Results;
    validate(userInput);
    autoOverlap = ¬isempty(regexp([p.UsingDefaults{:} ''],...
        'BlockOverlap','once'));
else
    if isPoints
        [userInput, autoOverlap] = codegenParseInputs(varargin{2:end});
    else
        [userInput, autoOverlap] = codegenParseInputs(varargin{:});
    end
    validate(userInput);
end

params = setParams(userInput,sz);
if autoOverlap
    params.BlockOverlap = getAutoBlockOverlap(params.BlockSize);
end
crossValidateParams(params);

if isPoints
    maxargs = 3;
    params.WindowSize = params.BlockSize .* params.CellSize;
else
    maxargs = 2;
    params.WindowSize = params.ImageSize;
end

% -----------------------------------------------------------------------
% Input image validation
% -----------------------------------------------------------------------
function validateImage(I)
```

```
% validate image
validateattributes(I, {'double','single','int16','uint8','logical'},...
    {'nonempty','real', 'nonsparse','size', [NaN NaN NaN]},...
    'extractHOGFeatures');

sz = size(I);
coder.internal.errorIf(ndims(I)==3 && sz(3) ≠ 3,...
    'vision:dims:imageNot2DorRGB');

coder.internal.errorIf(any(sz(1:2) < 3),...
    'vision:extractHOGFeatures:imageDimsLT3x3');

% ------------------------------------------------------------------------
% Input parameter parsing for codegen
% ------------------------------------------------------------------------
function [results, usingDefaultBlockOverlap] = codegenParseInputs(varargin)

% Check for string and error
for n = 1 : numel(varargin)
    if isstring(varargin{n})
        coder.internal.errorIf(isstring(varargin{n}), ...
            'vision:validation:stringnotSupportedforCodegen');
    end
end

pvPairs = struct( ...
    'CellSize',      uint32(0), ...
    'BlockSize',     uint32(0), ...
    'BlockOverlap', uint32(0),...
    'NumBins',       uint32(0),...
    'UseSignedOrientation', uint32(0));

popt = struct( ...
    'CaseSensitivity', false, ...
    'StructExpand'    , true, ...
    'PartialMatching', true);

defaults = getParamDefaults();

optarg = eml_parse_parameter_inputs(pvPairs, popt, varargin{:});

usingDefaultBlockOverlap = ¬optarg.BlockOverlap;

results.CellSize  = eml_get_parameter_value(optarg.CellSize, ...
    defaults.CellSize, varargin{:});

results.BlockSize = eml_get_parameter_value(optarg.BlockSize, ...
    defaults.BlockSize, varargin{:});

results.BlockOverlap = eml_get_parameter_value(optarg.BlockOverlap, ...
    defaults.BlockOverlap, varargin{:});

results.NumBins = eml_get_parameter_value(optarg.NumBins, ...
    defaults.NumBins, varargin{:});

results.UseSignedOrientation  = eml_get_parameter_value(...
    optarg.UseSignedOrientation, ...
    defaults.UseSignedOrientation, varargin{:});

% ------------------------------------------------------------------------
% Set block overlap based on block size
% ------------------------------------------------------------------------
function autoBlockSize = getAutoBlockOverlap(blockSize)
szGTOne = blockSize > 1;
autoBlockSize = zeros(size(blockSize), 'like', blockSize);
autoBlockSize(szGTOne) = cast(ceil(double(blockSize(szGTOne))./2), 'like', ...
    blockSize);

% ------------------------------------------------------------------------
% Default parameter values
% ------------------------------------------------------------------------
```

```
function defaults = getParamDefaults()
intClass = 'int32';
defaults = struct('CellSize'    , cast([8 8],intClass),...
    'BlockSize'   , cast([2 2],intClass), ...
    'BlockOverlap', cast([1 1],intClass), ...
    'NumBins'     , cast( 9   ,intClass), ...
    'UseSignedOrientation', false,...
    'ImageSize' , cast([1 1],intClass),...
    'WindowSize', cast([1 1],intClass));

% -------------------------------------------------------------------------
function params = setParams(userInput,sz)
params.CellSize     = reshape(int32(userInput.CellSize), 1, 2);
params.BlockSize    = reshape(int32(userInput.BlockSize), 1 , 2);
params.BlockOverlap = reshape(int32(userInput.BlockOverlap), 1, 2);
params.NumBins      = int32(userInput.NumBins);
params.UseSignedOrientation = logical(userInput.UseSignedOrientation);
params.ImageSize  = int32(sz(1:2));
params.WindowSize = int32([1 1]);

% -------------------------------------------------------------------------
% Input parameter validation
% -------------------------------------------------------------------------
function validate(params)

checkSize(params.CellSize,  'CellSize');

checkSize(params.BlockSize, 'BlockSize');

checkOverlap(params.BlockOverlap);

checkNumBins(params.NumBins);

checkUsedSigned(params.UseSignedOrientation);

% -------------------------------------------------------------------------
% Cross validation of input values
% -------------------------------------------------------------------------
function crossValidateParams(params)
% Cross validate parameters

coder.internal.errorIf(any(params.BlockOverlap(:) ≥ params.BlockSize(:)), ...
    'vision:extractHOGFeatures:blockOverlapGEBlockSize');

% -------------------------------------------------------------------------
function parser = getInputParser()
persistent p;
if isempty(p)

    defaults = getParamDefaults();
    p = inputParser();

    addOptional(p, 'Points', []);
    addParameter(p, 'CellSize',     defaults.CellSize);
    addParameter(p, 'BlockSize',    defaults.BlockSize);
    addParameter(p, 'BlockOverlap', defaults.BlockOverlap);
    addParameter(p, 'NumBins',      defaults.NumBins);
    addParameter(p, 'UseSignedOrientation', defaults.UseSignedOrientation);

    parser = p;
else
    parser = p;
end

% -------------------------------------------------------------------------
function checkPoints(pts)

if vision.internal.inputValidation.isValidPointObj(pts)
    vision.internal.inputValidation.checkPoints(pts, mfilename, 'POINTS');
else
    validateattributes(pts, ...
```

```
        {'int16', 'uint16', 'int32', 'uint32', 'single', 'double'}, ...
        {'2d', 'nonsparse', 'real', 'size', [NaN 2]},...
        mfilename, 'POINTS');
    % Use standard checkPoints to guard against gpuArrays
    if isa(pts, 'gpuArray')
        vision.internal.inputValidation.checkPoints(pts, mfilename, 'POINTS');
    end
end

% ------------------------------------------------------------------------
function checkSize(sz,name)

vision.internal.errorIfNotFixedSize(sz, name);
validateattributes(sz, {'numeric'}, ...
    {'real','finite','positive','nonsparse','numel',2,'integer'},...
    'extractHOGFeatures',name);

% ------------------------------------------------------------------------
function checkOverlap(sz)

vision.internal.errorIfNotFixedSize(sz, 'BlockOverlap');
validateattributes(sz, {'numeric'}, ...
    {'real','finite','nonnegative','nonsparse','numel',2,'integer'},...
    'extractHOGFeatures','BlockOverlap');

% ------------------------------------------------------------------------
function checkNumBins(x)

vision.internal.errorIfNotFixedSize(x, 'NumBins');
validateattributes(x, {'numeric'}, ...
    {'real','positive','scalar','finite','nonsparse','integer'},...
    'extractHOGFeatures','NumBins');

% ------------------------------------------------------------------------
function checkUsedSigned(isSigned)

vision.internal.errorIfNotFixedSize(isSigned, 'UseSignedOrientation');
validateattributes(isSigned, {'logical','numeric'},...
    {'nonnan', 'scalar', 'real','nonsparse'},...
    'extractHOGFeatures','UseSignedOrientation');

% ------------------------------------------------------------------------
function checkNumOutputsForCodegen(numOut, maxargs)

if ¬isempty(coder.target)
    % Do not allow HOG visualization if generating code
    coder.internal.errorIf(numOut > maxargs-1,...
        'vision:extractHOGFeatures:hogVisualizationNotSupported');
end






%function: visualization


%Visualization Displays HOG features.
%  Visualization is a Visualization of HOG features extracted from an
%  image. This Visualization is returned by the extractHOGFeatures function
%  and can be displayed using plot.
%
%  plot(Visualization) plots the HOG features as an array of rose
%  plots. Each rose plot shows the distribution of edge directions within a
%  cell. The distribution is visualized by a set of directed lines whose
%  lengths are scaled to indicate the contribution made by the gradients in
%  that particular direction. The line directions are fixed to the bin
%  centers of the orientation histograms and are between 0 and 360 degrees
%  measured counterclockwise from the positive X axis. The bin centers are
%  recorded in the BinCenters property.
```

```
%
%  plot(Visualization, AX) plots HOG features into the axes AX.
%
%  plot(..., Name, Value) specifies additional name-value pair arguments:
%
%   'Color'
%      <a href="matlab:helpview(fullfile(docroot, 'toolbox','matlab', ...
   'helptargets.map'),'colorspec')">ColorSpec</a>
%      Specifies the color used to plot HOG features.
%
%  Visualization properties:
%
%  CellSize              - Size of cells in pixels
%  BlockSize             - Number of cells in each block
%  BlockOverlap          - Overlap between adjacent blocks
%  NumBins               - Number of orientation bins
%  UseSignedOrientation  - Determines if signed orientation values are used
%  BinCenters            - Centers of the histogram bins
%
%  Example 1 - Visualize HOG features
%  ----------------------------------
%
%    I1 = imread('gantrycrane.png');
%    [¬, Visualization] = extractHOGFeatures(I1,'CellSize',[32 32]);
%    plot(Visualization)
%
%  Example 2 - Overlay HOG features on an image
%  --------------------------------------------
%
%    I2 = imread('gantrycrane.png');
%    [¬, Visualization2] = extractHOGFeatures(I2,'CellSize',[32 32]);
%    figure;
%    imshow(I2);
%    hold on
%    plot(Visualization2, 'Color', 'green')
%
%  See also extractHOGFeatures

classdef(HandleCompatible) Visualization < matlab.mixin.CustomDisplay
    % ---------------------------------------------------------------------
    % Public read-only properties
    % ---------------------------------------------------------------------
    properties (GetAccess = public)
        avgHogsLog

    end

    properties (GetAccess = public, SetAccess=protected)
        % CellSize - Size of a HOG cell in pixel units
        CellSize
        % BlockSize - Number of cells in each block
        BlockSize
        % BlockOverlap - Number of overlapping cells between adjacent
        %                blocks
        BlockOverlap
        % NumBins - Number of orientation bins
        NumBins
        % UseSignedOrientation - Determines if signed orientation values
        % are used. When false, the orientation histogram range is
        % from 0 to 180 degrees. Otherwise it is between 0 and 360.
        UseSignedOrientation
        Feature
        BlockStepSize

    end

    % ---------------------------------------------------------------------
    % Public read-only properties
    % ---------------------------------------------------------------------
    properties(GetAccess = public, SetAccess = protected, Dependent = true)
        % BinCenters - Centers of the histogram bins
```

```
        BinCenters
    end

    % ------------------------------------------------------------------------
    % Protected properties
    % ------------------------------------------------------------------------
    properties(Hidden, SetAccess = protected, GetAccess = protected)

        ImageSize
        Points
    end

    % ------------------------------------------------------------------------
    % Hidden read-only properties
    % ------------------------------------------------------------------------
    properties(Hidden, SetAccess = protected, GetAccess = public)
        % WindowSize is accessed by external helper functions
        WindowSize
    end

    % ------------------------------------------------------------------------
    % Private properties
    % ------------------------------------------------------------------------
    properties(Hidden, Access = private, Dependent = true)
        BlockSizeInPixels

    end

    methods
        % --------------------------------------------------------------------
        % Plot method for visualizing HOG features
        % --------------------------------------------------------------------
        function hData = plot(this,varargin)
            % plot(Visualization) plots HOG features as an array of
            % rose plots.
            %
            % plot(Visualization, AX) plots features into the axes AX.
            %
            % plot(..., Name, Value) specifies additional name-value pair
            % arguments:
            %
            %  'Color'
            %      <a href=”matlab:doc('ColorSpec')”>ColorSpec</a>
            %       Specifies the color used to plot HOG features.
            %
            % Example - Visualize HOG features
            % ------------------------------------
            %
            %   I1 = imread('gantrycrane.png');
            %   [¬, hogVis] = extractHOGFeatures(I1,'CellSize',[32 32]);
            %   plot(hogVis)

            [colorSpec, axes] = parseInputs(this, varargin{:});

            if isempty(this.Feature)
                warning(message('vision:extractHOGFeatures:nothingToPlot'));
                if nargout > 0
                    hData = [];
                end
            else

                nBins   = this.NumBins;

                % average HOGs over overlapping cells
                numHOGs      = size(this.Feature,1);
                featureClass = class(this.Feature);
                avgHogs = zeros([floor(this.WindowSize./this.CellSize) nBins numHOGs], ...
                     featureClass);
                for idx = 1:numHOGs
                    avgHogs(:,:,:,idx) = this.averageHOGs(idx);
                end
```

```
            this.avgHogsLog=avgHogs;
            [cellCentersXY, cIdx] = computeCellCenters(this);

            x = zeros(2, nBins, size(cellCentersXY,1), numHOGs);
            y = zeros(2, nBins, size(cellCentersXY,1), numHOGs);

            % compute spatial offset of HOG blocks when extracted around
            % point locations.
            if ¬isempty(this.Points)
                blockCenter = (this.WindowSize - mod(this.WindowSize,2))./2 + 1;
                dxdy = bsxfun(@minus, round(this.Points), fliplr(blockCenter));
            else
                dxdy = zeros(1,2);
            end

            endPoints = computeLineEndPoints(this);

            % scale factor based on cellSize, adjusted to look nice
            lineScale = min(this.CellSize);

            for k = 1:numHOGs
                f = avgHogs(:,:,:,k);
                blockOffset = dxdy(k,:);

                for idx = 1:size(cellCentersXY,1)
                    startPoints  = ones([nBins 1])*(cellCentersXY(idx,:) + ...
                        blockOffset);

                    vals = squeeze(f(cIdx(idx,2), cIdx(idx,1), :));

                    vals = vals./(norm(vals,2) + eps);

                    if this.UseSignedOrientation
                        x1y1 = startPoints;
                    else
                        x1y1 = startPoints + lineScale .* ...
                            bsxfun(@times,-endPoints,vals);
                    end

                    x2y2 = startPoints + lineScale .* bsxfun(@times,endPoints,vals);

                    pts = [x1y1 x2y2];
                    x(:,:,idx,k) = pts(:,[1 3])';
                    y(:,:,idx,k) = pts(:,[2 4])';
                end
            end

            x = reshape(x,2,[]);
            y = reshape(y,2,[]);
            x(end+1,:) = NaN;
            y(end+1,:) = NaN;

            try
                ax = newplot(axes);

                % plot the hog cell lines and markers for cell centers.
                lns = plot(x(:), y(:), '-', ...
                    cellCentersXY(:,1), cellCentersXY(:,2), '.',...
                    'Color', colorSpec, ...
                    'Parent', ax, ...
                    'MarkerSize', 1);

                rects = zeros(1,numHOGs);
                if ¬isempty(this.Points)
                    % add a rectangle around point locations
                    for k = 1:numHOGs
                        rects(k) = rectangle('Parent',ax,...
                            'EdgeColor',colorSpec,...
                            'Position',[dxdy(k,:)+0.5 ...
                            fliplr(this.CellSize.*this.BlockSize)]);
                    end
```

```
                    end
                catch aError
                    throwAsCaller(aError);
                end

                if ¬ishold
                    ax = get(lns(1),'Parent');
                    set(ax,'Ydir','reverse','Color',[0 0 0]);
                    axis(ax,'image');
                    set(ax, ...
                        'XLim',[0 this.ImageSize(2)]+0.5, ...
                        'YLim',[0 this.ImageSize(1)]+0.5, ...
                        'YTickLabel','', ...
                        'XTickLabel','');
                end

                if nargout == 1
                    hData = [lns(1) rects];
                end
            end
        end
    end

    % -----------------------------------------------------------------
    % Get methods for dependent properties
    % -----------------------------------------------------------------
    methods
        % -------------------------------------------------------------
        % Convert block size from cells to pixels
        % -------------------------------------------------------------
        function sz = get.BlockSizeInPixels(this)
            sz = this.CellSize .* this.BlockSize;
        end

        % -------------------------------------------------------------
        % Compute block step size from the overlap
        % -------------------------------------------------------------
        function sz = get.BlockStepSize(this)
            sz = this.CellSize.*(this.BlockSize - this.BlockOverlap);
        end

        % -------------------------------------------------------------
        % Compute bin centers based on NumBins and UseSignedOrientation
        % -------------------------------------------------------------
        function centers = get.BinCenters(this)
            centers = computeBinCenters(this);
            if ¬this.UseSignedOrientation
                centers = [centers; centers + 180];
            end
            centers = double(sort(mod(centers, 360)));
        end
    end

    methods (Hidden)
        % -------------------------------------------------------------
        % Constructor
        % -------------------------------------------------------------
        function this = Visualization(features, params)
            if nargin > 0
                this.Feature     = features;
                this.NumBins     = single(params.NumBins);
                this.CellSize    = single(params.CellSize);
                this.ImageSize   = single(params.ImageSize);
                this.BlockSize   = single(params.BlockSize);
                this.WindowSize = single(params.WindowSize);
                this.BlockOverlap = single(params.BlockOverlap);
                this.UseSignedOrientation = params.UseSignedOrientation;

                % check if HOG features are extracted around points
                if isfield(params,'Points')
                    if isnumeric(params.Points)
```

```
                        this.Points = params.Points;
                    else
                        this.Points = params.Points.Location;
                    end
                end
            end
        end
    end

    methods(Hidden, Access = private)
        % ----------------------------------------------------------------
        % Average HOG cells across overlapping blocks
        % ----------------------------------------------------------------
        function hog = averageHOGs(this, idx)

            numCellsPerWindow = floor(this.WindowSize./this.CellSize);
            accum = zeros([numCellsPerWindow this.NumBins], 'single');
            count = zeros(numCellsPerWindow);

            hBlockSize = [this.NumBins this.BlockSize];

            numBlocks = single(vision.internal.hog.getNumBlocksPerWindow(this));

            % reshape features to simplify averaging
            features = reshape(this.Feature(idx,:), [prod(hBlockSize) numBlocks]);

            blockStep = this.BlockStepSize ./ this.CellSize;
            for j = 1:numBlocks(2)
                for i = 1:numBlocks(1)
                    hBlock = reshape(features(:,i,j), hBlockSize);
                    % offset for cells based on current block position
                    ox = (j-1)*blockStep(2);
                    oy = (i-1)*blockStep(1);
                    for x = 1:this.BlockSize(2)
                        for y = 1:this.BlockSize(1)
                            accum(oy+y, ox+x,:) = ...
                                squeeze(accum(oy+y,ox+x,:)) + hBlock(:,y,x);
                            count(oy+y, ox+x)   = count(oy+y, ox+x) + 1;
                        end
                    end
                end
            end

            % average overlapping cells
            count = repmat(count,[1 1 this.NumBins]);
            hog   = accum./(count + eps);
        end
    end

    % ----------------------------------------------------------------
    % Custom display using matlab.mixin.CustomDisplay
    % ----------------------------------------------------------------
    methods(Hidden, Access = protected)

        % ----------------------------------------------------------------
        % Create header for disp method
        % ----------------------------------------------------------------
        function header = getHeader(this)
            if ¬isscalar(this)
                header = getHeader@matlab.mixin.CustomDisplay(this);
            else
                % Create a hyperlink that invokes the plot method
                headerStr = matlab.mixin.CustomDisplay.getClassNameForHeader(this);
                cmd = sprintf('<a href="matlab:plot(%s)">plot(%s)</a>',...
                    inputname(1),inputname(1));
                msg = sprintf('Type %s to visualize.', cmd);
                header = sprintf('%s\n\n   %s\n',headerStr,msg);
            end

        end
        % ----------------------------------------------------------------
```

```
        % Customize property display
        % -----------------------------------------------------------------
        function group = getPropertyGroups(¬)
            plist = {'CellSize', 'BlockSize', 'BlockOverlap', ...
                'NumBins', 'UseSignedOrientation','BinCenters'};

            title = sprintf('Read-only properties:');
            group = matlab.mixin.util.PropertyGroup(plist,title);

        end
    end

    % ---------------------------------------------------------------------
    % Helper methods
    % ---------------------------------------------------------------------
    methods(Hidden, Access = protected)

        % -----------------------------------------------------------------
        % Compute cell centers in spatial and pixel coordinates
        % -----------------------------------------------------------------
        function [centers, indices] = computeCellCenters(this)
            cellSize = this.CellSize;
            winSize  = this.WindowSize - rem(this.WindowSize,this.CellSize);

            % cell centers in spatial coordinates
            [cx,cy] = ndgrid(0.5 + (cellSize(2)/2:cellSize(2):winSize(2)),...
                0.5 + (cellSize(1)/2:cellSize(1):winSize(1)));

            % cell centers in pixel coordinates
            numCells = floor(this.WindowSize./this.CellSize);
            [cxIdx,cyIdy] = ndgrid(1:numCells(2),1:numCells(1));

            centers = [cx(:) cy(:)];
            indices = [cxIdx(:) cyIdy(:)];
        end

        % -----------------------------------------------------------------
        % Compute the bin centers in degrees
        % -----------------------------------------------------------------
        function binCenters = computeBinCenters(this)
            if this.UseSignedOrientation
                binRange = 360;
            else
                binRange = 180;
            end
            binWidth = binRange/this.NumBins;

            binCenters = (binWidth/2:binWidth:binRange)';
            binCenters = binCenters + 90; % rotate to show edges
        end

        % -----------------------------------------------------------------
        % Compute the end points of the lines used to represent bin centers
        % -----------------------------------------------------------------
        function endPoints = computeLineEndPoints(this)
            centers = (computeBinCenters(this)) * pi/180;
            endPoints = [cos(centers) -sin(centers)];
        end
    end
end

% -------------------------------------------------------------------------
% Input parser for plot method
% -------------------------------------------------------------------------
function [colorSpec, axes] = parseInputs(x,varargin)

validateattributes(x,{'Visualization'},...
    {'scalar'},'plot','',1);

p = inputParser;
addOptional  (p, 'axes', [], ...
```

```
    @vision.internal.inputValidation.validateAxesHandle);
addParameter(p, 'Color', 'white');

parse(p, varargin{:});

colorSpec = p.Results.Color;
axes      = p.Results.axes;

end
```

E

Checks

Figure E.1: End checks in board’s E/F face (dry group)

Figure E.2: Overview of end checks (dry group)

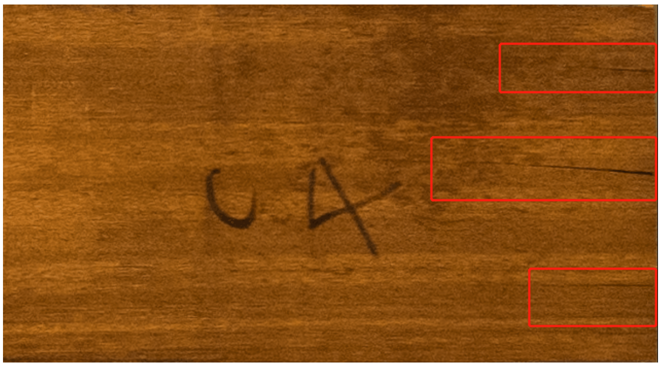

Figure E.3: Example of end checks at the 4C face

Figure E.4: Example of surface check

Figure E.5: End checks in board’s E/F face (wet group)

Figure E.6: Overview of end checks (wet group)

F

Crack angle measurement from DIC

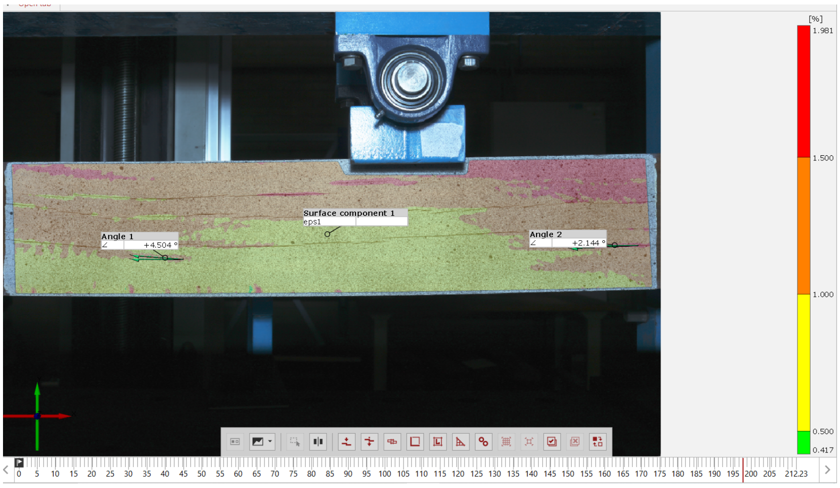

Figure F.1: Okan NO.4

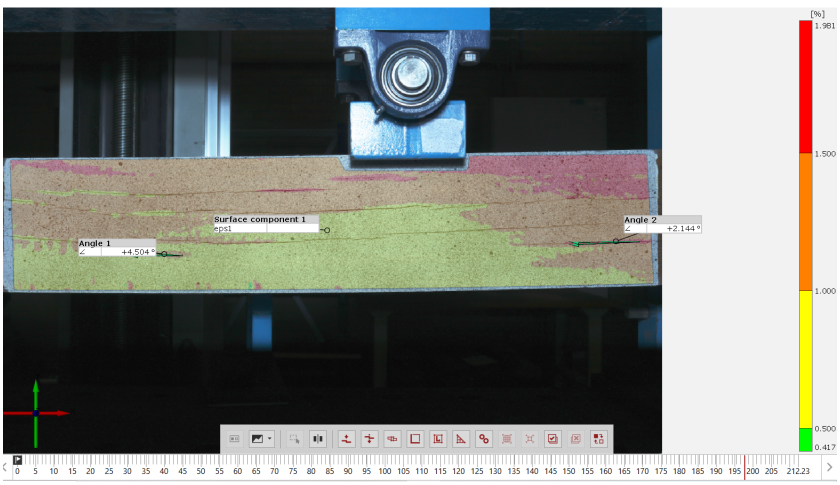

Figure F.2: Okan NO.6

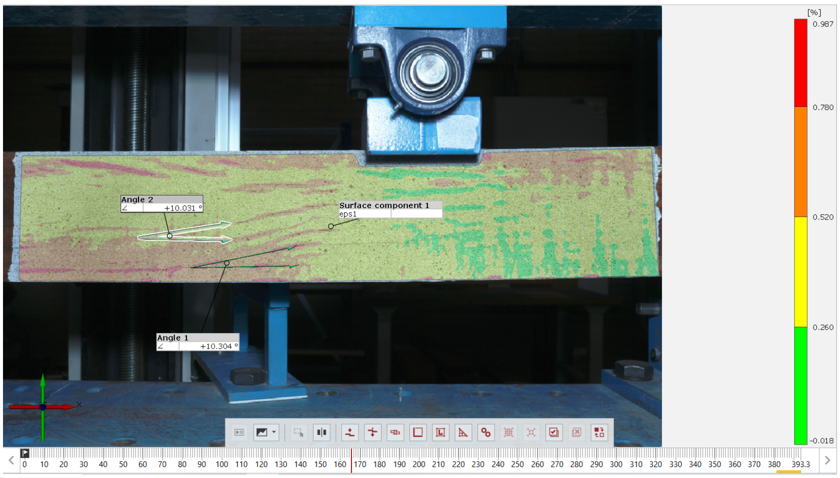

Figure F.3: Okan NO.9

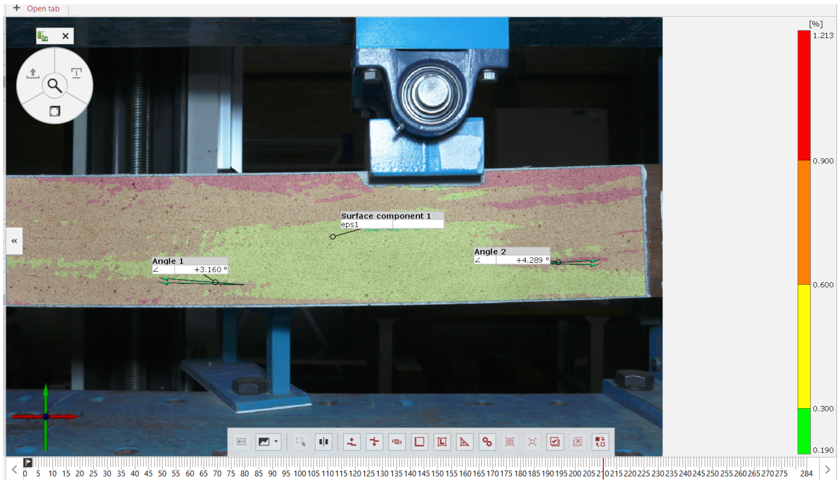

Figure F.4: Okan NO.18

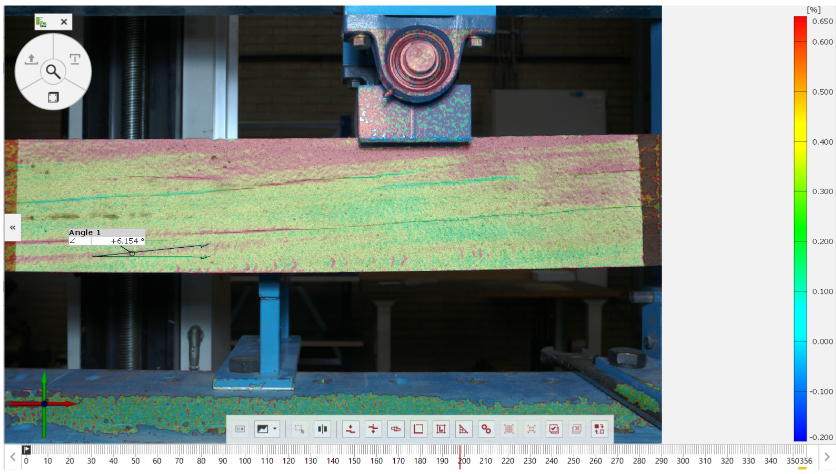

Figure F.5: Okan NO.24

G

Failure pictures

Figure G.1: Failure of beam No.4

Figure G.2: Failure of beam No.6

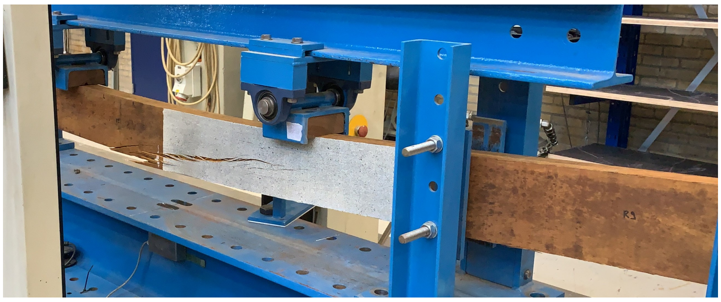

Figure G.3: Failure of beam No.9

Figure G.4: Failure of beam No.12

Figure G.5: Failure of beam No.18

Figure G.6: Failure of beam No.31

Figure G.7: Failure of beam No.34

Figure G.8: Failure of beam No.35

Figure G.9: Failure of beam No.38

Figure G.10: Failure of beam No.41

Figure G.11: Failure of beam No.45

Figure G.12: Failure of beam No.53

Figure G.13: Failure of beam No.54

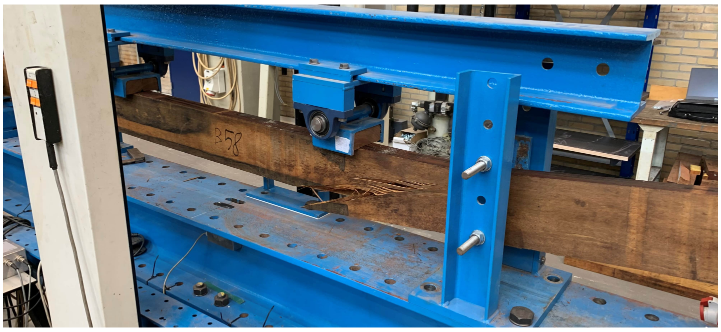

Figure G.14: Failure of beam No.58

H

Fracture section details

Figure H.1: Fracture section of beam NO.6

Figure H.2: Fracture section of beam NO.6

Figure H.3: Fracture section of beam NO.18

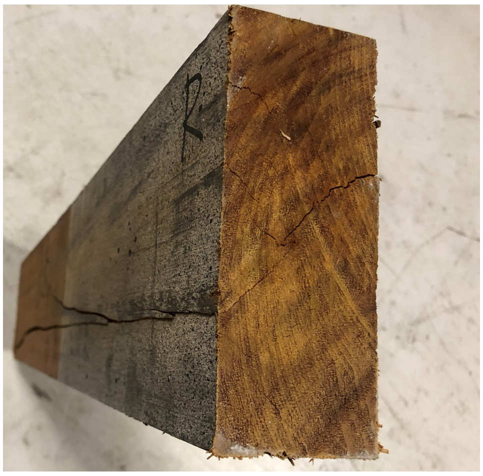

Figure H.4: Fracture section of beam NO.31

Figure H.5: Fracture section of beam NO.32

Figure H.6: Fracture section of beam NO.45

Figure H.7: Fracture section of beam NO.54

Figure H.8: Fracture section of beam NO.54

Bibliography

[1] Grain direction. https://tropicalwoods.weebly.com/grain-direction.html#.

[2] Histogram of oriented gradients. https://www.learnopencv.com/histogram-of-oriented-gradients/. Accessed: 2016-12-06.

[3] Interlocked grain. http://www.hobbithouseinc.com/personal/woodpics/_anatomy/_anatomy.htm. Accessed: 2020-05-24.

[4] How logs are turned into boards. https://www.core77.com/posts/24890/how-logs-are-turned-into-boards-part-1-plainsawn-24890. Accessed: 2013-06-05.

[5] Trees in tropical country. https://www.theforestacademy.com/tree-knowledge/annual-growth-rings/#.X28MHGgzZPY.

[6] Digital image correlation and tracking. https://en.wikipedia.org/wiki/Digital_image_correlation_and_tracking, . Accessed: 2020-01-23.

[7] Feature (computer vision). https://en.wikipedia.org/wiki/Feature_(computer_vision), . Accessed: 2020-05-14.

[8] Laszlo Bejo. *Simulation Based Modeling of the Elastic Properties of Structural Wood Based Composite Lumber*. PhD thesis, 2001.

[9] Blaß, Hans Joachim, Sandhaas, and Carmen. *Timber engineering – Principles for design*. 2017. ISBN 978-3-7315-0673-7. doi: 10.5445/KSP/1000069616.

[10] Thomas Ehrhart, René Steiger, and Andrea Frangi. A non-contact method for the determination of fibre direction of european beech wood (fagus sylvatica l.). *Holz als Roh- und Werkstoff*, 76: 925–935, 05 2018. doi: 10.1007/s00107-017-1279-3.

[11] EN14081-1: 2016+A1(EN). Timber structures, Strength graded structural timber with rectangular cross section. Part 1: General requirements. European Committee for Standardization. Standard, Dutch Standardization Institute, Brussels, 08 2019.

[12] EN338:2016(EN). Structural timber – Strength classes. European Committee for standardization. Standard, Dutch Standardization Institute, Brussels, 04 2016.

[13] W.F. Gard, G.J.P. Ravenshorst, and J.W.G. Van de Kuilen. Consistency of visual strength grading of tropical hardwood in europe. 2013. ISCHP.

[14] Amy Grotta, Robert Leichti, Barbara Gartner, and Randy Johnson. Effect of growth ring orientation and placement of earlywood and latewood on moe and mor of very-small clear douglas-fir beams. *Wood and Fiber Science*, 37, 04 2005.

[15] R. L. Hankinson. Investigation of crushing strength of spruce at varying angles of grain. *Air Force Information Circular No. 259*, 07 1921.

[16] Christian Jenkel and Michael Kaliske. Finite element analysis of timber containing branches – an approach to model the grain course and the influence on the structural behaviour. *Engineering Structures*, 75:237–247, 09 2014. doi: 10.1016/j.engstruct.2014.06.005.

[17] S.N. Jonkman, R.D.J.M. Steenbergen, O.Morales-Nápoles, A.C.W.M. Vrouwenvelder, and J.K. Vrijling. *PROBABILISTIC DESIGN: RISK AND RELIABILITY ANALYSIS IN CIVIL ENGINEERING*. 2017.

[18] Hae-Young Kim. Statistical notes for clinical researchers: Assessing normal distribution (2) using skewness and kurtosis. *Restorative dentistry endodontics*, 38:52–54, 02 2013. doi: 10.5395/rde.2013.38.1.52.

[19] Andriy Kovryga, Peter Stapel, and J.W.G. van de Kuilen. Tensile strength classes for hardwoods. 2016. International Network on Timber Engineering Research Proceedings: Meeting 49 Graz, Austria.

[20] NEN 5493:2010 (EN). Quality requirements for hardwoods in civil engineering works and other structural applications. Standard, Dutch Standardization Institute, Delft, 05 2010.

[21] NEN-EN 13183-1 (EN). Moisture content of a piece of sawn timber - Part 1: Determination by oven dry method. Standard, Dutch Standardization Institute, Brussels, 05 2002.

[22] NEN-EN 14358(EN). Timber structures - Calculation and verification of characteristic values. Standard, Dutch Standardization Institute, 11 2016.

[23] NEN-EN 384(EN). Structural timber - Determination of characteristic values of mechanical properties and density. Standard, Dutch Standardization Institute, 9 2016.

[24] NEN-EN 408+A1 (EN). Timber structures - Structural timber and glued laminated timber - Determination of some physical and mechanical properties. Standard, Dutch Standardization Institute, Brussels, 09 2012.

[25] NEN-EN 844-9 (EN). Round and sawn timber - Terminology - Part 9: Terms relating to features of sawn timber. Standard, Dutch Standardization Institute, Brussels, 04 1997.

[26] NEN-EN1309-3 (EN). Round and sawn timber - Methods of measurements - Part 3: Features and biological degradations. Standard, Dutch Standardization Institute, Brussels, 01 2018.

[27] G.J.P. Ravenshorst. *Species independent strength grading of structural timber*. PhD thesis, 07 2015.

[28] G.J.P. Ravenshorst and J.W.G. Van de Kuilen. Species independent strength modelling of structural timber for machine grading. 2016. WCTE 2016, Vienna.

[29] G.J.P. Ravenshorst and J.W.G. Van de Kuilen. Relationships between non-destructive measurements and mechanical properties of tropical hardwood. 2018. WCTE 2018, Seoul.

[30] G.J.P. Ravenshorst, W.F. Gard, and J.W.G. Van de Kuilen. Influence of slope of grain on the mechanical properties of tropical hardwoods and the consequences for grading. *European Journal of Wood and Wood Products*, 78, 09 2020. doi: 10.1007/s00107-020-01575-0.

[31] Slomp, Robert, Knoeff, Han, Bizzarri, Alessandra, Bottema, Marcel, and de Vries, Wout. Probabilistic flood defence assessment tools. *E3S Web Conf.*, 7:03015, 2016. doi: 10.1051/e3sconf/20160703015. URL https://doi.org/10.1051/e3sconf/20160703015.

[32] Mark van Benthem and Boris Bakker (intern Probos). Lesser-known timber species are part of it too. http://www.houtdatabase.nl/?q=node/243. Accessed: 2011-07.

[33] J.W.G. Van de Kuilen. Engineered wood structures with tropical hardwoods. 2013. ISCHP.